The use of controlled radical techniques to form polymer architectures suitable for use as Gear Oil Viscosity Modifiers

by

Peter Wright

A thesis submitted in partial fulfilment of the requirements for the degree of Doctor of Philosophy in Chemistry

Department of Chemistry

THE UNIVERSITY OF WARWICK

December 2008

“One must try by doing the thing: for though you think you know it, you have no certainty until you try.”

Sophocles

“...man will occasionally stumble over the truth, but usually manages to pick himself up, walk over or around it, and carry on.”

Winston S. Churchill

“Failures are finger posts on the road to achievement.”

C. S. Lewis

Table of Contents

Abbreviations

AA	Acrylic Acid
ADPA	*N*-phenyl-1,4-phenylenediamine
ATRP	Atom transfer living racial polymerisation
BA	*n*-butyl acrylate
bipy	2,2-dipyridyl
BMA	*n*-butyl methacrylate
BV40	Absolute viscosity measured on a Brookfield viscometer at -40°C
$C_{12/15}MA$	A monomer based on Neodol 25 made by Shell
DMAEMA	Dimethylaminoethyl methacrylate
DoE	Design of experiment
DP	Degree of polymerisation
DVB	Divinyl benzene
DVM	Dispersant viscosity modifier
EGDMA	Ethylene glycol dimethacrylate
EHMA	2-ethylhexyl methacrylate
GPC	Gel permeation chromatography
KV	Kinematic viscosity
LRP	Living radical polymerisation
MA	Methyl acrylate
Me_6TREN	Tris(2-(dimethylamino)ethyl)amine
MMA	Methyl methacrylate
M_n	Number average molecular weight
M_w	Weight average molecular weight
NMP	Nitroxide mediated polymerisation
NMR	Nuclear magnetic resonance
RAFT	Radical addition fragmentation chain transfer
OVAT	One variable at a time
PAMA	Poly alkyl methacrylate
PDI	Polydispersity index
SET-LRP	Single electron transfer living radical polymerisation
SSI	Shear stability index
STY	Styrene
t-BuMA	*t*-butyl methacrylate
TE	Thickening efficiency

TEGDMA	Triethylene glycol dimethacrylate
TMM LRP	Transition metal mediated living radical polymerisation
VI	Viscosity index
VM	Viscosity modifier
VT-I	Viscosity temperature improver
UV-VIS	Ultra Violet - Visible

Acknowledgements

Among the many people I wish to thank perhaps the first is David Haddleton. His constant enthusiasm and optimism helped me battle through those moments when the chemistry was just not working.

I also thank post-docs past and present for their help, guidance and patience even when asked the silliest questions. Particular mention must go to Beppe Mantovani and Josefina Lindqvist. The polymer group at large, again past and present, who have provided the answers to many questions and also asked many good ones of me – I thank you all.

I would like to thank Lubrizol for funding this project and in particular Will Barton, David Price, Mark Davis and Tim Smith, who either helped set up the project or have guided me through the industrial angle of this work.

Lastly I wish to thank my wife, Hayley, for helping me to achieve what I have.

Declaration

Experimental work contained in this thesis is the original research carried out by the author, unless otherwise stated, in the Department of Chemistry at the University of Warwick or at Lubrizol's Chemical Synthesis department, Hazelwood, Derbyshire between October 2005 and October 2008. No material herein has been submitted for any other degree, or at any other institution.

Results from other authors are referenced in the usual manner throughout the text.

Signed:_____ Date:_____

Peter Wright

Abstract

This project is concerned with the synthesis of Viscosity Modifiers (VMs) for use in gear box oils. The use of amines as precursors for initiators is also of interest due to their dispersant properties.

Atom transfer radical polymerisation (ATRP) was used to prepare statistical copolymers of *n*-Butyl methacrylate and $C_{12/15}$ methacrylate for use as VMs. These copolymers were first of a linear nature demonstrating that ATRP could be used to polymerise this monomer combination to give well defined polymers with a high degree of control. Thereafter, multi-functional initiators were used to synthesise core first stars with differing numbers of arms. Three, four, five and eight arm stars were successfully synthesised giving well defined polymers. These polymers were tested by Lubrizol for their viscometric properties. All were found to give significant improvements versus Lubrizol's existing linear polymers in almost all respects.

Although the core first stars gave a significant improvement in viscometric properties the costs of the core are relatively high for the application. Therefore the synthesis of arm first stars via ATRP was carried out. Design of experiment (DoE) was used to aid in the optimisation process and to interrelate any factors used in the design. The DoE process indicated two relationships between input factors, one of which was defined numerically. A range of polymers were synthesised on a larger scale for testing by Lubrizol for their viscometric properties. The polymers were found to have exceptional viscosity properties, compared to the baseline sample.

The use of amines as precursors for initiators (forming amide initiators) was investigated. 4-Aminodiphenylamine (ADPA) was synthesised into an initiator suitable for ATRP and used in several polymerisations. It was found to have very low initiator efficiency. For this reason Single Electron Transfer Living Radical Polymerisation (SET-LRP) was employed to polymerise methyl acrylate from this initiator with near 100% initiator efficiency. A range of other amide initiators were also successfully used in polymerisations. A new solvent system for SET-LRP was also demonstrated. The addition of phenol to toluene promoted the disproportionation of Cu(I) allowing SET-LRP to take place. Polymers were synthesised in this solvent mixture with high degrees of control over molecular weight with narrow Polydipersity indexs (PDI).

Chapter 1
-
Polymers as Oil Additives

Table of Contents

List of Figures

List of Tables

1 Introduction

1.1 The Oil Additive Industry

Lubricating oil additives are designed to improve the efficiency of the oil and to increase the lifespan of the part(s) being lubricated and of the oil itself. The additive package is devised to enhance an existing property or properties of the base oil or to give it a new property which is desirable for the application. Typically, lubricating oils for use in cars or lorries would contain:

Additive	Role in the Oil
Dispersants	Sludge & varnish control
Antioxidants	Prohibit oxidation
Antiwear	Planetary gear, bushing, thrust washer protection
Friction modifier	Modify clutch plate and band friction
Corrosion inhibitor	Prevent corrosion and rust
Seal swell agent	Prevent loss of fluid via seals
Viscosity Improver	Reduce rate of change of viscosity
Pour Point Depressant	Improve low temperature fluidity
Foam inhibitor	Foam control

Today, the market for the sale of these additive packages is highly competitive with a number of companies selling highly effective products. This research is concerned with the synthesis of Viscosity Modifiers (VMs) and soot dispersants which represent a significant proportion of the total oil additives market. Therefore any improvement gained through innovation and the development of new products could be result in significant commercial benefit.

In order to understand how these two additives work and how they might be improved it is first necessary to explore what viscosity is and how it is measured. After this is explained, the mechanism of action of dispersants is discussed.

1.2 Viscosity

Viscosity can simply be described as a fluid's resistance to flow - that is the resistance arising from intermolecular forces and internal friction as the molecules move past each other. In a situation where two surfaces in motion are fully separated by a fluid the friction is due solely to the internal friction of the liquid; its viscosity.

Different fluids have different viscosities. Water and honey are two liquids with vastly different viscosities; at ambient temperature water is free-flowing and honey is highly viscous. However, a more interesting observation is that water's free-flowing nature does not change enough between 5°C and 50°C for the human eye to detect the difference. Honey, on the other hand, will be almost solid at 5°C and a free-flowing liquid at 50°C. This change in viscosity, however large or small, can be described as the Viscosity Index (VI) which will be expanded upon later.

The original work describing viscosity of fluids was by Newton in 1668. He stated that "*The internal friction* (*i.e.* viscosity) *of a fluid is constant with respect to the rate of shear*".[1] Newton's work allowed scientists to later group fluids into two categories; those which obey the above statement, and later came to be described as 'Newtonian', and those which do not are known as 'Non-Newtonian'. An example of a Newtonian fluid is water; irrespective of the speed of stirring or mixing (or shear) it remains a free-flowing liquid. The viscosity of a Newtonian fluid is dependent only on temperature but not on shear rate and time. Non-Newtonian fluids' viscosities are dependant on temperature, time and shear rate. Depending on how the viscosity changes with time, they can be further defined as either; *thixotropic* – time thinning, i.e. viscosity decreases with time at constant shear, or *rheotropic* - time thickening i.e. viscosity increases with time at constant shear. Non-Newtonian fluids can also be subdivided by their response to shear rate: *shear thinning* – the viscosity decreases with increasing shear rate, *shear thickening* – the viscosity increases with increasing shear rate. Polymers are classed as Non-Newtonian fluids.

1.2.1 Absolute (or Dynamic) Viscosity

The viscosity of a fluid can be stated in a number of different ways. Firstly, the absolute or dynamic viscosity. This is measured in Poise (usually stated in Centi-Poise cP), Equation 1. The equation derives from the shear stress and the shear strain (rate of shear). The absolute viscosity is defined as *the force in dynes required to move a surface one square centimetre in*

area past a parallel surface at a speed of one centimetre per second (U), with the surfaces separated by a fluid film one centimetre thick (h) and is represented in Equation 2. Typically, the absolute viscosity would be measured using a Brookfield Viscometer.

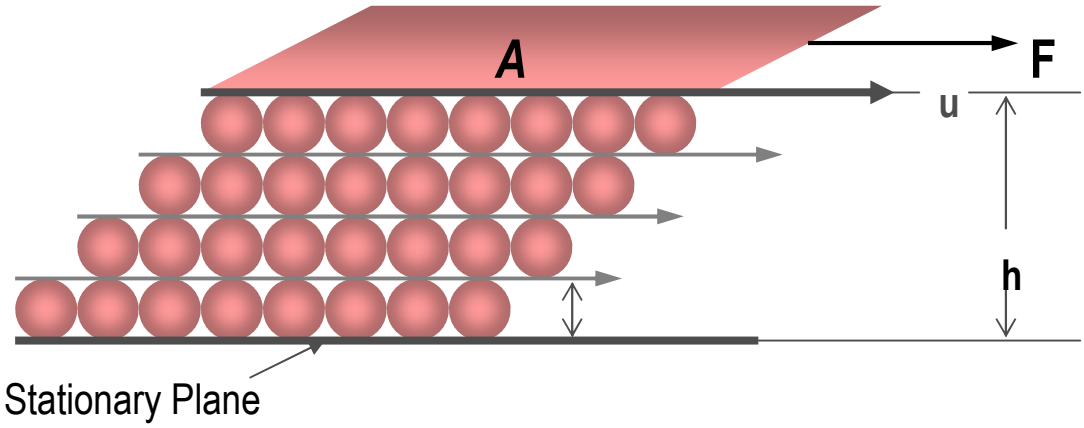

Figure 1 – Absolute viscosity model

$$F = \eta A \frac{U}{h}$$

Equation 1

This equation can then be rearranged to give the absolute viscosity, η:

$$\eta = \frac{F/A}{U/h} = \frac{shear\ stress}{rate\ of\ \ shear} = \frac{dynes/cm^2}{s^{-1}} = Poise$$

Equation 2

1.2.2 Kinematic Viscosity

The Kinematic Viscosity (KV- stated in Centistokes, cSt), Equation 3, is the measure of a fluids resistance to flow under gravity. The KV, as shown by Equation 3, is related to the fluid density. The density of a fluid changes with temperature; it is important to use values for density and absolute viscosity measured at the same temperature when determining KV in this manor. The KV is often measured using a capillary viscometer.

$$Kinetmatic\ Vis\cos ity = \frac{Absolute\ Vis\cos ity}{Fluid\ \ Density} = Stokes$$

Equation 3

The prediction of the change in KV with temperature is important for assessing oil suitability. The majority of lubricating fluids give a straight line response on a viscosity temperature plot; when the Walther equation, Equation 4, is used to calculated the KV, the graph plotted from it allows for the prediction of the KV between two points, Figure 2.

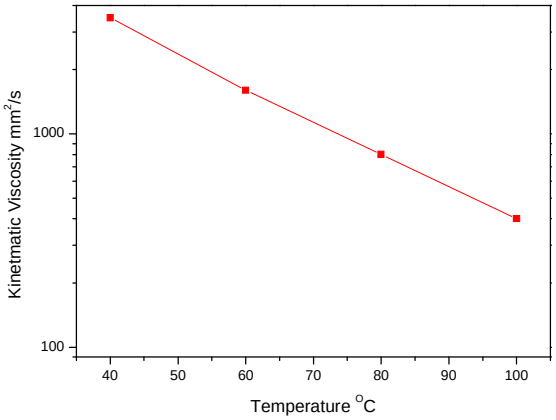

Figure 2 – Typical log plot of the Kinematic Viscosity against temperature for a lubricating oil.

$$Log_{10}\ Log_{10}\ (KV + a) = b + c\ LOGT$$

Equation 4

In this equation KV is the kinematic viscosity, a, b and c are constants and machine dependant, while T is the absolute temperature.

However, KV is often measured by using a capillary viscometer so the equation used is a derivation from the above Equation 3, to give Equation 5. Equation 5 can be simplified to give Equation 6 which shows that the length of the capillary used squared dived by the time taken to move that length gives the KV.

$$Kinematic\ Viscos\,ity = \frac{force \times length}{area \times velocity} \Big/ \frac{mass}{volume}$$

Equation 5

$$Kinematic\ Vis\cos ity = \frac{(length)^2}{time}$$

Equation 6

1.2.3 Viscosity Index

The viscosity index of a fluid describes to what extent its viscosity changes between two different temperatures and is calculated from the KV. The VI system was established in 1929 by Dean and Davis, who worked for the Standard Oil Development Company (now part of ExxonMobil).[2] The system was developed to show the difference between oils from Pennsylvania, Texas and California. At that time, Pennsylvania oils thinned much less rapidly than the oils from Texas when subjected to a temperature increase. These Pennsylvania oils were rated 100 on their VI scale. The Texan oils were rated 0. This system meant that the identification of oils was now possible by measuring its VI by using Equation 7 and Figure 3. However, now that refinement techniques have improved significantly, the same oils which were previously rated 0-10 VI can be prepared with 30-50 VI. Similarly, oils with higher VI such as from Pennsylvania can often be found with 100+ VI.

A similar problem of differentiating between oils also arose when polymeric additives started to be widely used to improve the viscosity-temperature properties of oils. These additives have relatively greater effects on the viscosities at high temperature than those at low temperature and therefore increase the VI considerably above 100 VI. This results in Equation 7 no longer holding true for VI>100. Any additives that improve the VI are defined as viscosity index improvers (VII).

$$VI = \frac{L-U}{L-H} \times 100$$

Equation 7

where L is the 40°C KV of a fictitious oil having the same KV of the test oil at 100°C, defined as having a VI of 0. H is also the 40°C KV of another fictitious oil having the same viscosity as the test oil at 100°C but defined as having a VI of 100. The VI of the test oil is defined by the relationship of its 40°C KV (called U).

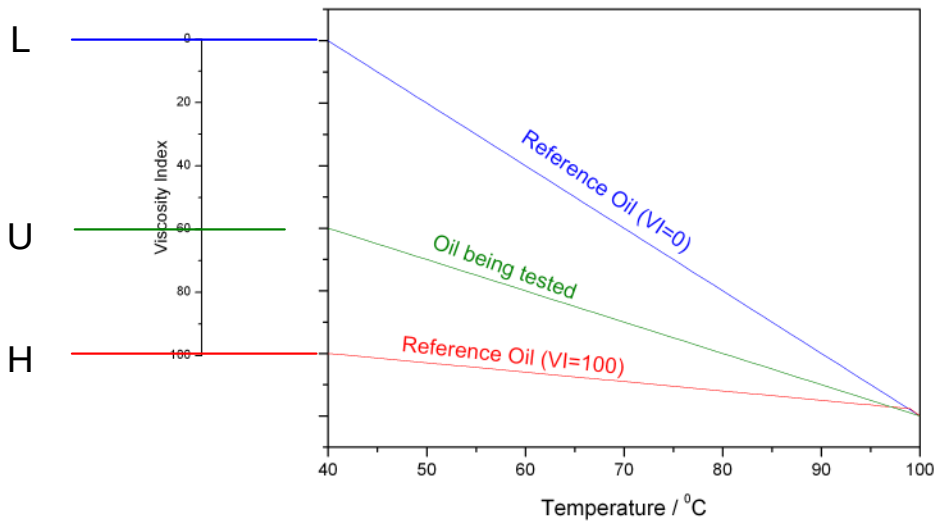

Figure 3 – Graph showing how calculation of Viscosity Index (VI) is based on viscosities at 40°C and 100°C.

1.2.4 Viscosity Index Extension (VI_E)

To overcome this issue of the original Dean and Davis system no longer holding true for VIs over 100, extensional work was undertaken to allow the satisfactory calculation also of these VIs. This new method was designed to provide continuity between the two systems so that an oil of VI 100 also has a VI_E of 100. The VI_E values can be calculated as described here:

$$VI_E = 100 + 140 * ((10 \wedge n) - 1)$$

Equation 8

$$\text{where} \quad n = \frac{(\log H - \log U)}{\log KV_{100}}$$

Equation 9

where U and H are as previously described for Equation 7.

1.2.5 Viscosity-Temperature Improvers

After the initial work on the VI system by Dean and Davis,[2] Selby, a Senior Research Engineer at General Motors, published a paper on the Non-Newtonian characteristics of lubricating oils.[3] In this work Selby describes the mechanisms by which VMs modify the VI. Selby suggests that *"the viscosity of a fluid may be attributed to the difficulty the molecules experience in getting past one another during flow of the fluid mass; the greater the difficulty, the higher the viscosity."*.[3] Therefore, upon addition of a high molecular weight polymer (a VM with M_n > 100 000 g mol^{-1}), which is spatially quite large, the small molecules of the mineral oil have a greater difficulty to move past each other and the polymer. The polymer chains also have a high impedance to moving past one another and therefore the solution viscosity will increase. The relative size or hydrodynamic volume of the VM molecule should ideally change with temperature. Selby attributes this change to the alteration in solubility of the VM in the chosen oil. At low temperature, the VM should be sparingly soluble, while at higher temperature it should be completely dissolved. This change in solubility also causes a change in the hydrodynamic volume. At low temperature, the polymer molecule is contracted to minimise its contact with the oil, while at higher temperatures it is much less densely packed, ideally fully elongated in the oil, Figure 4.

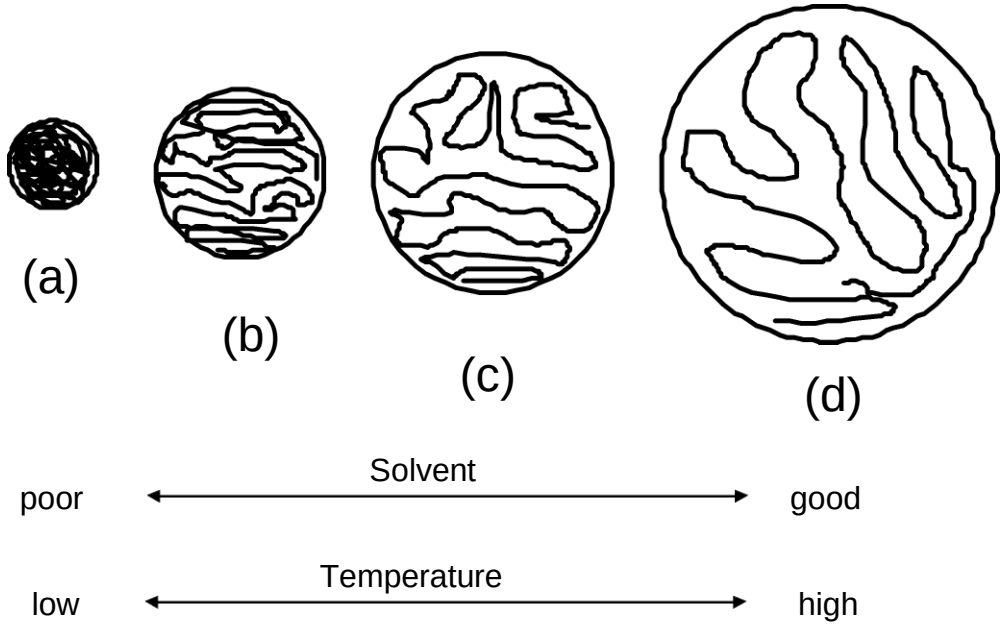

Figure 4 – The expansion and contraction of a macromolecule depending on the solvent and temperature

However, in a case where the VM is soluble in the oil at low temperatures the additive may not act as a VM. In fact, its influence on the viscosity of the oil may well be the same or less at high temperatures as it is at low; Selby classes this type of additive as a thickener.

In order to differentiate between an actual VM and a thickener, Selby reclassified a VII as a viscosity-temperature improver (V-TI). These are additives which give a greater viscosity contribution at higher temperature than low describing the use of Equation 10 to aid in the differentiation between a thickener and a V-TI.

$$\mu_{sp} = \frac{\mu - \mu_0}{\mu_0}$$

Equation 10

where μ_{sp} = specific viscosity
μ = blend viscosity
μ_0 = base oil viscosity

The viscosity temperature characteristics can be calculated by using Equation 11 where if the ratio for V-T characteristic exceeds 1 the polymer is indeed a V-TI, while when less than 1 the polymer is a thickener. The greater the value above or below 1 shows how effective a thickener or V-TI the polymer is.

$$V - T\ Characteristic = \frac{\mu_{sp_{100}}}{\mu_{sp_{40}}}$$

Equation 11

In this way Selby suggests that his system for the characterisation of oil VM additives better separates V-TI from thickeners. However, other than Selby's discussion of the mechanism of action of VMs most citations of this paper ignore the additional calculations proposed by the author.

1.2.6 Shear Stability

The shear stability of polymers is an important factor as it is the measure of the ability of the oil/polymer mixture to resist permanent viscosity loss under high shear – the more shear stable the oil mixture the smaller the viscosity loss when subjected to shear.[4] The viscosity of lubricants drops significantly during the early stages of use due to shearing of the VM.[5] Generally, lower molecular weight polymers exhibit lower shear rates. However, due to the lower molecular weights, increasing amounts of additive are needed to obtain the necessary viscosities, increasing the overall cost the additive package. The balance between shear stability and treatment rate (the amount of the additive put in the oil mixture), through tailoring the molecular weight, is important.

The shear stability index (SSI) of an oil VM can be defined by the following equation:

$$SSI = \frac{m_i - m_f}{m_f - m_0} \times 100$$

Equation 12

where:

m_i = initial viscosity of lubricant with the viscosity modifier

m_f = final viscosity of lubricant after shear

m_0 = viscosity of the lubricant without the viscosity modifier

The equation can be explained as follows: a VM with a low SSI number is more shear-stable, while a VM with a high SSI number is less shear stable. Higher molecular weight VMs will have the greatest thickening efficiency for a given weight of polymer but will have the lowest shear stability (highest SSI).[6]

1.2.7 Thickening Efficiency

The thickening efficiency (TE) is a measure of a VMs ability to thicken a given oil with reference to the amount of it added to the oil. Equation 13 shows how the TE is calculated; KV100 is the kinematic viscosity of the oil blend at 100°C, KV oil is the kinematic viscosity of the base oil at 100°C, and the TR is the treat rate, or the amount of the VM added to the oil as a weight percentage.

$$Thickening\,Efficiency = (Log(\frac{KV100}{KV\,oil})) * TR$$

Equation 13

The thickening efficiency increases with the molecular weight of a polymer. However, the shear stability decreases as molecular weight increases, Figure 5. Therefore, the molecular weight of the polymer is paramount to optimising the shear stability and the thickening efficiency of the VM.

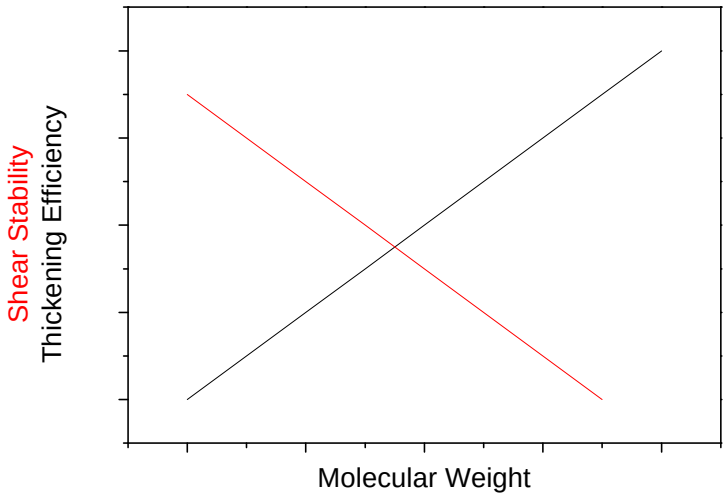

Figure 5 – A demonstration of how the shear stability and thickening efficiency change with the molecular weight of the polymer used as a VM.

1.3 Lubricating oil additives

1.3.1 Dispersants

Dispersants are used in automotive applications to keep impurities, particularly those formed during the use of mechanical devices such as automatic transmissions, internal combustion engines and brake fluid, in suspensions rather than allowing them to accumulate as sludge or other deposits on the surfaces of the lubricated parts. The insoluble materials are often formed by oxidation and other mechanisms during the use of the oil. Dispersants prevent the agglomeration of soot particles, therefore reducing increases in viscosity of the lubricating oil upon use.

Figure 6 – The difference between a soiled piston head on the left, and a new one on the right.

The mechanism by which they prevent agglomeration is by either electrostatic or steric stabilisation,[7] Figure 7. Dispersants usually use steric stabilisation as they are non-ionic species. This is where the steric interactions of the polymer chains attached to the particles cause the particles to repel one another preventing agglomeration. They also prevent corrosion by these often highly polar by-products. Although a dispersants primary role is to prevent deposition of soot, they must also have other properties in order to function effectively. These properties include oxidative and thermal stability, good low temperature properties i.e. maintenance of low viscosity and the dispersant head group not degrading seals of the unit, gear box/engine that it is in.[4, 8] Those dispersants that are not oxidative or thermally stable will firstly break down, reducing its ability to suspend soot and sludge deposits in solution. Secondly, it will add to the deposits causing oil thickening and deposit formation. [8]

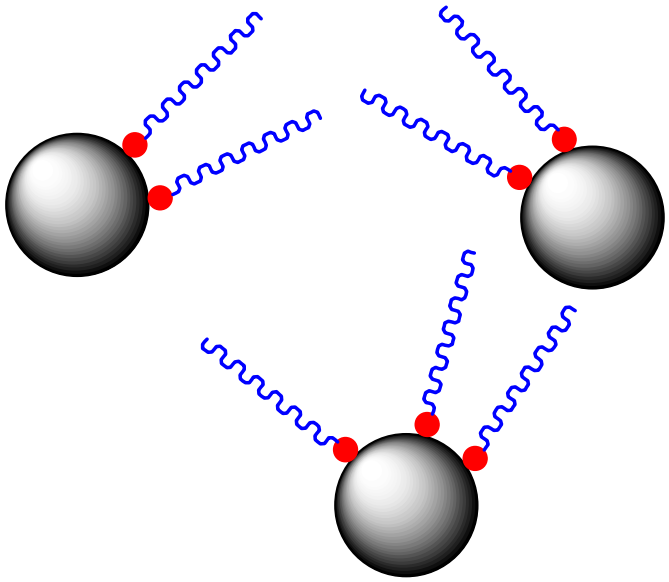

Figure 7 – Steric stabilisation of a soot particle,the polymer chains prevent the particles getting to close and flocculating.

Dispersants can be separated into two categories: (1) Dispersant viscosity modifiers (DVM), or (2) Dispersant polymers. In DVMs, the dispersency and viscosity modifying properties are combined into the same product. They are derived from hydrocarbon polymers, often olefin or (meth)acrylate based, of molecular weights between 25,000 and 500,000 g mol^{-1}. Alternatively, polymers used to make DVMs include olefin copolymers such as ethylene-propylene copolymers[9], ethylene-propylene-diene copolymers[11, 12] and polymethacrylates[13-17], styrene diene rubbers[10] and styrene-ester copolymer[19]. Dispersant polymers have a low molecular weight, usually between 3000 and 7000 g mol^{-1} and do not usually have any additional properties besides dispersing insoluble materials.

Polymer-based dispersants have been used to stabilise paints,[20, 21] ink systems[22, 23] and carbon impurities in automotive applications.[9, 24] The system has a three component structure which combines the different requirements, Figure 8, which is summarised here.

1. The anchoring group, which must be capable of strongly attaching, via different methods, to the surface of particles.
2. The polymeric chain, which must dissolve the polymer in the desired solvent and stabilise the particle it is anchored onto.
3. A linking group between the polymeric chain and the polar anchoring group.

The polar group is usually nitrogen or oxygen-based. The polar entity can be varied depending on the nature of the particle/sludge being adsorbed. Nitrogen-based groups are

generally derived from amines and are usually basic in nature whilst oxygen-based groups are derived from alcohols and are neutral.[7]

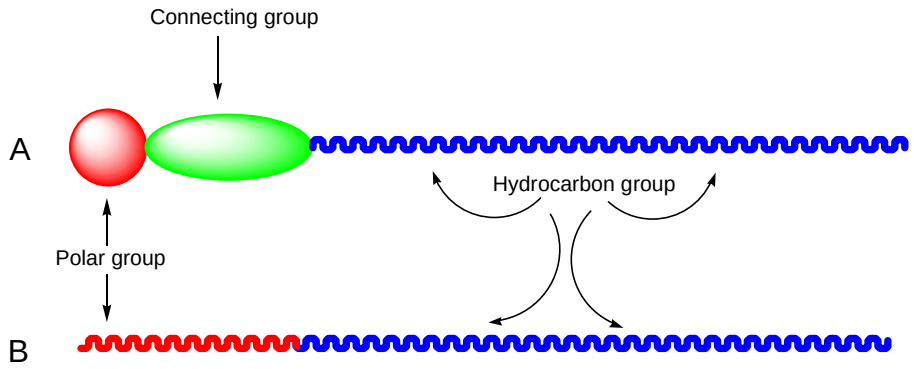

Figure 8 - Representation of how polar groups are incorporated into a dispersant molecule through (A) Polar head groups (B) Polar monomers

The two ways of incorporating these properties into polymers are shown in Figure 8. The anchoring groups can either be by polar head groups or as part of the polymeric chain. The solvating part is always a polymer with six common configurations for solvation, Figure 9.

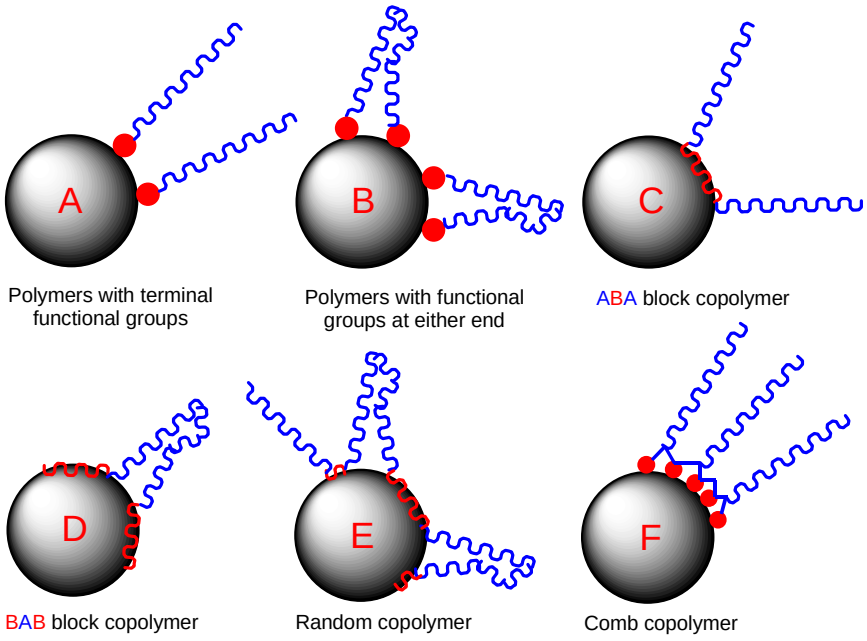

Figure 9 - The different methods of anchoring polymeric dispersants onto particles: Polymeric blocks (C, D, E, F) or functional groups (A, B)

Each type of interaction has its own distinct advantages with methods A and C being considered to be the optimum. This is because they prevent flocculation by bridging of the particles by the dispersant, where a polymer chain is anchored onto two particles. However, flocculation by chain interaction, where chains on different particles interact is still possible. Method A is preferable to C because a closer packed monolayer can be formed on the

particles surface allowing for greater dispersion. Methods B-F all have multiple anchor points and give a greater possibility of anchoring successfully onto a particles surface, however bridging of particles is more likely.

The dispersing group almost always contains secondary nitrogen and often aromatic groups as these are the most effective at binding to soot and sludge. Although the exact mechanism is not known, it is likely to be a combination of hydrogen bonding of the nitrogen to the soot surface; soot has a significant amount of carboxylic acid groups on its surface, and electrostatic interactions.[11] Soot is known to have a significant amount of aromatic groups in its structure along with carboxylic acids and hydroxyl groups and therefore π- π stacking and acid/base interactions can be used to absorb the dispersant head groups onto the surface. Polar head groups used as dispersants are wide ranging from amines such as ethylenediamine[8], through to dyes such as disperse orange 3.[24] Maleic anhydrides,[12] succinimides,[13, 14] Mannich bases products,[27, 28] carboxylic functionalities[13] have been used to react with the desired amine functionality - aromatic amines[13, 14] such as phenyl-1,4-phenylene diamine[31, 32] and other amines.[12, 14] A further way of anchoring polymeric dispersants onto soot/sludge is using a monomer which has nitrogen incorporated in it such as dimethylaminoethyl methacrylate or dimethylaminoethyl methacrylamide. [15] Sludge is best dispersed by non-aromatic amines for miscibility reasons.

The nature of the polymer chain is very important for dispersants. If the chains are not long enough and are not soluble enough, the dispersant will not provide a thick enough barrier to prevent flocculation. This will cause an increase in viscosity and a decrease in performance. Alternatively, if the chains are too long, then the chain will collapse onto the particles surface allowing it to aggregate or flocculate. Ideally, the polymer chains should be of a length where it can move freely in solution.

1.3.2 Viscosity Modifiers

Viscosity modifiers (VM, viscosity improver, VI, or viscosity index improver, VII) reduce the extent of the increase in kinematic viscosity as the temperature is lowered, or reduce the extent of the decrease in kinematic viscosity as the temperature is raised, or both.[4] They should have good thickening capability while remaining cost effective, be shear stable and have minimal deposits at high temperature.[6] This should mean that the oil maintains a more consistent viscosity over a broad range of temperatures. If the oil is too thin then it is moved away from the interface of two surfaces and poor lubrication occurs leading to surface

damage. When the oil is too viscous it either does not flow into the interface causing certain surface damage, or it consumes too much energy which is converted to heat and the system can overheat. The kinematic viscosity is usually measured between 40°C and 100°C and a graph plotted to show the change over the temperature range, Figure 10. The effect of adding a VM is demonstrated with the viscosity variance being smaller over the same temperature range.

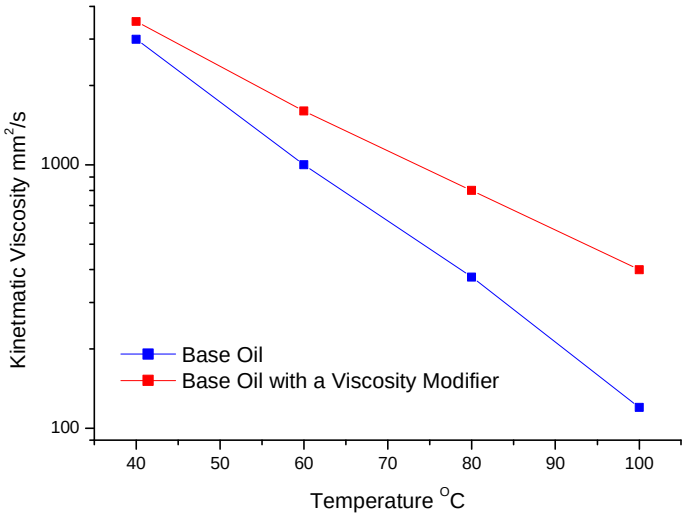

Figure 10 – Plot showing the difference between a base oils viscosity drop (blue) against the same base oil with a viscosity modifier added to it (red).

A simplified explanation for this phenomenon is that the polymer-oil interaction at low temperature is minimal but increases as temperature rises. This interaction of the polymer with the base oil at higher temperatures increases the hydrodynamic volume of the polymer causing an increase in the effective volume fraction of the VM. This leads to an increase in lubricant viscosity.[6]

VM's have previously been made from polyolefin,[17, 18] polyisobutylene[16-20] and more recently poly(alkyl methacrylate)s.[14-16, 39] They are usually linear, although stars and other branched architectures have been used. The stars have exceptional low-temperature properties but undergo more permanent viscosity loss under severe conditions.[6] The alkyl methacrylates are of particular interest as they are a blend of chain lengths from C_{11} to C_{18} to give the desired properties, e.g., de-waxing, solubility and VM. Carbon chains with 8 to 13 carbons give solubility in hydrocarbon solutions. Long chains of 14 or more carbons give de-waxing properties to act as a pour point depressant. Polyolefins are usually copolymers of ethylene, propylene and a third monomer, often a non-conjugated diene.[21] They have high thickening efficiencies and relatively low cost. The polymers can be tailored for different applications

by varying the copolymer composition, particularly low temperature ones. The desirable property of the poly(alkylmethacrylates) (PAMAs) are the ability to contribute relatively little viscosity at lower temperatures but have a much higher contribution to viscosity at elevated temperatures. [22] They have been previously made by free radical polymerisation. However, more recently living radical polymerisation techniques such as radical addition fragmentation chain transfer (RAFT), nitroxide mediated polymerisation (NMP) and TMM LRP (transition metal mediated living radical polymerisation or commonly known as atom transfer radical polymerisation – ATRP) have all shown great potential for making PAMAs due to their molecular weight control and narrow PDIs. The VM block can be made into a block copolymer with the dispersant block to reduce the number of components that are needed in the final product.

1.3.3 Transition Metal Mediated Living Radical Polymerisation

The non-linear structures that are of interest for VMs are not easily accessible by conventional free radical polymerisation. However, living radical techniques can be used to access a variety of non-linear structures. The polymerisation technique being used for this project, TMM LRP has seen extensive research in the 13 years since it was originally published by Sawamoto[23] and Matyjaszewski[24] in 1995. Pioneering work on this system used Ru(II) and Cu(I) catalysts respectively.[23,24] ATRP has been further developed to use different transition metals as catalysts including low valent iron, [25, 26] palladium, [27] rhodium[28] and nickel.[29]

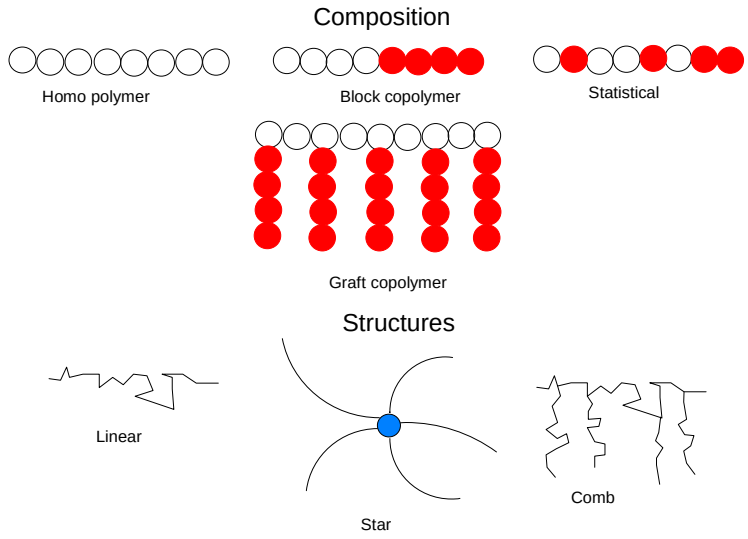

Figure 11 - Different structures of polymers obtainable via ATRP

The appeal of this chemistry is the high degree of molecular weight control, the variety of structures that can be synthesised, Figure 11, and low PDI of the products giving more mono-disperse properties (PDI < 1.2). In addition each polymer chain retains a terminal initiating group giving α-functional polymers. ATRP is relatively insensitive to impurities such as water, making it a robust technique for scale up to industrial levels of production. The polymerisations can be carried out in bulk or in solution. A wide range of solvents can be used, including: toluene, dimethoxybenzene (DMB), diphenyl ether (DPE), ethylene carbonate, acetonitrile, *N*,*N*-dimethylformamide (DMF), acetone, most alcohols (especially methanol and isopropanol), water, benzene and anisole.[30] The solvent can be tailored to the monomer system being polymerised. Depending on the solvent being used, the ligand can also be altered to ensure that the transition metal is soluble in the chosen solvent. The ligands can vary dramatically from the original diamine reported by Matyjaszewski *et al*. in 1995,[31] to the Schiff base ligands, Figure 12, reported by Haddleton *et al*. in 1998.[32]

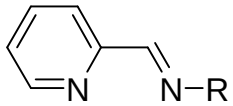

R=Et, n-Pr, n-Bu, n-Pen, n-Hex, n-Oct, n-Non, n-Octadec

Figure 12 - Schiff base ligands developed and used at by Haddleton *et al.* [32]

All the features mentioned make ATRP an attractive technique relative to anionic polymerisation which requires exceptionally pure reagents, very clean glassware along with low temperatures (often < –78°C) causing difficulty in industrial scale up for commercialisation. It also gives the molecular weight control which free radical processes do not have.[33] Unfortunately, ATRP does have several drawbacks. Transition metals tend to be difficult to remove from the final product which is consequently contaminated with the metal to some extent. Also, the presence of oxygen has an adverse effect on the metal catalyst causing the rate to be abnormally slow and so the evacuation of oxygen is an important part of this chemistry. The reactions are sensitive to acidic impurities which have a negative effect on the polymerisation.

ATRP can be described as living if the rate of termination/chain transfer events is equal to zero. In a living polymerisation there is a linear increase in the number average molecular weight (M_n) as conversion increases. The first order kinetic plot should also be linear, indicating a constant concentration of propagating species, Figure 13. Since there is the same concentration of radical species throughout the reaction and termination equals zero, after consumption of all the monomer, the chain end should still be active so that upon addition of a second portion of monomer, the chain will start growing again. These are the 3 classical tests for a living polymerisation.

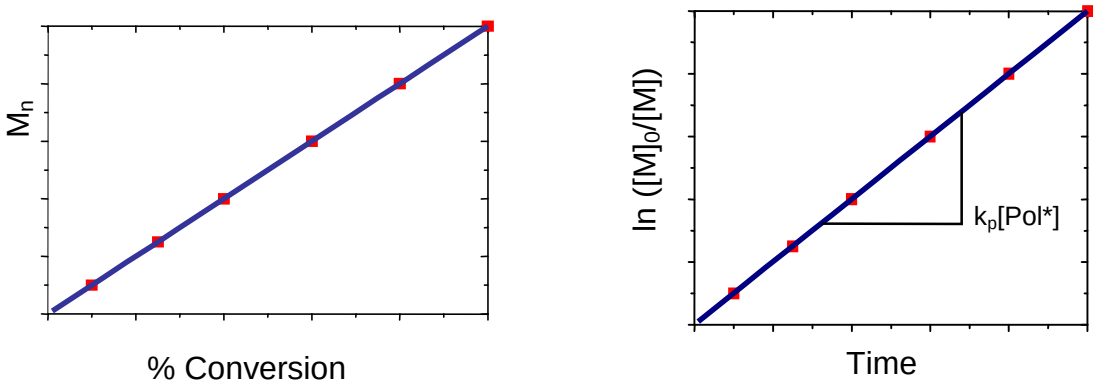

Figure 13 - The two graphs plotted to test for a living polymerisation, a first order kinetic plot and number average molecular weight (M_n) evolution with conversion of monomer

The constant concentration of propagating species is brought about by a redox equilibrium between oxidation states of the transition metal. The metal should have 2 accessible oxidation states separated by 1 formal charge, have good affinity for halogens and should have a coordination sphere that can expand to accommodate a halogen ligand.[34] In the case of copper, Cu(I)X (X = Br or Cl, usually Br) is added to the polymerisation. Homolytic cleavage of the C-X bond of the initiator results in a radical or radical-like species. The initiator is then able to initiate polymerisation. Ideally, the initiation is at least as fast as propagation and the transfer and termination negligible, therefore the number of growing chains is constant and equal to the original initiator concentration. When the rate of initiation is faster than or equal to the rate of propagation, the obtained polymers have narrow PDI (~1.1). The free halogen is then captured by the copper complex causing it to be oxidised to the Cu(II) state. The transfer of the halogen between the end-capped position on the end of the polymer chain and the copper complex is fast and the equilibrium such that termination is a minimum, Figure 14.

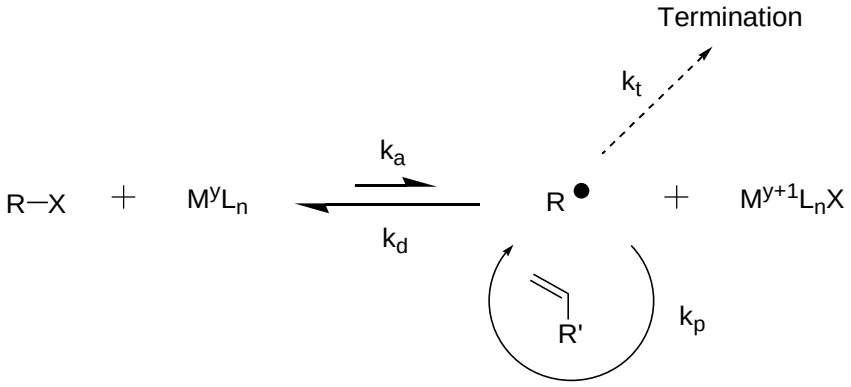

Figure 14 – A proposed mechanism of ATRP

There are cases where the rate of initiation is too fast e.g. amide initiators. This type of polymerisation commonly results in very low initiator efficiencies and slightly broader

PDIs.[35] The low efficiency causes the molecular weight to be much higher than predicted. Very little work has been done on how to increase the efficiencies of this type of initiators although work by Haddleton *et al.*[36] details how the due of a short induction period at ambient temperature and replacing Cu(I)Br with Cu(I)Cl reduces the rate of initiation and increases the efficiency of the initiator.

ATRP has been widely used to produce polymers that can be used for applications ranging from polymer-drug bioconjugates,[37] mucoadhesive polymers for drug delivery,[38] to conjugation to carbon nanotubes for numerous applications.[39] It has not, however, been widely used to produce polymeric additives for fuels or lubricating oils, specifically DVMs or VMs. Traditionally, free radical polymerisation has been used to produce polymers for use in fuels and lubricating oils. Using free radical polymerisation is relatively easy to approach 100% monomer conversion, it can be run in bulk and that there are low levels of volatile organics (VOC's) to remove post reaction.[33] However, polymers from free radical processes tend to have broad PDI (typically PDI > 2)[40] causing the bulk properties of the polymer to be less defined. There is also little architectural control. The strengths of ATRP have not been fully utilised as yet for commercial applications. Among the reasons for this are high metal (and to a lesser extent ligand) content in the product and an elevated concentration of halogens particularly in the lower molecular weight polymers. Halogens containing compounds that will be used in formulations that are handled by metallic devices such as pumps, tubing, containers or spraying devices can cause corrosion problems.[41]

Removal of the halogen end-group has been attempted by several approaches. Several were detailed by Haddleton *et al.* using a range of approaches.[42] Method 1 involves the homolysis of the ω-CBr bond with a subsequent reaction, via coupling or disproportionation, with an external radical species such as TEMPO. Organotin compounds can be used, specifically tributyltin hydride to remove the halogen leaving a hydrogen atom at the ω-terminus.[43] Method 2 utilizes monomers that are able to fragment after undergoing radical addition to the polymer chain such as trimethylsilyl enol ethers used as quenchers, previously reported by Sawamoto *et al.*[44] This reaction gives polymers with ω-ketone functionality and the corresponding trimethylsilyl halide as a by-product. Reaction with allyl bromide under similar conditions yields an allyl-functionalized polymer material as a result of its addition and subsequent fragmentation, that is, the elimination of a bromide radical. Method 3 involves the reaction of the polymer chain with ethylene. This results in the formation of a primary carbon-bromine bond which is much less reactive in ATRP. Method 4 is the reaction of a monomer that yields a relatively more stable secondary, or primary, carbon–halogen bond. This method also includes a patented method is the addition of a "limited polymerisable

carbon double bond containing compound or LPDP compound"[41] the resulting in a secondary carbon on the end of the polymer chain allowing elimination of HBr to occur.

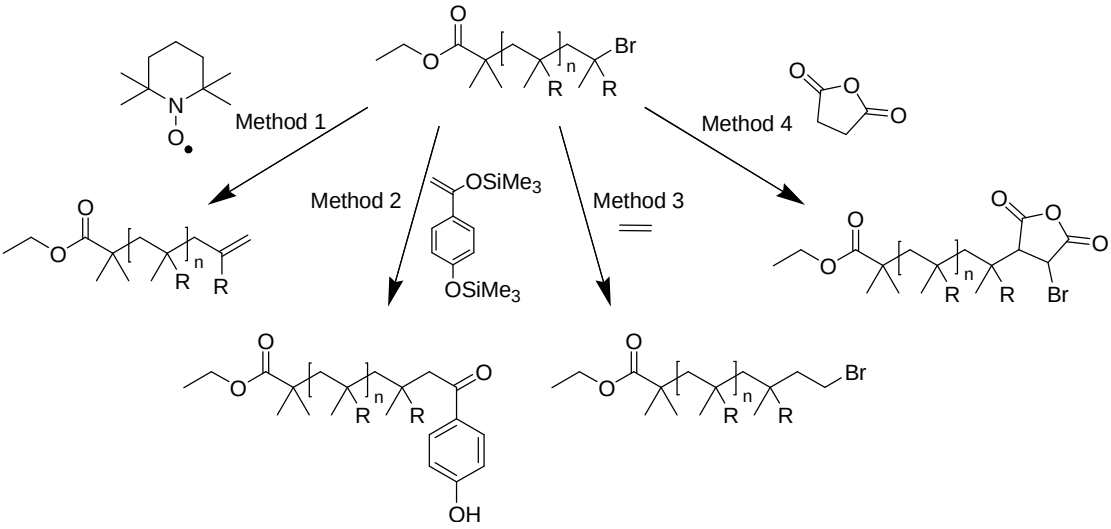

Figure 15 – Four techniques for the removal or reduction in reactivity, of the bromine end group which are detailed further in the text.

ATRP, as already described, can be carried out in bulk (absence of solvent), although does have ligand and copper to remove from the polymer before it can be used commercially. For gear oil applications the copper levels would have to be parts per million (ppm) as elevated copper levels are a sign of corrosion/degradation of the gears. Copper can be removed by bubbling the reaction mixture with air immediately following the polymerisation process whilst cooling. This aids oxidation of the Cu(I) to Cu(II) and precipitation of less soluble copper(II) salts. The reaction mixture is then passed over alumina, silica, ion exchange resins or activated carbon removing the copper.[63] In work by Dubois *et al.*[63] they showed the relative effectiveness of these different copper removal processes. They found that for poly(dimethyl aminoethyl methacrylate), which binds to copper, the most effective method was sulfonated ion exchange resin, although it was quite a slow process. After filtration, the polymer can be precipitated into, in the case of PMMA, methanol with 5% sulphuric acid which removes residual copper salts. This precipitation process has been developed and used exclusively at Warwick. However, the extensive work up required to remove the catalyst is both expensive and wasteful. The Schiff base ligands used at Warwick are not always easily removed and can give the polymers a yellow tinge.

In an attempt to find a catalyst that is homogeneous at reaction temperature, but insoluble at ambient temperature several groups varied their ligand structure. Poly(ethylene)-*block*-poly(ethylene glycol) (PE-PEG)[45] was used to support ligands by Shen *et al*. This was found to be insoluble below 70°C which is ideal for the majority of ATRP reactions. The PDIs were

< 1.2 and the catalyst showed good activity even after being recycled twice. Barré *et al*. took a different approach in that they used highly hydrophobic groups on their ligands to render them insoluble in highly polar media causing them to precipitate in high yield, ~97%.[46] They found that the copper concentration was approximately 200 ppm, ~190 ppm more than by filtering existing complexes with basic alumina.[49]

Other methods have been attempted to reduce the copper levels in the polymers made by ATRP. One approach was to attach the ligand onto a solid support.[47] This allows the ligand and most of the copper to be removed by a filtration process. However, when the solid supported ligand is reused, its activity drops reducing its effectiveness at catalysing the polymerisation.[47] The PDI also broadens to ~1.4. Although this is a good method for keeping the work-up of the polymers to a minimum, the advantages of ATRP are reduced by using the solid supported ligand and is therefore not as advantageous as anticipated. Duquesne *et al.* have attempted to optimise the conditions for using solid supported catalysts.[67] They investigated the effect of changing, among other factors the temperature of polymerisation, catalyst concentration, ligand, monomer concentration, ligand to catalyst molar ratio and the influence of catalyst recycling on further polymerisations. They found that although the PDI could be narrowed and good molecular weight control improved upon previous work, the polymerisations were still not as controlled as homogenous catalysts.

1.3.4 Industrial use of ATRP

A number of companies have taken advantage of the benefits of ATRP. RohMax Additives[48] has used it to synthesise copolymers which act as pour point depressants for lubricating oils. They polymerised using a 50:50 mixture of mineral oil:toluene as their solvent mixture to give molecular weight control and allow ease of handling of the end product.[49] This polymerisation process has also been used by CIBA Speciality Chemicals Inc[50] to synthesise phenolic antioxidants for fuels and lubricating oils.[51, 52] They take particular interest in block copolymers and end group modification to remove the halogen as they are undesirable in polymers for applications with high temperatures, since elimination of hydrogen halide may occur at elevated temperature.[52] The double bond formed is very sensitive to reactions with oxygen, which in the case of CIBA Speciality Chemicals antioxidants reduces their effectiveness. The hydrogen halide released may also react with other functionalities in the polymer such as ester groups present in acrylates giving unwanted side products which may decrease the performance of the product.[51] Although free radical processes are traditionally used to synthesise polymers for use as lubricating oil additives,[12] Lubrizol[53] has recently

started using several living radical polymerisations to synthesise high molecular weight multi-arm stars[54] for viscosity modifying applications. These processes include NMP, RAFT along with ATRP. They describe how linear polymers are made and then a cross linking agent, as discussed in more detail in chapter 3, is added causing star formation.

1.3.5 Monomer Selection

For this work certain monomers were chosen to give optimal performance as a VM. The three monomers used were $C_{12/15}$ methacrylate ($C_{12/15}$MA), *n*-butyl methacrylate (BMA) and 2-ethylhexyl methacrylate (EHMA), Figure 16. The $C_{12/15}$ MA is used to provide solubility in the oil, while the addition of either BMA or EHMA prevents the polymer solidifying when the longer alkyl chains co-crystallise with the wax in the lubricating oil at low temperature. The $C_{12/15}$MA is made from Neodol 25, an alkyl alcohol from Shell Chemicals and modified by Lubrizol to a methacrylate, Table 1 (2).

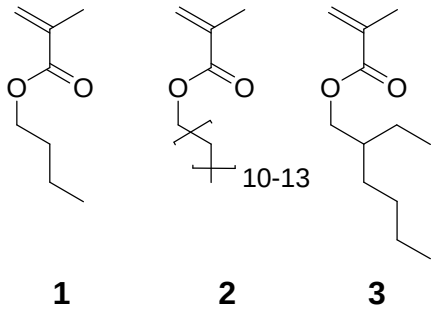

Figure 16 – Monomers used in this study, chosen to balance the low and high temperature properties. (1) *n*-butyl Methacrylate, (2) $C_{12/15}$ Methacrylate, (3) 2-ethylhexyl Methacrylate.

The ratio of monomers used for the synthesis of the stars was decided by Lubrizol. This ratio was 70 wt % $C_{12/15}$MA, 30 wt % BMA or EHMA (close to a 1:1 molar ratio), which is known to provide good viscosity-modifying properties at a wide range of temperatures.

Chain Length	Percentage of mixture
C11 and shorter	<1
C12	21
C13	29
C14	25
C15	25
C16 and longer	<1

Table 1 – The relative amounts of the different alcohols in Neodol 25[55]

The relative rates of polymerisations for these monomers are similar as demonstrated by their k_p in free radical polymerisation, Table 2. The data shows that the rates of propagation do not

change dramatically from MMA to dodecyl methacrylate (structurally closed to $C_{12/15}$ MA). Therefore a statistical copolymer is expected to be formed

Monomer	k_p L mol^{-1} s^{-1}	Reference
Methyl Methacrylate	1620	[56]
n-Butyl Methacrylate	1930	[57]
2-Ethylhexyl Methacrylate	2180	[58]
Dodecyl Methacrylate	2390	[76, 77]

Table 2 – The relative rates of propagation at 90°C in free radical polymerisation of several methacrylates.

2 References

1. I. Newton, *The mathematical principles of natural philosophy.*, printed for Benjamin Motte, London, Printed 1729.
2. E. W. Dean and G. H. B. Davis, *Chem. and Metall. Engng*, 1929, **36**, 618-9.
3. T. W. Selby, *ASLE*, 1958, **1**, 68-76.
4. S. Srinivasan, Y. S. Song, J. S. Strukl, P. Growcott, P. G. Griffin and A. Duggal, 2005-17288, 1637580, 2006.
5. M. J. Covitch, J. Weiss and I. M. Kreutzer, *Lubrication Science*, 1999, **11**, 337-64.
6. E. A. Bardasz and G. D. Lamb, *Chemical Industries*, 2003, **90**, 387-428.
7. S. Q. A. Rizvi, *Chemical Industries*, 2003, **90**, 137-70.
8. A. S. Oldfield and D. J. Irvine, WO2006054045, 2006.
9. K. Okada and R. Kaneshige, WO2000034420, 2000.
10. D. Vargo, D. Visger, B. Schober, S. Patterson, P. Mosier, C. Friend, J. Pudelski, M. J. Covitch, D. Price and et al., WO2005103093, 2005.
11. E. Ghzaoui, M. Lindheimer, A. Lindheimer, S. Lagerge and S. Partyka, *Colloids Surf., A*, 2004, **233**, 79-86.
12. C. J. Kolp, P. A. Lewis and J. G. Dietz, US6165235, 2000.
13. T. E. Nalesnik, US4863623, 1989.
14. B. A. Grisso, D. A. Hutchison and R. T. Dittmeier, EP1574559A1, 2005.
15. J. T. Loper and R. M. Sheets, US2005143265, 2005.
16. J. D. Burrington, S. L. Bartley, P. W. Pike and C. J. Kolp, WO2001098387, 2001.
17. M. J. Covitch, J. K. Pudelski, C. Friend, M. D. Gieselman, R. A. Eveland, M. G. Raguz and B. J. Schober, US2006025316, 2006.
18. J. N. Vinci, C. D. Tipton and R. W. Cain, WO2002083825, 2002.
19. T. S. Coolbaugh, F. C. Loveless, J. E. Marlin, II, D. N. Matthews and J. M. Klosek, WO2000034421, 2000.
20. B. P. Gracey and D. J. Moreton, EP889113, 1999.
21. M. J. Covitch, *Chemical Industries*, 2003, **90**, 293-327.
22. B. G. Kinker, *Chemical Industries*, 2003, **90**, 329-53.
23. M. Kato, M. Kamigaito, M. Sawamoto and T. Higashimura, *Macromolecules*, 1995, **28**, 1721-3.
24. J.-S. Wang and K. Matyjaszewski, *Journal of the American Chemical Society*, 1995, **117**, 5614-15.
25. T. Ando, M. Kamigaito and M. Sawamoto, *Macromolecules*, 1997, **30**, 4507-10.
26. K. Matyjaszewski, M. Wei, J. Xia and N. E. McDermott, *Macromolecules*, 1997, **30**, 8161-64.
27. P. Lecomte, I. Drapier, P. Dubois, P. Teyssie and R. Jerome, *Macromolecules*, 1997, **30**, 7631-33.
28. V. Percec, B. Barboiu, A. Neumann, J. C. Ronda and M. Zhao, *Macromolecules*, 1996, **29**, 3665-8.
29. C. Granel, P. Dubois, R. Jerome and P. Teyssie, *Macromolecules*, 1996, **29**, 8576-82.
30. K. Masami, A. Tsuyoshi and S. Mitsuo, *Chemical Reviews*, 2001, **101**, 3689-745.
31. J.-S. Wang and K. Matyjaszewski, *J. Am. Chem. Soc.*, 1995, **117**, 5614-15.
32. D. Haddleton, D. Duncalf, D. Kukulj, A. Heming, A. Shooter and A. Clark, *J. Mater. Chem.*, 1998, **8**, 1525-32.
33. K. Matyjaszewski and S. G. Gaynor, *App. Pol. Sci.*, 2000, 929-77.
34. K. Matyjaszewski and J. Xia, *Chem. Rev.*, 2001, **101**, 2921-90.
35. A. Postma, T. P. Davis, G. Moad and M. S. O'Shea, *React. Funct. Polym.*, 2006, **66**, 137-47.
36. A. Limer and D. M. Haddleton, *Macromolecules*, 2006, **39**, 1353-58.
37. F. Lecolley, L. Tao, G. Mantovani, I. Durkin, S. Lautru and M. Haddleton David, *Chem. Commun.*, 2004, 2026-7.
38. S. Keely, A. Rullay, C. Wilson, A. Carmichael, S. Carrington, A. Corfield, D. M. Haddleton and D. J. Brayden, *Pharm. Res.*, 2005, **22**, 38-49.
39. H. Kong, C. Gao and D. Yan, *J. Am. Chem. Soc.*, 2004, **126**, 412-13.
40. C. J. Hawker, A. W. Bosman and E. Harth, *Chem. Rev.*, 2001, **101**, 3661-88.
41. G. J. McCollum, J. B. O'Dwyer and S. Coca, WO9954365, 1999.
42. S. A. F. Bon, A. G. Steward and D. M. Haddleton, *J. Polym. Sci., Part A: Polym. Chem.*, 2000, **38**, 2678-86.

43. V. Coessens and K. Matyjaszewski, *Macromol. Rapid Commun.*, 1999, **20**, 66-70.
44. T. Ando, M. Kamigaito and M. Sawamoto, *Macromolecules*, 1998, **31**, 6708-11.
45. Y. Shen, S. Zhu and R. Pelton, *Macromolecules*, 2001, **34**, 3182-85.
46. G. Barre, D. Taton, D. Lastecoueres and J.-M. Vincent, *J. Am. Chem. Soc.*, 2004, **126**, 7764-65.
47. D. M. Haddleton, D. Kukulj and A. P. Radigue, *Chem. Commun.*, 1999, 99-100.
48. http://www.rohmax.com/en/oiladditives, Accessed 9th December 2005.
49. M. Scherer and J. Souchik, US6391996B1, 2002.
50. http://www.cibasc.com/, Accessed 9th December 2005.
51. B. Camenzind, P. Dubs, P. Haenggi, R. Martin, A. Muehlebach and F. Rime, WO2003095512, 2003.
52. B. Camenzind, P. Dubs, P. Hanggi, R. Martin, A. Muhlebach and F. Rime, US0272717A1, 2005.
53. http://corporate.lubrizol.com/, Accessed 12th June 2006.
54. D. Visger, M. Davies, D. Price, M. Baum and B. J. Schober, WO2006047398, 2006.
55. http://www.shell.com/home/content/chemicals/products_services/our_products/alpha_olefins_detergent_alcohols/neodol/product_data/neodol_product_data.html, Accessed 6th June 2009.
56. S. Beuermann, M. Buback, T. P. Davis, R. G. Gilbert, R. A. Hutchinson, O. F. Olaj, G. T. Russell, J. Schweer and A. M. Van Herk, *Macromol. Chem. Phys.*, 1997, **198**, 1545-60.
57. S. Beuermann, M. Buback, T. P. Davis, R. G. Gilbert, R. A. Hutchinson, A. Kajiwara, B. Klumperman and G. T. Russell, *Macromol. Chem. Phys.*, 2000, **201**, 1355-64.
58. R. A. Hutchinson, S. Beuermann, D. A. Paquet, Jr. and J. H. McMinn, *Macromolecules*, 1997, **30**, 3490-93.

Chapter 2

-

Core-first stars as viscosity modifiers synthesised by copper(I) mediated living radical polymerisation

Table of Contents

List of Figures

List of Tables

1 Introduction

1.1 Core First stars by copper(I) mediated living radical polymerisation (ATRP)

After the publication of the independent discovery of ATRP by Sawamoto[1] and Matyjaszewski[2] in 1995, a range of possible monomers and architectures was investigated by a number of groups across the world. Among this work, both Sawamoto and Matyjaszewski investigated multi-arm architectures. Similar structures had been previously synthesised by ionic polymerisation processes; which are not as tolerant to as wide a range of functional groups as living radical polymerisation and the initiators for these ionic systems are not as easily synthesised. This led to the publication of a number of articles by Sawamoto[3, 4] and Matyjaszewski[5] in 1998 describing the use of multiple arm, core first stars synthesised by ATRP.

Following these first publications, a number of groups demonstrated the wide range of molecules that can be transformed into ATRP initiators and used for successful polymerisation to form stars. They can be broken down into 4 broad categories; 1) halo-esters; 2) sulphonyl halides based; 3) (haloalkyl) benzenes; 4) miscellaneous.

1.2 Halo Ester Initiators

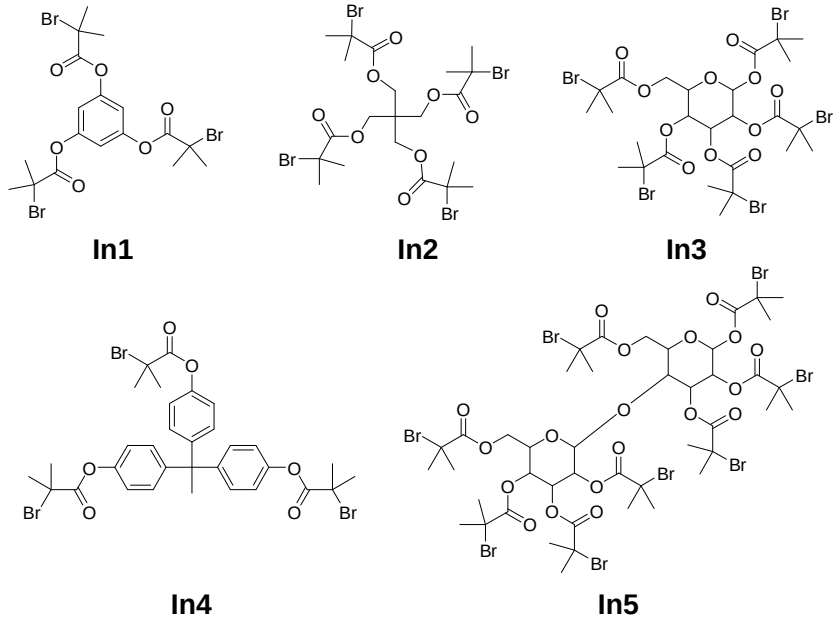

Figure 1 – Multi-arm organic halo-ester initiators for ATRP

The first of these initiators to be used as cores for ATRP stars were **In2** and **In4**, reported by Matyjaszewski *et al*.[6] In this work, they detailed the polymerisation of *n*-butyl acrylate or styrene using a Cu(I)Br di-nonyl bipyridine catalyst. The authors demonstrated how the polymerisations were of a living nature yielding well-defined polymers. Soon after, Haddleton and coworkers published on the use of phenolic initiators.[6] Of particular interest was the use of **In1**. Here the authors used Cu(I)Br in combination with *N*-(*n*-octyl)-2-pyridylmethanimine as catalyst for the polymerisation of methyl methacrylate and styrene. Using this initiator, they noted that while changing the halide to chlorine (and the copper salt to Cu(I)Cl) a drop in rate could be observed for the polymerisation of MMA. This drop could, however, not be observed when styrene was used as monomer, indicating that further optimisation of the MMA polymerisation is possible. The PDIs of the resulting polymers were found to be slightly broader for the chlorine initiator/catalyst system which may be of importance for certain applications. Also in 1999, Haddleton *et al.* published the use of glucose as a core for a five arm core first star polymer.[7] This initiator, **In3**, was used to polymerise both MMA and styrene, using a Cu(I)Br/ *N*-(n-pentyl)-2-pyridylmethanimine catalyst system. The glucose-based 5 arm initiator was later used by the same group to polymerise dimethylaminoethyl methacrylate (DMAEMA).[8] The high amine content was incorporated to give the polymer high muco-adhesion and was used to adhere to the outside of fish. DMAEMA polymers were also made using **In1** and **In5** to demonstrate that a range of star polymers with different numbers of arms would all muco-adhere.[8] **In5** was also used to synthesise polymers suitable for core-cross-linking to form reverse micelles. This work was by Lerourx and coworkers.[9] They polymerised glycidyl methacrylate which was then hydrolyzed to give di-alcohol functional monomer units. These were then partially esterified with alkyl groups to give a hydrophobic nature to the polymer, Figure 2. This polymer was cross-linked to give the micelle-like structure. The obtained structure may be of particular interest for drug delivery systems and potentially nanoreactors [9].

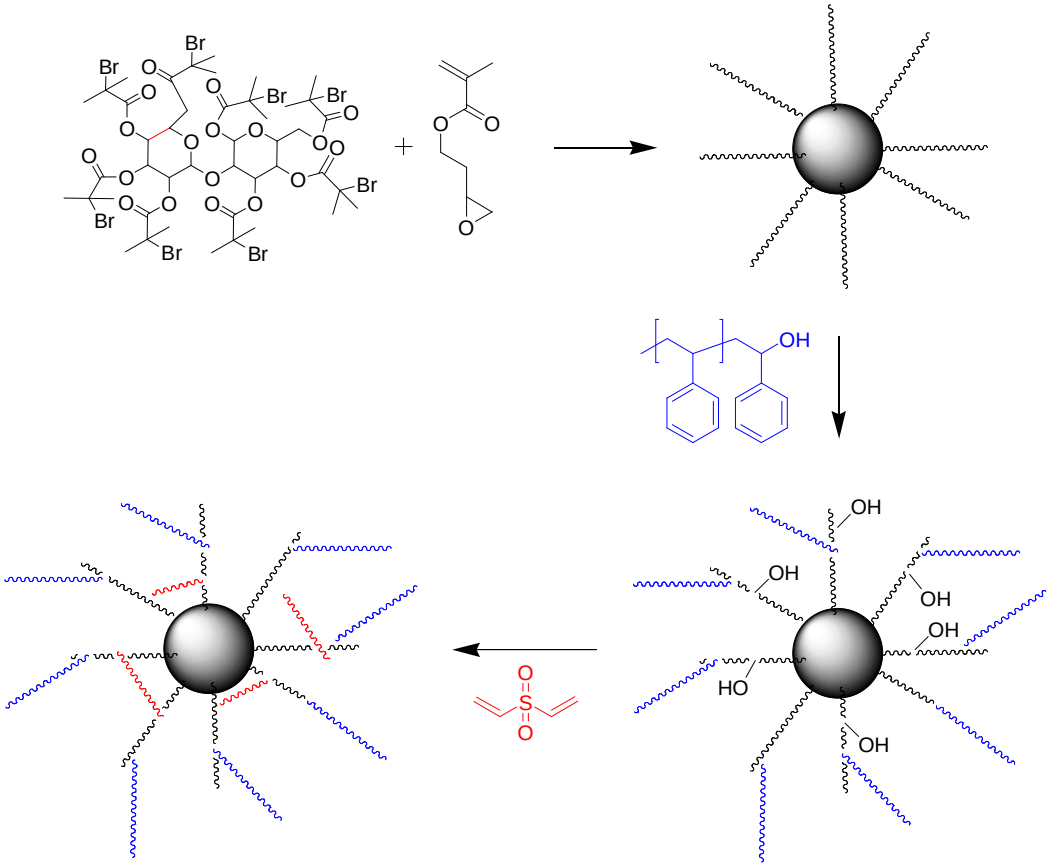

Figure 2 – Core-cross linked star polymers synthesised from **In5**.

1.3 (Haloalkyl) benzene initiators

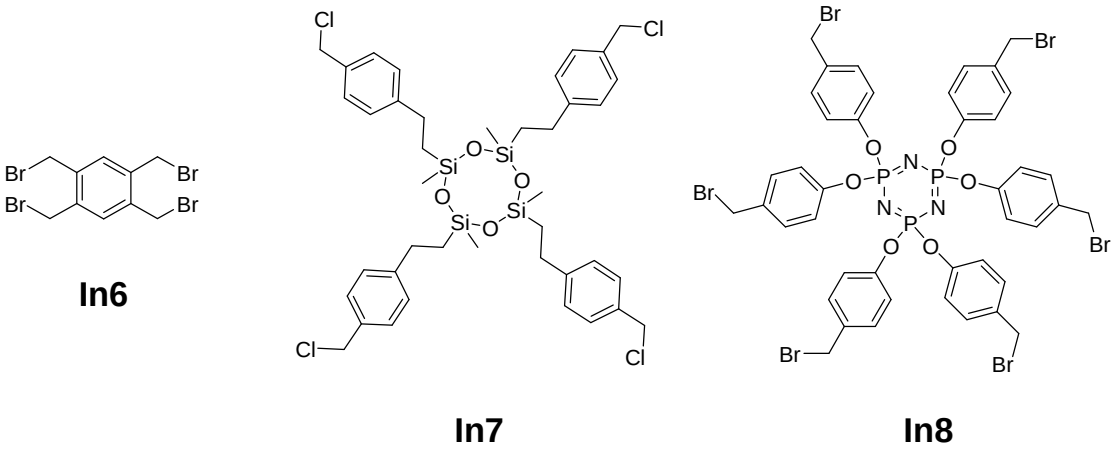

Figure 3 - Multi-arm organic and inorganic (Haloalkyl) benzenes initiators for ATRP.

In the range of initiators used by Matyjaszewski and coworkers in his original paper on core-first star polymers the synthesis of 4 and 6 arm stars based on **In7** and **In8,** respectively, was described.[10] The authors polymerised styrene, MA and *n*-BA with

high degrees of control and narrow molecular weight distributions. The authors furthermore suggest that these star polymers could find applications in areas such as "surfactants, viscosity modification, or adhesives technologies".[9] Later, Wang *et. al*. synthesised four arm stars using **In7** with MMA or styrene.[11] Due to the non-trivial nature of the synthesis of the initiators **In7** and **In8** they have not become as widely used as **In1**-**5**.

Matyjaszewski and coworkers published on their range of initiators for star polymers, Hadjichristidis *et al.*[12] published on the synthesis of four arm stars using the initiator **In6**. They used a Cu(I)Br/bipy catalyst system to polymerise MMA, *t*-BuMA and styrene. The same initiator was later used by Wu *et al.* to synthesise polymers of styrene or MMA.[13] These polymers were post-functionalised with C_{60} to give optical-limiting properties to the polymer. Optical limiters, as defined by the authors, are devices that strongly attenuate optical beams at high intensities while exhibit higher transmittance at low intensities.[13] They can be useful for protecting the human eye and optical sensors from intense laser beams. By attaching the C_{60} to the polymer the poor solubility and processability of the C_{60} is overcome.

1.4 Sulphonyl Chloride initiators

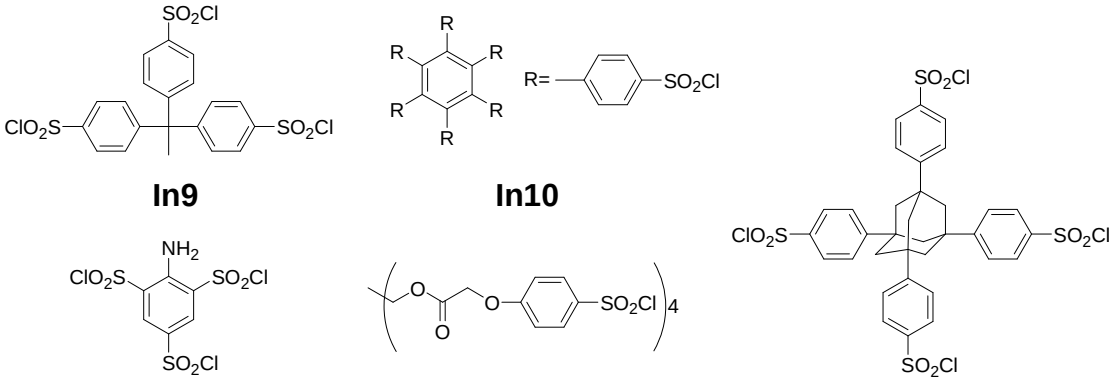

Figure 4 - Multi-arm organic sulphonyl chloride based initiators for ATRP.

This type of initiator was first used to polymerise linear polymers of styrene by Percec *et al.*[14] in 1995. The use of this type of mono-functional initiator led to the development of the corresponding multi-functional initiators, shown in Figure 4. First published of these were **In9**, **11** and **12** by Percec and co-workers.[15] In their report, they detailed the polymerisation of MMA or BMA using a Cu_2O/bipy catalyst system. Interestingly, the initiator **In12** is based on pentaerytritol showing how a core can be used to give a variety

of initiating systems. Soon after, the polymerisation of acrylonitrile, using a variety of catalyst systems, was detailed also by Percec and co-workers.[15] This polymerisation was initially carried out with mono-functional initiators, but later also using **In9**. The use of this type of initiator culminated in their use to form dendritic stars by the process coined Irreversible TERminator Multifunctional INItiator (TERMINI). Here, a three arm star based on **In9** was polymerised after which the chloro-functional end group reacted with the terminating agent,[16] Figure 5. The terminating agent can be made into a di-functional initiator for ATRP; meaning that each initial arm of the polymer now has a branching point and two further polymer chains growing from it. This process can be repeated, leading to the introduction of multiple branching points in the chain, yielding a dendritic polymer.

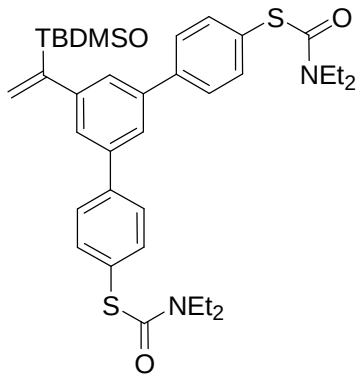

TERMINI

Figure 5 – The terminating agent, used by Percec *et al.*, which can be transformed into a di-functional initiator suitable for ATRP.[16]

The group of Robello also contributed to the development of multi-functional sulphonyl chloride initiators for ATRP. They demonstrated how a simple benzene moiety could be transformed into either a 5 or a 6 arm core suitable for use as an ATRP initiator,[17] such as **In10** and **13**. A range of monomers were polymerised from these initiators including MMA, *t*-BuMA, MA and styrene.

1.5 Shear Stability of Core First Stars

Some studies have been carried out as to the extent of shear stability depending on the nature of the core of the star. This is the permanent breaking of the chemical bonds in the polymer either by mechanical or chemical processes; in this case mechanical. Two different cores were compared to see if there was any noticeable shearing within the core depending on its structure, Figure 6. They showed that in the case of these polymers, the relative shear rates at the core were similar, being very low and the shear rate of the

arms once again similar, showing that the core has little effect on the shear rate.[18] The polymers had an M_w over 2×10^6 g mol^{-1}. They were exposed a high strain rate cross-slot flow cell under 1-5 bar pressure and pumped around varying number of cycles before being analysed. They found that although the cores did not break up, the arms were easily sheared. This is unexpected due to the difference in structures of the cores.

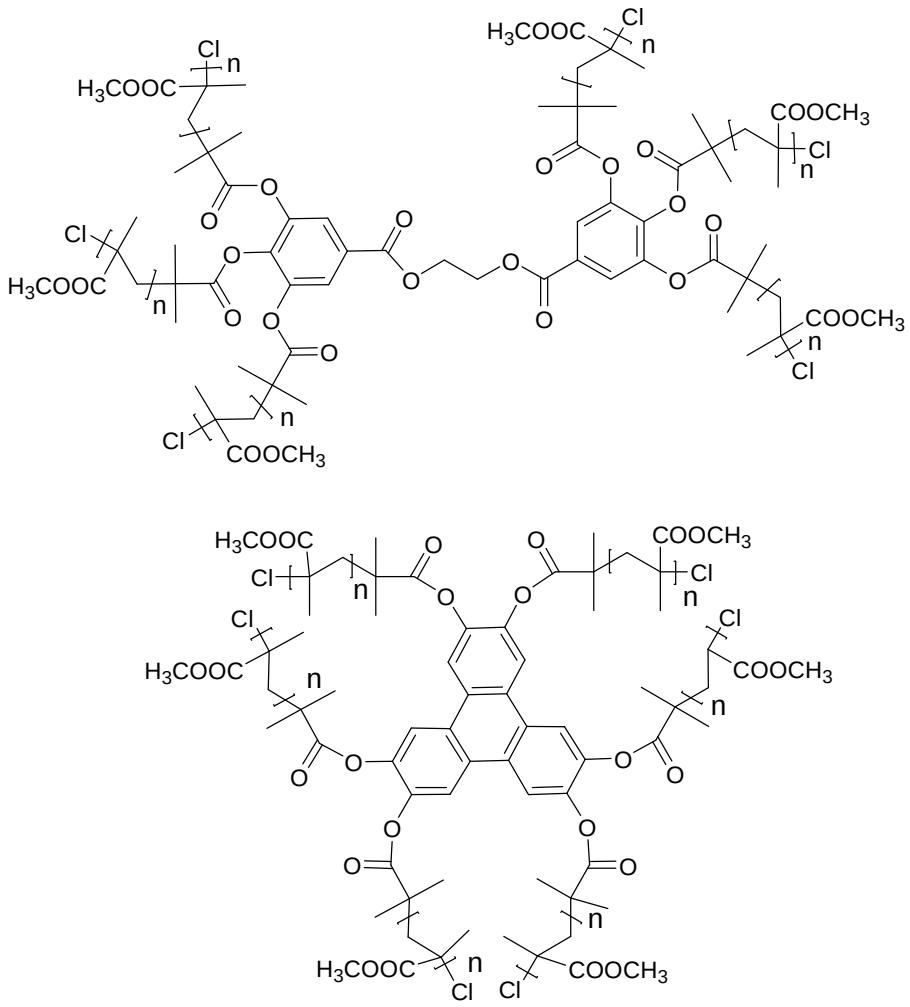

Figure 6 - Chemical Structures of the 6-arm PMMA stars compared for shear stability[18]

2 Results and Discussion

Although polymers have been used widely for a number of years as VMs,[19] the structure-activity relationships are not well documented in the literature. Therefore, a study was undertaken to investigate how a linear polymer compares to star polymers with varying numbers of arms. The effect of changing molecular weight of the polymers on the viscometric properties was also investigated. To this end, a series of polymers was synthesised and is documented in Table 1. The data obtained for these polymers would be compared to a linear VM commonly used by Lubrizol.

Total polymer $M_{n\ target}$ / g mol $^{-1}$	Number of arms
10000 and 20000	One
10000 and 20000	Three
10000 and 20000	Four
10000 and 20000	Five
10000 and 20000	Eight

Table 1 - Polymers synthesised to compare the effect of molecular weight and arm number on preformance as a VM

A core-first synthetic method was chosen as it allowed for a well-defined polymer to be made with a definite number of arms which could be varied by changing the initiator. The range of arm numbers were chosen to give a good cross-section of lower molecular weight stars. Increasing the amount of arms would mean that at higher than ~10 arms the M_n of each arm would be below that of the core and therefore the properties of the star may come from the core rather than the arms. Consequently, the number of arms was limited to 8.

Throughout this work it was noted that the theoretical value of M_n was different from the value obtained experimentally from GPC. This can be explained by the fact that the samples were measured against a PMMA calibration and that the samples were star polymers of different hydrodynamic volume to the linear standards. Both these factors combined to show that the GPC molecular weight data could only be used to suggest trends and give a guide to the M_n. However, GPC data from two separate systems were compared both the chloroform system used at Warwick and a THF GPC at Lubrizol. This data is included in Chapter 5.

2.1 Overview of the synthesis of core-first multi-arm star polymer

This section aims to provide a summary of the key points for the synthesis of the following core-first stars. Each synthesis is essentially identical with the initiator being changed to give a linear polymer or a star with a differing numbers of arms. The polymerisations used a Cu(I)Br/n-propyl-2-pyridiylmethanamine catalyst system. All the polymerisations were carried out at 90 °C in toluene at 50 % solids. They all exhibit linear first order kinetics shown in Figure 8, Figure 11, Figure 15, Figure 19 and Figure 23. The different initiators exhibit expected behaviour of the lower $M_{n\ target}$ giving a higher rate of reaction. This linear nature of the plot shows that there is a constant concentration of propagating chains in the reaction. The polymerisations also all have linear growth of molecular weight with conversion of monomer. This feature is indicative of living radical polymerisations Figure 9, Figure 12, Figure 16, Figure 20 and Figure 24.

To allow good structure-activity correlation, the polymerisations were monitored for star-star cross-linking to ensure that the polymers were mono-disperse with reference to the number of arms per star. Polymerisations were stopped at around 80 % monomer conversion to prevent star-star coupling. GPC analysis of the polymers indicated that no star-star coupling had occurred, as shown by the narrow PDI, Figure 13, Figure 17, Figure 21 and Figure 25. Although in certain cases polymerisations were left to proceed to about 90 % monomer conversion, star-star coupling could still not be observed. In all cases the PDI dropped as monomer conversion increased due to the percentage difference in the length of chains dropping as the chains grew towards their target M_n. All the polymerisations have a rapid build up of molecular weight in the first few minutes of the reaction while still at low monomer conversion. This is indicative of a rapid initiation step. The polymers were synthesised at two molecular weights, M_n=10,000 g mol^{-1} and M_n=20,000 g mol^{-1}. The difference in M_n should allow the comparison of change in VI against SSI as M_n increases. Linear polymers were synthesised to directly compare with the Lubrizol linear baseline chosen as the reference sample. They should show whether having a narrow PDI is sufficient to give an increase in VI without changing the architecture. It will also allow better correlation of the number of arms to VI performance.

The reactions yielded polymers with molecular weights that were, in the majority of cases, close to that targeted, Table 2. The five arm stars were both slightly higher than ideal but still within the molecular weight range for testing.

Number of Arms	Conversion % - ^{1}H NMR	$M_{n\ target}$ g mol^{-1}	$M_{n\ GPC}$ g mol^{-1}	$M_{n\ theoretical}$ g mol^{-1}	PDI
Linear	84	10000	7500	8400	1.17
Linear	83	20000	19800	16600	1.14
3	77	10000	11700	7700	1.08
3	74	20000	18900	14800	1.09
4	95	10000	8600	9500	1.14
4	86	20000	12000	17200	1.14
5	81	10000	15300	8100	1.14
5	75	20000	26200	15000	1.12
8	95	10000	10800	9500	1.15
8	87	20000	12300	17400	1.09

Table 2 - An overview of the core-first stars synthesised by ATRP

The reactions shown were carried out in a 2 L jacketed reactor to give sufficient material for viscosity testing, for which about 500 g of polymer is required. A small induction period could be noted for all the polymerisations. This is most likely due to the large quantity of monomer being added last to the reaction flask at room temperature and the resulting reaction mixture taking a few minutes to heat up to the required temperature of 90 °C.

2.2 Synthesis of the linear polymers

2.2.1 Synthesis of the 4-Methylphenyl 2-bromoisobutyrate initiator

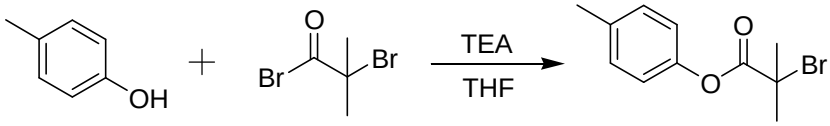

Figure 7 – Synthesis of the initiator based on 4-methyl phenol using the ratios [phenol]:[acid bromide]:[TEA] – [1.2]:[1]:[1.5].

The initiator for the linear polymers was synthesised from 4-methyl phenol in good yield (95%). The product was isolated by washing with sodium hydrogen carbonate solution to remove the excess phenol. The aromatic ring has the added benefit of the ^{1}H NMR peaks corresponding to the initiator being significantly different to that of the polymers that will be synthesised from it and thus will potentially allow determination of molecular weight from ^{1}H NMR, should they be visible. The methyl group on the aromatic ring should also be visible in the ^{1}H NMR spectrum. Phenolic initiators are well known in the literature for having high initiator efficiencies and are therefore ideal for the careful targeting of particular molecular weight polymers.[6]

2.2.2 Synthesis of the Polymers

The ATRP of the mixture of $C_{12/15}$ MA and *n*-BMA was undertaken at 90°C using the 4-methyl phenol based initiator shown above. The reactions were complete in less than four hours. Reactions were controlled as described above in the section 2.1. The polymerisations vary in the initiator:monomer ratio. The reaction targeting M_n=10K g mol^{-1} has twive the amount of initiator than the reaction targeting M_n=20K g mol^{-1}. Therefore the relative rates should be a factor of two different. However, when the initiator concentration is doubled, the reaction rate only increased from Kp=0.0073 min^{-1} to 0.012 min^{-1}. The rapid increase of molecular weight at the start of the reaction is most likely due to the low concentration of Cu(II) in the reaction. At this time, the persistent radical effect suggests that some bimolecular termination of the initiator or oligomeric species is happening to produce the Cu(II) which leads to greater control at later stages in the polymerisation.

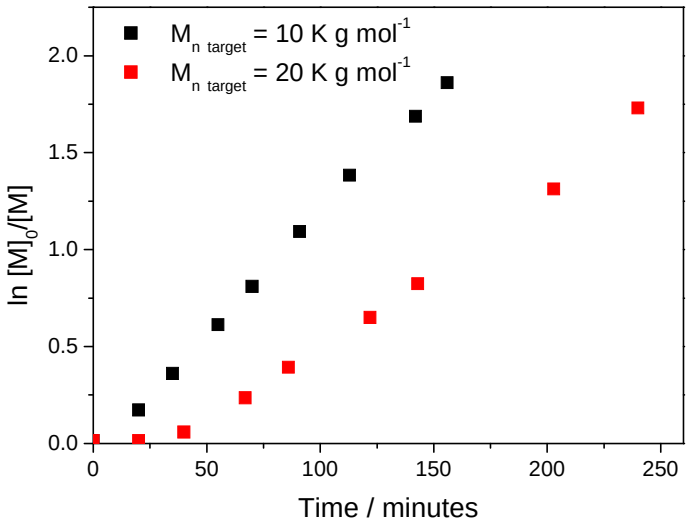

Figure 8 - First order kinetic plot for the synthesis of the linear $C_{12/15}$ MA/*n*-butyl methacrylate copolymer. [$C_{12/15}$ MA]:[*n*-BMA]:[Ligand]:[$Cu^{I}Br$]:[Initiator] - [51]:[42]:[2.1]:[1]:[1] (red), [25]:[21]:[2.1]:[1]:[1] (black) 90°C, 50% solids in toluene solution.

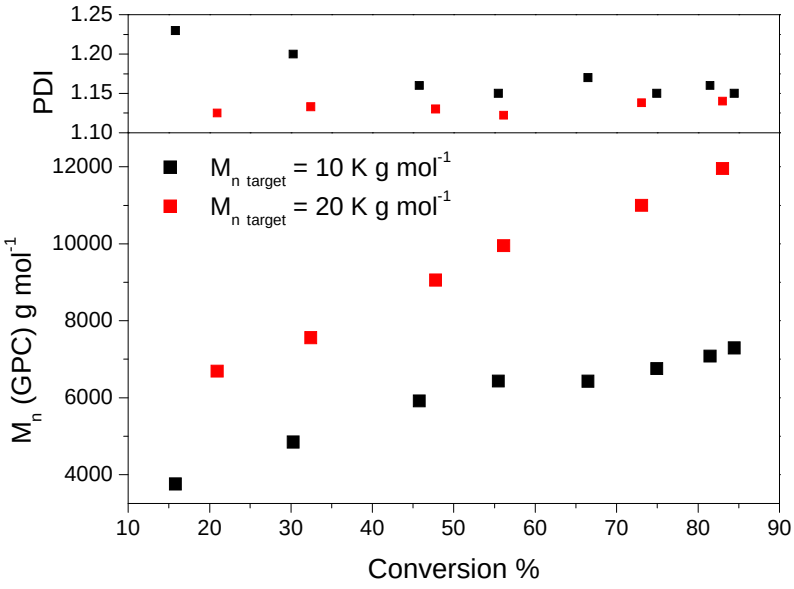

Figure 9 - M_n and PDI versus conversion for the co-polymerisation of $C_{12/15}$ MA and *n*-butyl methacylate**.** [$C_{12/15}$ MA]:[*n*-BMA]:[Ligand]:[$Cu^{I}Br$]:[Intiator] - [51]:[42]:[2.1]:[1]:[1] (red), [25]:[21]:[2.1]:[1]:[1] (black) 90°C, 50% solids in toluene solution.

2.3 Synthesis of a three arm star polymer

2.3.1 Synthesis of three arm initiator

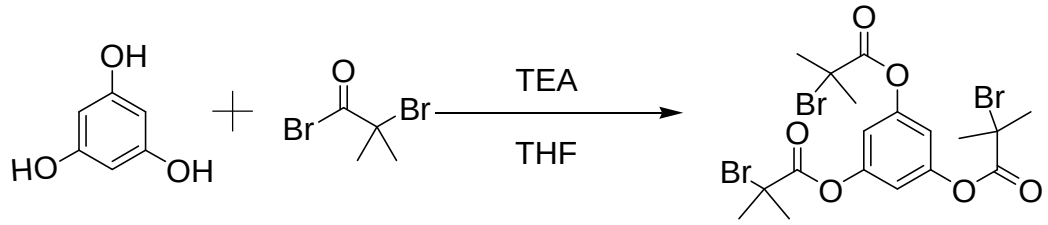

Figure 10 - Synthesis of a 3 arm initiator based on 1,3,5-benzenetriol using ratios [triol]:[acid bromide]:[TEA] - [1]:[3.3]:[3.3]

The three arm initiator was synthesised from a tri-functional benzene moiety in good yield (>85%). The product was isolated by recrystallisation from methanol with a high degree of purity achieved. The aromatic ring has the added benefit of the peaks on the initiator being significantly different to that of the polymers that will be synthesised from it and will potentially allow determination of molecular weight from ^{1}H NMR should they be visible.

2.3.2 Synthesis of the Polymers

Polymerization of the mixture of $C_{12/15}$ MA and *n*-BMA was undertaken at 90°C using the 1,3,5-benzenetriol based initiator, figure 10. The reactions were complete in less than three hours. Reactions were controlled as described above in the section 2.1. As with the linear polymer synthesis in section 2.2, the rate of polymerisation does not double when the amount of initiator is doubled. Here the rate increases from Kp=0.01 min^{-1} to 0.015 min^{-1} when changing the targeted M_n from 20 K g mol^{-1} to 10 K g mol^{-1}.. These polymers demonstrate how the GPC gives incorrect results for star polymers. The plot of M_n versus monomer conversion shows how both polymers, targeting different molecular weights have given very similar plots. This is unexpected and could be due to the change in hydrodynamic volume when changing the targeted M_n.

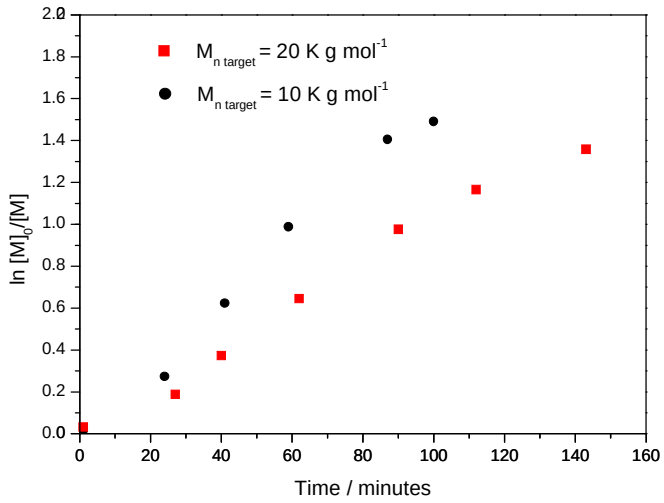

Figure 11 - First order kinetic plot for the synthesis a 3 arm star $C_{12/15}$ MA/*n*-butyl methacrylate copolymer**.** [$C_{12/15}$ MA]:[*n*-BMA]:[Ligand]:[$Cu^{I}Br$]:[Initiator] - [51]:[42]:[2.1]:[1]:[1] (red), [25]:[21]:[2.1]:[1]:[1] (black) 90°C, 50% solids intoluene solution.

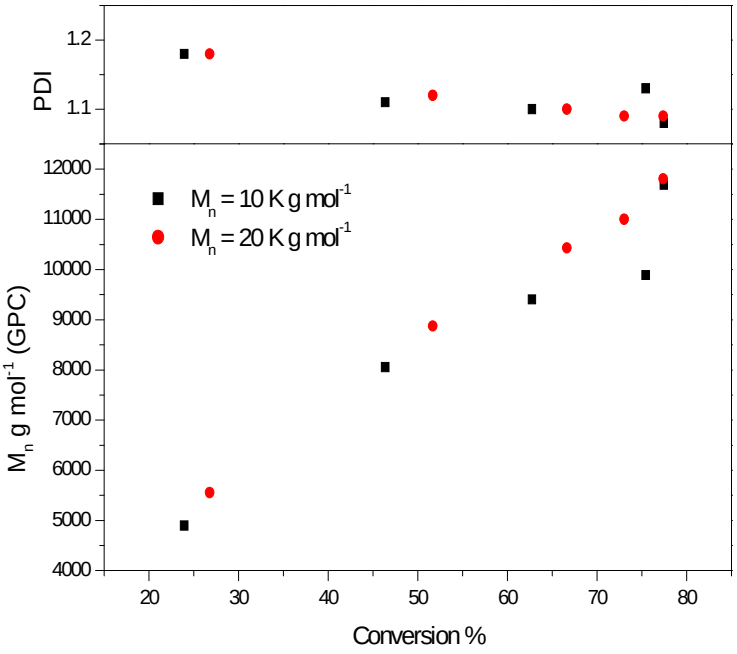

Figure 12 - M_n and PDI verus conversion for the co-polymerisation of $C_{12/15}$ MA and *n*-butyl methacylate. [$C_{12/15}$ MA]:[*n*-BMA]:[Ligand]:[$Cu^{I}Br$]:[Intiator] - [51]:[42]:[2.1]:[1]:[1] (red), [25]:[21]:[2.1]:[1]:[1] (black) 90°C, 50% solids, toluene solution.

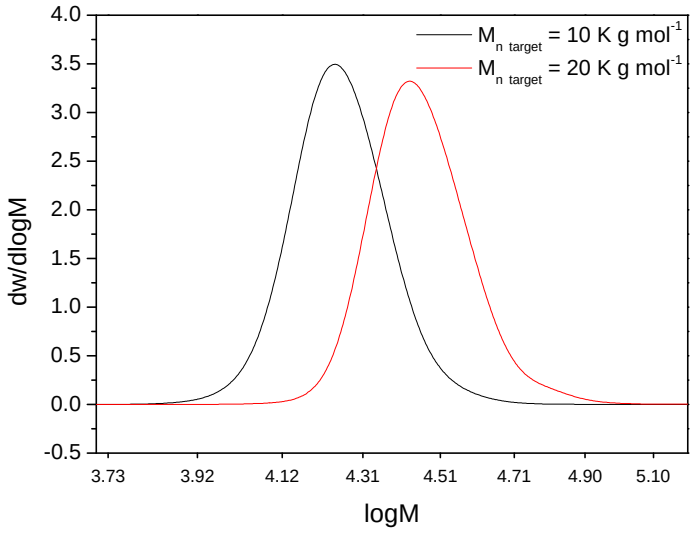

Figure 13 - Normalised GPC trace showing the difference between the two 3 arm star polymers made. It can be seen that there are no tailing effects to lower or higher molecular weight

2.4 Synthesis of a four arm star polymer

2.3.3 Synthesis of a four arm initiator

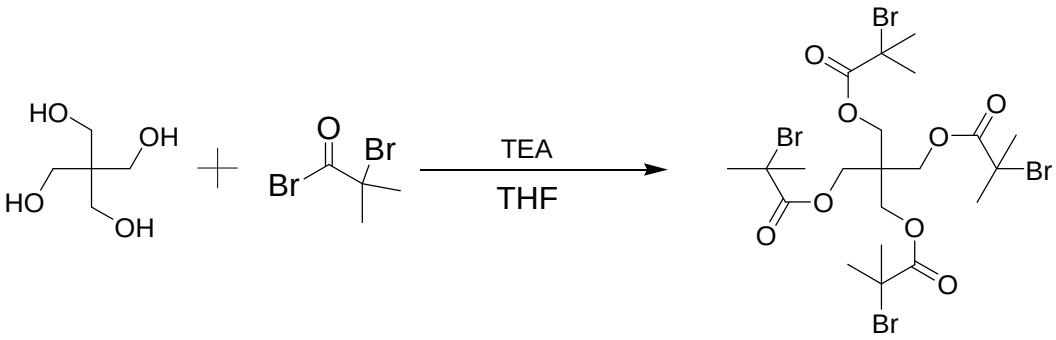

Figure 14 - Synthesis of a four arm initiator based on pentaerytritol using the ratios – [pentaerytritol]:[acid bromide]:[TEA]-[1]:[4.4]:[4.4].

The synthesis of the four arm initiator based on pentaerytritol yielded product with high purity but a low yield (50%). This was attributed to the poor solubility of the pentaerytritol in THF; however, switching solvent to DCM did not give a higher yield. The product was isolated by recrystallisation from methanol. Sufficient product was obtained for the synthesis of the polymers and therefore optimisation was not attempted.

2.3.4 Synthesis of the Polymers

The ATRP of the mixture of $C_{12/15}$ MA and *n*-BMA was undertaken at 90°C using the pentaerytritol based initiator shown above. The reactions were complete in less than three hours. Reactions were controlled as described above in the section 2.1. The relative rates of polymerisation here vary considerably. When targeting M_n=10 K g mol^{-1} the Kp=0.037 min^{-1}. By halving the initiator concentration to target M_n=20 K g mol^{-1} the rate drops to Kp=0.013 min^{-1}. This is a drop of a factor of 3, which is unexpected.

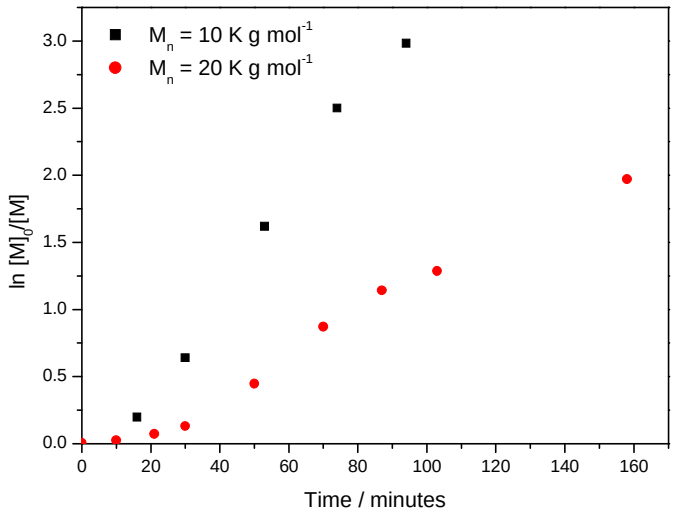

Figure 15 - First order kinetic plot for the synthesis a 4 arm star $C_{12/15}$ MA/n-butyl methacrylate copolymer**.** [$C_{12/15}$ MA]:[*n*-BMA]:[Ligand]:[Cu^{I}Br]:[Initiator] - [59]:[49]:[2.1]:[1]:[1] (red), [30]:[25]:[2.1]:[1]:[1] (black) 90°C, 50% solids in toluene solution.

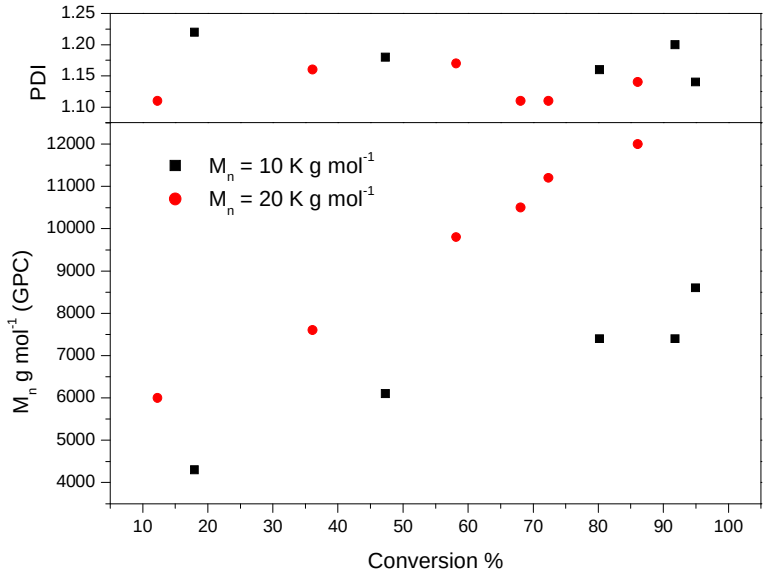

Figure 16 - M_n and PDI verus conversion for the co-polymerisation of $C_{12/15}$ MA and *n*-butyl methacylate**.** [$C_{12/15}$ MA]:[*n*-BMA]:[Ligand]:[Cu^{I}Br]:[Initiator] - [59]:[49]:[2.1]:[1]:[1] (red), [30]:[25]:[2.1]:[1]:[1] (black) 90°C, 50% solids, in toluene solution.

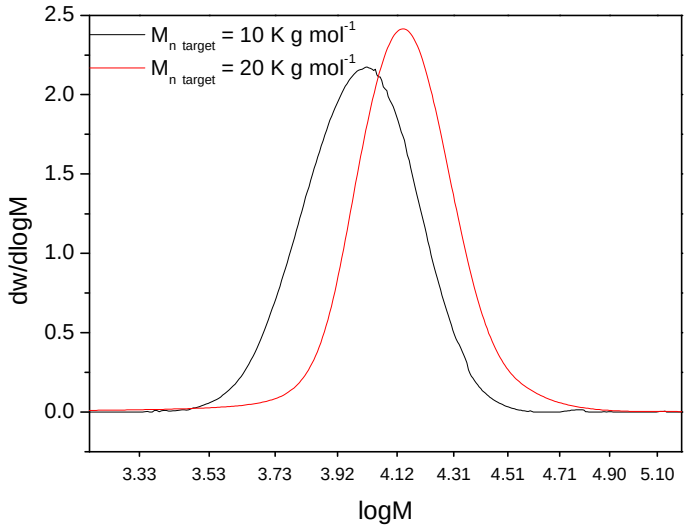

Figure 17 - Normalised GPC trace showing the difference between the two 4 arm star polymers made. It can be seen that there are no tailing effects to lower or higher molecular weight.

2.4 Synthesis of a five arm star polymer

2.4.1 Synthesis of the five arm initiator

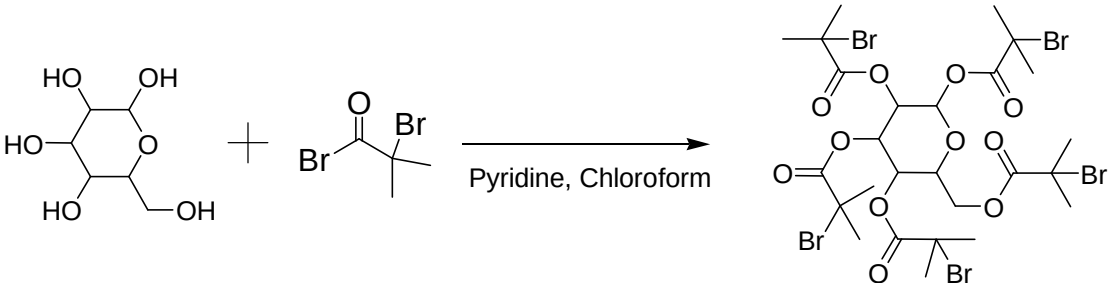

Figure 18 - Synthesis of a 5 arm initiator based on glucose in a 50:50 (v:v) mixture of pyridine and solvent using the ratios – [glucose]:[acid bromide] – [1]:[5.5].

The initiator was synthesised in good yield, 78%, with a high degree of purity. It was isolated by recrystallisation from methanol to give the desired product. Unfortunately, using this initiator for polymerisation it is problematic to obtain accurate molecular weight data for the polymer by ^{1}H NMR, since the peaks corresponding to the initiator, which are not overlapping those of the polymer in the spectrum, are very weak and not easily identified.

2.4.2 Synthesis of the Polymers

Polymerisation of the mixture of $C_{12/15}$ MA and *n*-BMA was undertaken at 90°C using the glucose based initiator shown above. The reactions were complete in less than three hours. Reactions were controlled as described above in the section 2.1. The observed rate of polymerisation only changes slightly for these two reactions. By halving the initiator concentration, the rate decreases from Kp=0.015 min^{-1} to 0.010 min^{-1}. This is similar to the linear polymer synthesis and the 3 arm stars where the rate of polymerisation also only varied a little..

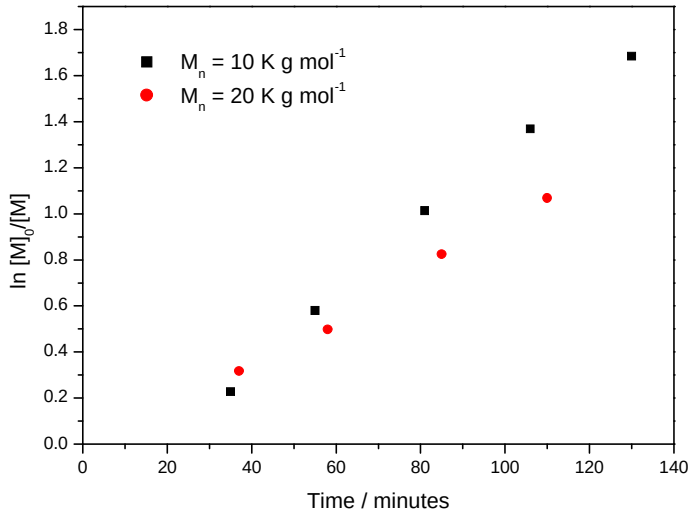

Figure 19 - First order kinetic plot for the synthesis a 5 arm star $C_{12/15}$ MA/*n*-butyl methacrylate copolymer**.** [$C_{12/15}$ MA]:[*n*-BMA]:[Ligand]:[$Cu^{I}Br$]:[Initiator] - [51]:[42]:[2.1]:[1]:[1] (red), [25]:[21]:[2.1]:[1]:[1] (black) 90°C, 50% solids in toluene solution.

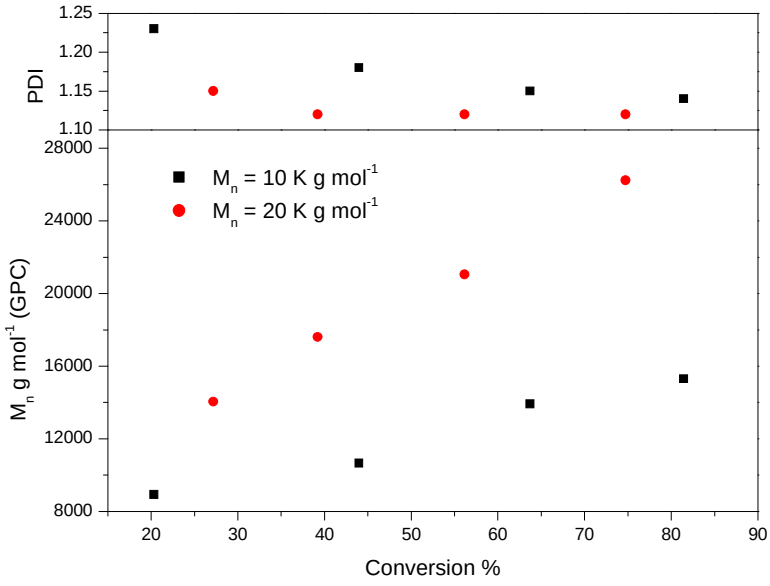

Figure 20 - M_n and PDI verus conversion for the co-polymerisation of $C_{12/15}$ MA and *n*-butyl methacylate**.** [$C_{12/15}$ MA]:[*n*-BMA]:[Ligand]:[$Cu^{I}Br$]:[Initiator] - [51]:[42]:[2.1]:[1]:[1] (red), [25]:[21]:[2.1]:[1]:[1] (black) 90°C, 50% solids, in toluene solution.

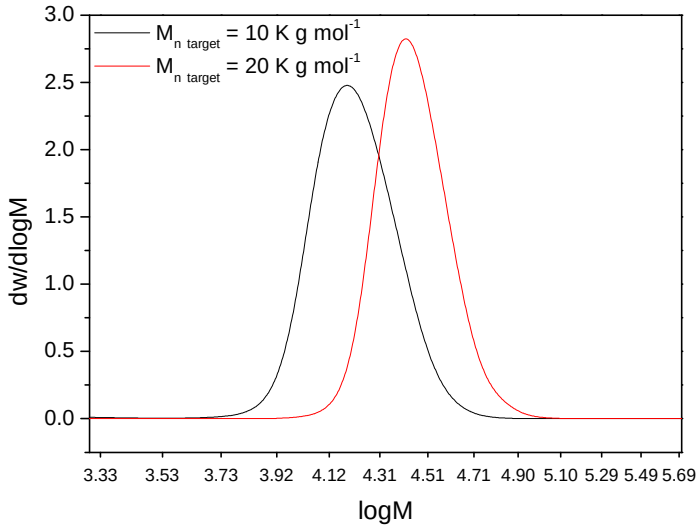

Figure 21 - Normalised GPC trace showing the difference between the two 5 arm star polymers made. It can be seen that there are no tailing effects to lower or higher molecular weight.

2.5 Synthesis of an eight arm star polymer

2.5.1 Synthesis of an eight arm initiator

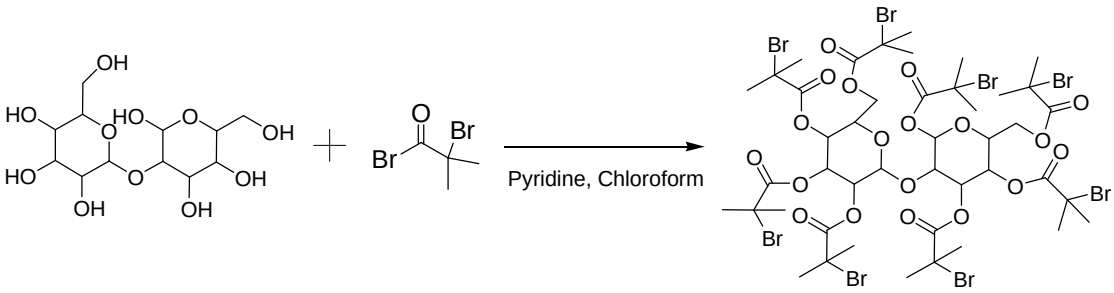

Figure 22 - Synthesis of an eight arm initiator based on lactose using ratios - [lactose]:[acid bromide] - [1]:[8.8]

The synthesis of this eight arm initiator gave very low yields, 15%, which was unsatisfactory and significantly lower than in the literature.[8] However, sufficient amounts of product were obtained to carry out the necessary polymerisation and therefore further optimisation was not attempted. The product obtained was of a high degree of purity and suitable for use in the polymerisations.

2.5.2 Synthesis of the Polymers

Polymerisation of the mixture of $C_{12/15}$ MA and *n*-BMA was undertaken at 90°C using the lactose based initiator shown above. The reactions were complete in less than two hours. Reactions were controlled as described above in the section 2.1. The rates of polymerisation vary as expected with initiator concentration. When targeting M_n=10 K g mol^{-1}, the rate is Kp=0.050 min^{-1}. This drops to Kp=0.022 min^{-1} when targeting M_n=20 K g mol^{-1}. This is close to the expected drop when halving the initiator concentration.

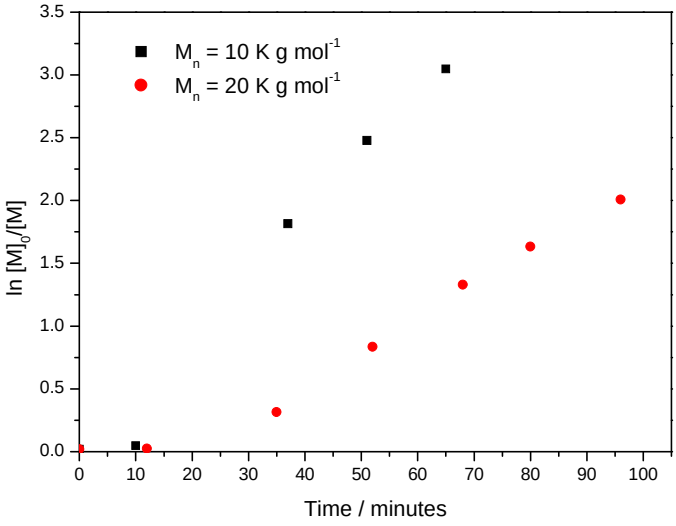

Figure 23 - First order kinetic plot for the synthesis a 8 arm star $C_{12/15}$ MA/*n*-butyl methacrylate copolymer**.** [$C_{12/15}$ MA]:[*n*-BMA]:[Ligand]:[$Cu^{I}Br$]:[Initiator] - [51]:[42]:[2.1]:[1]:[1] (red), [25]:[21]:[2.1]:[1]:[1] (black) 90°C, 50% solids.

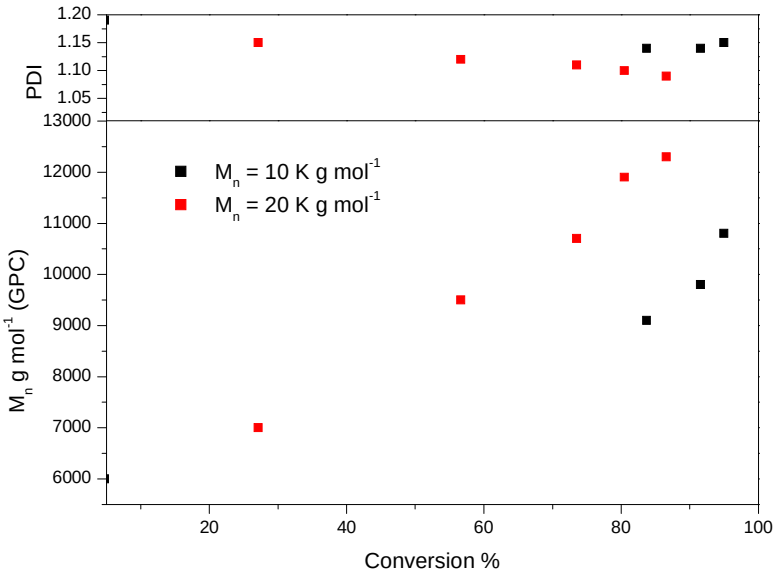

Figure 24 - M_n and PDI verus conversion for the co-polymerisation of $C_{12/15}$ MA and *n*-butyl methacylate to form an 8 arm star polymer**.** [$C_{12/15}$ MA]:[*n*-BMA]:[Ligand]:[$Cu^{I}Br$]:[Initiator] - [51]:[42]:[2.1]:[1]:[1] (red), [25]:[21]:[2.1]:[1]:[1] (black) 90°C, 50% solids.

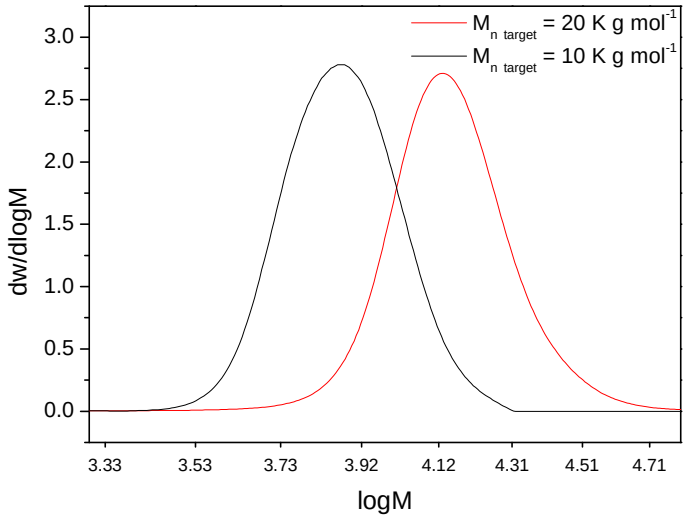

Figure 25 - Normalised GPC trace showing the difference between the two 8 arm star polymers made. It can be seen that there are no tailing effects to lower or higher molecular weight.

2.6 Discussion of results.

These results demonstrate how the rate of polymerisation does not always vary in the expected way with initiator concentration. A number of other factors could affect this such as: catalyst concentration, temperature and the presence of oxygen. These are all controlled to the greatest degree of accuracy possible; however the actual reason is unknown at this stage.

3 Conclusions

A library of polymers with varying number of arms from 3 to 8 have been synthesised by a core first approach. The polymerisations were found to be controlled with PDIs; below 1.3 in all cases and molecular weights found to be close to that predicted. The polymerisations were found to be suitable for scale up from the 5 g scale for kinetic experiments, to the 2 L scale for the synthesis of samples for viscosity testing. The scaled up reactions exhibited the same living characteristics as the smaller scale reactions.

The polymers were analysed by GPC using a DRI detector. These results demonstrate that this method of obtaining molecular weights of star polymers is not accurate enough to give absolute values. They do give trends in molecular weights however. In order to obtain more accurate molecular weight data other detectors would be needed such as a multi-angle light scatterer or a viscometer. These detectors may allow a more accurate determination of molecular weight. ^{1}H NMR could have been used as previously discussed to calculate the molecular weight. However, the initiator peaks could be seen, and therefore no molecular weights could be calculated.

4 Experimental

4.1 Materials and Instrumentation

All reagents were purchased from Aldrich, with the exception of $C_{12\text{-}15}$ MA which was provided by the Lubrizol Corporation (based on Neodol 25). All solvents were purchased from Fisher Chemicals. Monomers were degassed with N_2 for 45 minutes prior to use. Toluene was also degassed with N_2 for 45 minutes prior to use. All other reagents and solvents were used as received. Gel Permeation chromatography (GPC) was carried out using a Polymer Laboratories (PL) modular system equipped with a differential refractive index (DRI) detector calibrated with linear poly (methyl methacrylate) (PMMA) standards (M_p = 200–1.577×10^6 g mol^{-1}). The mobile phase used was 95% $CHCl_3$, 5% triethylamine and the elution time was standardised against toluene with a flow rate of 1.0 mL min^{-1}. The system was equipped with a PL-gel 5 μm (50 · 7.5 mm) guard column and two PL-gel 5 μm (300 · 7.5 mm) mixed C columns. Samples were compared against narrow standards of poly(methyl methacrylate), M_p = 200 to 1.577 ×10^6 g mol^{-1}, obtained from Polymer Laboratories, except for the methyl methacrylate dimer, trimer and tetramer which were prepared by catalytic chain transfer at the University of Warwick. ^1H and ^{13}C NMR spectra were recorded on a Bruker DPX400 spectrometer using deuterated solvents from Aldrich. UV-VIS spectra were recorded on a Perkin Elmer Lambda 25 spectrophotometer. Infra red absorption spectra were recorded on a Bruker Vector 22 spectrometer equipped with a Golden Gate diamond attenuated total reflection (ATR) sample platform.

4.2 Copper mediated living radical polymerisation – General procedure

All polymerisation were carried out using either Schlenk apparatus or a 3 necked round bottomed flask – whichever was more appropriate – under dry nitrogen. Typically, all solids were added to the pre-dried reaction vessel prior to sealing with a rubber septum. The vessel was then either purged with nitrogen, in the case of the round bottomed flask, or evacuated and flushed with nitrogen three times, in the case of the Schlenk tubes, so as to remove oxygen. All remaining liquid reagents, apart from the ligand, which had previously been deoxygenated with nitrogen, were added to the reaction vessel via dried, degassed syringes and the mixture further deoxygenated by three freeze-pump-thaw cycles. The reaction vessel was brought up to reaction temperature in a stirred,

thermostated oil bath and the deoxygenated ligand added. Samples for kinetic data were taken using degassed syringes and polymer conversion data obtained by ^{1}H NMR. Molecular weight data was obtained from GPC. Reactions were stopped by exposure to air and by further dilution in the reaction solvent. Polymers were typically purified by stirring with basic alumina to remove the copper and then filtered over a bed of celite to remove the solids. The dilute polymer-solvent mixture was concentrated *in vacuo* and precipitated by stirring in IPA:methanol (9:1) for 1 hour before cooling using a dry-ice acetone mixture to cause precipitation of the polymer. The IPA-methanol mixture was decanted off and the viscous polymer and washed with cold IPA (approximately 100 ml × 3) Polymers were collected after precipitation as a viscous liquid and dried in a vacuum oven at 40°C overnight.

4.3 Purification of copper (I) bromide

Copper(I) bromide was purified by a method based on that of Keller and Wycoff.[20] Typically copper(I) bromide (50 g, 0.35 mol) was placed in a large beaker and the solid washed with glacial acetic acid (300 ml), absolute ethanol (300 ml) and anhydrous diethyl ether (300 ml) ensuring that the copper species was exposed to oxygen for the minimum time possible. 38.2 g of a off-white coloured powder was obtained and dried at 100°C under vacuum overnight.

4.4 Synthesis of *N*-Propyl-2-pyridiylmethanamine

N-Propyl amine (126 g, 1.77 mol) was slowly added drop wise to a stirred solution of pyridine-2-carboxaldehyde (190 g, 2.15 mol) in diethyl ether (ca. 600 ml) at 0 °C and stirred for four hours. Dried magnesium sulphate (ca. 100 g) was added and the solution stirred at ambient temperature for two hours. The solution was filtered and the solvent removed *in vacuo* to yield an orange oil. This oil was distilled under reduced pressure to yield N-n-propyl-2-pyridyl-methanimne as a clear yellow liquid (boiling range 77-79 °C at 10^{-1} Torr). Obtained 158.21 g (60%).

^{1}H NMR δ (ppm) - 8.63 (d, 1H, Pyr-H), 8.39 (s, 1H, Pyr-CH=N-), 8.00 (d, 1H, Pyr-H), 7.69 (t, 1H, Pyr-H), 7.27 (t, 1H, Pyr-H), 3.64 (t, 2H, *J* = 4.4 Hz, -C=N-C$\underline{H}_2$-), 1.76 (sextet, 2H, *J* = 4.4 Hz, -CH_2-C$\underline{H}_2$-CH_3-), 0.70 (t, 3H, *J* = 4.4 Hz, -CH_2-C$\underline{H}_3$).

^{13}C NMR δ (ppm) -161.0 (Pyr-CH=N-), 154.1, 148.7, 135.8, 123.9, 120.5 (Pyr), 62.6 (-C=N-CH2-), 22.3 (-CH2-CH2-CH3-), 11.3 (-CH2-CH3).

IR absorption: ν (cm-1) = 3054, 3009 (Ar C-H str.), 2961-2834 (Alkyl C-H str.), 1651 (C=N str.), 1587, 1568, 1468, 1436 (Ar ring str.).

Mass spectrum: (+EI, m/z) = 149 [M + H].

CHN Analysis: Theoretical C-72.9%, H-8.2%, N=18.9%, Found C-71.1%, H-8.0%, N-18.5%.

4.5 Synthesis of *N*-Octyl-2-pyridiylmethanamine

N-Octyl amine (140 g, 1.09 mol) was slowly added drop wise to a stirred solution of pyridine-2-carboxaldehyde (80 g, 0.74 mol) in diethyl ether (ca. 300 ml) at 0 °C and stirred for four hours. Dried magnesium sulphate (ca. 40 g) was added and the solution stirred at ambient temperature for two hours. The solution was filtered and the solvent removed *in vacuo* to yield an orange oil. This oil was distilled under reduced pressure to yield N-n-octyl-2-pyridyl-methanimne as a clear yellow liquid (boiling range 101-103 °C at 10^{-1} Torr). Obtained 120.21 g (0.55 mol, 75%).

^{1}H NMR ($CDCl_3$) δ (ppm) 8.62 (d, 1H, Pyr-H, *J* = 3.5 Hz), 8.35(s, 1H, Pyr-CH=N), 7.97 (d, 1H, Pyr-H, *J* = 7.7 Hz,), 7.71 (t, 1H, Pyr-H, *J* = 7.5 Hz,), 7.28 (t, 1H, Pyr-H, *J* = 4.5 Hz,), 3.65 (t, 2H, C=N-CH_2, *J* = 7.1 Hz,), 1.70 (m, 2H), 1.30 (m, 10H), 0.85 (t, 3H, CH_2-CH_3, *J* = 3.2 Hz).

^{13}C NMR ($CDCl_3$) δ (ppm) 162.0 (Pyr-CH=N), 154.6, 149.3, 136.4, 124.5, 121.1 (Pyr), 61.5 (C=N-CH_2), 31.8, 30.6, 29.3, 29.2, 27.3, 22.6 (-CH_2-), 14.0 (C=N-$(CH_2)_7$-CH_3).

IR (solid, ATR cell) υ (cm^{-1}) 3053, 3008 (Aromatic. C-H stretch.), 2930-2850 (alkyl C-H stretch.), 1650 (C=N stretch), 1587, 1567, 1467, 1435 (Aromatic Ring stretch.).

Mass spectroscopy (+EI, m/z): 218.1

CHN analysis: Theoretical C-77.01%, H-10.16%, N-12.83%. Found C-76.67%, H-10.25%, N-12.68%.

4.6 Synthesis of 1,3,5-Tri-O-isobutyryl bromide benzene

1,3,5-Trihydroxybenzene (11 g, 87 mmol) was dissolved in anhydrous THF (250 mL) at 25 °C under an atmosphere of nitrogen. Triethylamine (42 mL, 305 mmol) was added and the mixture was cooled to 0 °C (ice bath). A solution of 2-bromoisobutyryl bromide (37.6 mL, 305 mmol) in anhydrous THF (50 mL) was added dropwise over a period of 30 minutes. A white precipitate of triethylammonium bromide forms almost immediately. After addition of 2-bromoisobutyryl bromide, the mixture was stirred for 2 h. The reaction mixture was filtered and the solvent evaporated under reduced pressure. The white/yellow powder was recrystallised from methanol and the product dried under vacuum to give the 3-arm initiator) as a white crystalline solid (45.0 g, 90%, Mp 48–50 °C).

^{1}H NMR δ (ppm) - 2.04 (s, 18H, CH_3), 6.96 (s, 3H).

^{13}C NMR δ (ppm) - 30.5 (CH_3), 54.8, 112.5, 151.3, 169.4 (C=O).

CHN analysis: Theoretical C-37.73%, H-3.69%,. Found C-37.70%, H-3.63%.

IR absorption: ν (cm-1) = 1750 (C=O), 1607 (aromatic ring C=C), 1452 (CH_3), 1255 (C-O-C=O).

4.7 Synthesis of 1,1,1,1-Tetrakis(2'-bromo-2'-methylpropionyloxymethyl)methane.

Pentaerythritol (6.83 g, 50.2 mmol), THF (200 mL) and triethylamine (30.6 mL, 220 mmol) were placed into a 500 mL round bottom flask. 2-Bromoisobutyryl bromide (27.2 mL, 220 mmol) was added dropwise with stirring over a period of 15 minutes. A white precipitate of triethylammonium bromide formed immediately upon addition of the acid bromide and the reaction was left to react for 12 hours. Upon completion the ammonium salt was removed by filtration. The filtrate was passed through a column of basic alumina and the solvent was removed under reduced pressure. The crude product was dissolved in dichloromethane (100 mL) and washed with 6×20 mL of 10% aq. HCl. The organic layer was dried with $MgSO_4$, filtered, and the solvent removed under

reduced pressure to give an off white powder which was recrystallised from methanol. (Yield = 50% Mp 134-135 °C)

^{1}H NMR δ (ppm) – 1.93 (s, 24H, CH_3), 4.32 (s, 8H, CH_2)

^{13}C NMR δ (ppm) –30.7($\underline{C}H_3$), 43.8 ($\underline{C}(CH_2)_4$), 55.4 ($\underline{C}(CH_3)_2Br$), 64.0 (CH_2), 171.0 ($\underline{C}$=O)

CHN analysis: Theoretical C-34.45%, H-4.41%,. Found C-34.47%, H-4.36%.

IR absorption: ν (cm-1) = 1732 (C=O), 1459 (CH_3/CH_2), 1267 (C-O-C=O).

4.8 Synthesis of 1,2,3,4,6-Penta-O-isobutyryl bromide-a-*D*glucose,

Glucose (50 g, 0.278 mol) was suspended in a mixture of anhydrous pyridine (200 mL) and anhydrous chloroform (300 mL) under an atmosphere of nitrogen at 25 °C. The suspension was cooled to 0 °C and a solution of 2-bromoisobutyryl bromide (205 mL, 1.67 mol) in anhydrous chloroform (100 mL) was added dropwise over a period of 30 minutes. The reaction mixture was allowed to warm to ambient temperature and stirred for 4 days. The reaction mixture was diluted with chloroform (300 mL) and washed successively with ice–water (500 mL), saturated aqueous sodium hydrogen carbonate solution (500 mL × 3), water (500 mL), dried ($MgSO_4$), filtered and evaporated to give a pale orange cake. Methanol (1 L) was added and the suspension stirred to break up the cake to give a fine suspension. The solid was filtered, washed with methanol (2 × 500 mL) and dried to give product (196.1 g, 78%, Mp 207–208 °C) as a white powder.

^{1}H NMR δ (ppm) - 1.82 (s, 3H, CH3), 1.85 (s, 3H, CH3), 1.86 (s, 3H, CH3), 1.88 (·2) (s, 3H, CH3), 1.90 (s, 3H, CH3), 1.91 (s, 3H, CH3), 1.94 (s, 3H, CH3), 1.85 (s, 3H, CH3), 2.01 (s, 3H, CH3), 4.31–4.42 (m, 3H), 5.23 (dd, 1H, J = 3.8, 10.2 Hz), 5.27–5.36 (m, 1H), 5.67 (t, 1H, J = 9.8 Hz), 6.39 (d, 1H, J = 3.8 Hz).

^{13}C NMR δ (ppm) - 30.1 (CH3), 30.2 (CH3), 30.3 (CH3), 30.4 (x3) (CH3), 30.5 (CH3), 30.6 (·2) (CH3), 30.7 (CH3), 54.8, 54.9, 55.0, 55.3 (·2), 62.5, 68.0, 70.1, 70.4, 70.5, 89.4, 169.2 (C=O), 169.7 (C=O), 170.2 (C=O), 170.3 (C=O), 171.1 (C=O).

CHN analysis: Theoretical C-33.76%, H-4.03%, Found C-34.00%, H-4.09%.

IR absorption: ν (cm-1) = 1738 (C=O), 1459 (CH_2), 1268 (C-O-C=O)

4.9 Synthesis of 8-arm initiator derived from lactose

Lactose (30 g, 87.63 mmol) was suspended in a mixture of anhydrous pyridine (200 mL) and anhydrous chloroform (200 mL) under an atmosphere of nitrogen at 25 °C. The suspension was cooled to 0 °C and a solution of 2-bromoisobutyryl bromide (104 mL, 0.841 mol) in anhydrous chloroform (100 mL) was added dropwise over a period of 1 h. The reaction mixture was allowed to warm to 25 °C and stirred for 3 days. The reaction mixture was diluted with chloroform (300 mL) and washed successively with ice–water (500 mL), saturated aqueous sodium hydrogen carbonate (3 × 500 mL), water (500 mL), dried (MgSO4), filtered and evaporated to give an orange transparent solid/syrup. Ethanol (500 mL) was added to the solid and heated to boiling to break up the solid. The mixture was allowed to cool and the solid filtered, washed with light petroleum and dried to give the product (20.5 g, 15%, Mp 219–220 °C) as a white powder.

^{1}H NMR δ (ppm) - 1.77 (CH3), 1.86 (CH3), 1.87 (CH3), 1.88 (CH3), 1.89 (CH3), 1.90 (CH3), 1.92 (CH3), 1.93 (CH3), 1.94 (CH3), 1.94 (CH3), 1.95 (CH3), 1.96 (CH3), 2.00 (CH3), 2.00 (CH3), 2.00 (CH3), 2.02 (CH3), 4.16–4.26 (m, 3H), 4.29–4.39 (m, 2H), 4.48 (dd, 1H, J = 2.0, 12.8 Hz), 4.69 (dd, 1H, J = 2.5, 12.8 Hz), 4.73 (d, 1H, J = 8.3 Hz), 5.00 (dd, 1H, J = 3.3, 10.5 Hz), 5.07 (dd, 1H, J = 3.8, 10.3 Hz), 5.25 (dd, 1H, J = 8.0, 10.5 Hz), 5.49 (d, 1H, J = 3.3 Hz), 5.63 (t, 1H, J = 9.8 Hz), 6.32 (d, 1H, J = 3.5 Hz).

^{13}C NMR δ (ppm) - 30.0, 30.1, 30.2, 30.3 (·2), 30.4, 30.5 (·4), 30.6 (·3), 30.7, 30.8, 31.1 (CH3 · 16), 54.4, 54.9, 55.1, 55.2, 55.3, 55.5, 55.6, 56.4, 62.3, 62.8, 68.3, 69.6, 70.2, 70.8, 70.8, 71.0, 72.9, 73.0, 89.1, 99.6, 169.2, 169.3, 170.3, 170.4 (C=O), 170.5 (C=O), 170.6 (C=O), 170.9 (C=O), 171.0 (C=O).

CHN analysis: Theoretical C34.81-%, H-4.12%,. Found C-34.69%, H-4.12%.

IR absorption: ν (cm-1) = 1737 (C=O), 1462 (CH_2), 1264 (C-O-C=O)

5 References

1. M. Kato, M. Kamigaito, M. Sawamoto and T. Higashimura, *Macromolecules*, 1995, **28**, 1721-3.
2. J.-S. Wang and K. Matyjaszewski, *J. Am. Chem. Soc.*, 1995, **117**, 5614-15.
3. J. Ueda, M. Kamigaito and M. Sawamoto, *Macromolecules*, 1998, **31**, 6762-68.
4. J. Ueda, M. Matsuyama, M. Kamigaito and M. Sawamoto, *Macromolecules*, 1998, **31**, 557-62.
5. K. Matyjaszewski, P. J. Miller, E. Fossum and Y. Nakagawa, *Appl. Organomet. Chem.*, 1998, **12**, 667-73.
6. D. M. Haddleton and C. Waterson, *Macromolecules*, 1999, **32**, 8732-39.
7. D. M. Haddleton, R. Edmonds, A. M. Heming, E. J. Kelly and D. Kukulj, *New J. Chem.*, 1999, **23**, 477-79.
8. A. J. Limer, A. K. Rullay, V. San Miguel, C. Peinado, S. Keely, E. Fitzpatrick, S. D. Carrington, D. Brayden and D. M. Haddleton, *React. Funct. Polym.*, 2006, **66**, 51-64.
9. H. Gao, M.-C. Jones, J. Chen, R. E. Prud'homme and J.-C. Leroux, *Chem. Mater.*, 2008, **20**, 3063-67.
10. K. Matyjaszewski, P. J. Miller, J. Pyun, G. Kickelbick and S. Diamanti, *Macromolecules*, 1999, **32**, 6526-35.
11. T.-L. Wang and C.-G. Tseng, *Polym. Int.*, 2006, **55**, 558-64.
12. P. Moschogianni, S. Pispas and N. Hadjichristidis, *J. Polym. Sci., Part A: Polym. Chem.*, 2001, **39**, 650-55.
13. H.-X. Wu, W.-M. Cao, R.-F. Cai, Y.-L. Song and L. Zhao, *J. Mater. Sci.*, 2007, **42**, 6515-23.
14. V. Percec and B. Barboiu, *Macromolecules*, 1995, **28**, 7970-2.
15. B. Barboiu and V. Percec, *Macromolecules*, 2001, **34**, 8626-36.
16. V. Percec, B. Barboiu, C. Grigoras and T. K. Bera, *J. Am. Chem. Soc.*, 2003, **125**, 6503-16.
17. D. R. Robello, A. Andre, T. A. McCovick, A. Kraus and T. H. Mourey, *Macromolecules*, 2002, **35**, 9334-44.
18. L. Xue, U. S. Agarwal and P. J. Lemstra, *Macromolecules*, 2005, **38**, 8825-32.
19. B. G. Kinker, *Chemical Industries*, 2003, **90**, 329-53.
20. R. N. Keller and H. D. Wycoff, *Inorganic syntheses. 1. Copper(I) chloride*, 1946.

Chapter 3

-

Arm first star polymers by copper(I) mediated living radical polymerisation

Table of Contents

List of Figures

List of Tables

1 Introduction

1.1 Arm-First Stars

1.1.1 Non-functionalised Stars

The first example of the synthesis of arm-first stars by ATRP was in 1999 by Xia *et al.*[1] using a copper(I) halide based catalyst system. They polymerised styrene to linear arms and following isolation and purification used to reinitiate polystyrene arms as macroinitiators to react with added divinyl benzene (DVB) to form the star architecture, Figure 1. It was found that 85-90% of arms were incorporated into star. Xia and co-workers further investigated how the ratio of cross-linker to arm changed the star molecular weight. As more cross-linker was added, an increase in molecular weight was seen; however, when too much DVB was added, gelation was observed in early stages of the polymerisation. Another important factor investigated was the effect of different cross-linkers on the formation of the star. It was noticed that DVB gave the slowest star formation and little gelation after 30 hours of reaction, followed by 1,4-butanediol diacrylate (BDA) which gelled after 3 hours, and ethylene glycol dimethacrylate which gelled after 20 minutes. The authors observe that these results show the necessity of careful choice of cross-linker for each polymerisation system.

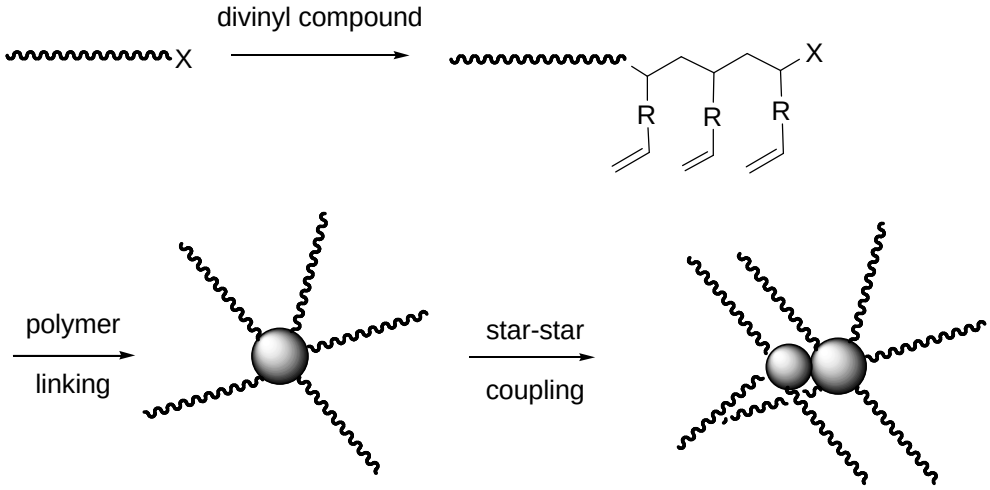

Figure 1 - Arm-first star formation, where an arm is grown prior to divinyl addition to link the growing chains together. If the polymerisation continues to very high conversion, or the cross-linker density is too high, star-star coupling can be observed

Soon after this seminal work, Sawamoto and coworkers showed how to synthesise similar structures using ruthenium-based catalysts [2]. Unlike Xia *et al.* [1], Sawamoto and coworkers synthesised the polymers in a one-pot fashion by adding the cross-linker to a

polymerisation of methyl methacrylate at approximately 90% monomer conversion. They also compared the use of different cross-linkers, Figure 2, finding that the soft aliphatic linkers (**1**, **2** and **3**) gave polymers with high percentages of star formation. Cross-linker **4** was found to give very little star-formation, which the authors suggest was due to intramolecular cyclisation reactions. However, **6** was found to give the highest percentage star formation, 92%, although they did not attribute why this is the case. It could be due to the rigidity of the linking group ensuring that the chains remained separated, reducing the steric crowding of the core. The decreased crowding of the cores could be the cause of the increased star formation.

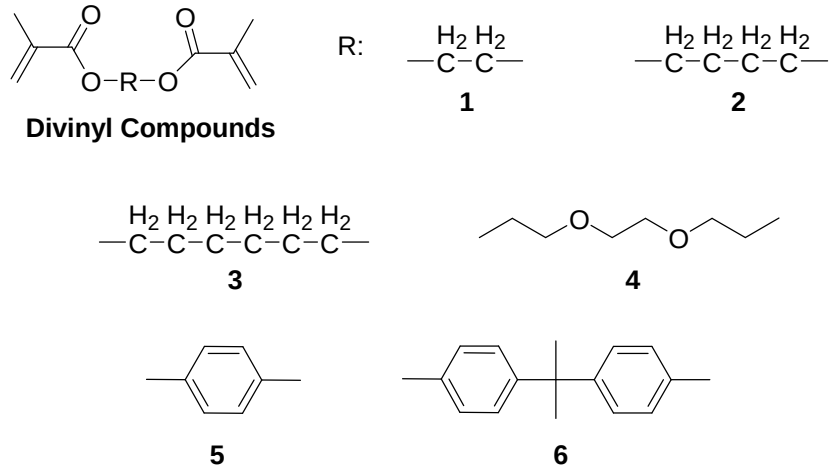

Figure 2 - Cross-linkers used by Sawamoto *et al.* in their first paper on arm-first stars[2]

Like Xia *et al.* [1], Sawamoto and co-workers noted that the choice of cross-linker could change depending on the monomer being polymerised. When switching to *n*BMA in place of MMA, they found that in this case 1, and no longer 6, gave the highest percentage star formation.

Later, Baek *et al*. further advanced the technique of synthesising arm-first star block copolymers.[3] They polymerised block copolymers of MMA and BMA, followed by addition of the divinyl compound to cross-link the arms into a star. The effect of using the different cross-linkers 1 and 6 (Figure 2) on the star formation was investigated also in this work. The authors detailed that nearly pure blocks or random copolymers can be synthesised, depending on the application.

More recently, Solomon *et al.* [4] were able to demonstrate a simple application for these star polymers. They polymerised MMA arms and cross-linked them with EGDMA, much like in previous examples. The polymers formed stars with typically >80% of the arms incorporated into the stars. Films of the polymer were cast using the advantageous

self-assembly of water droplets into hexagonal arrays, producing a honeycomb film. They found that with increasing molecular weight and arm number, the pores of the honeycomb film became smaller.

1.1.2 End-Functional Stars

A simple way of adding functionality into polymers made by ATRP is via the initiator. Almost any compound containing an alcohol group can be esterified into an initiator for ATRP. A number of initiators for ATRP are detailed in several reviews.[5-7] Matyjaszewski and coworkers showed how ATRP could be used to produce end-functional star polymers.[8] A variety of initiators was synthesised, Figure 3, from a simple non-reactive methyl-functional initiator, through to epoxy- and alcohol-functional. A number of these initiators have the potential for further reaction on the α end of the polymer chain. The authors noted that the polymerisations, using these functional initiators, proceeded in a similar fashion to that of with a non-functional initiator.

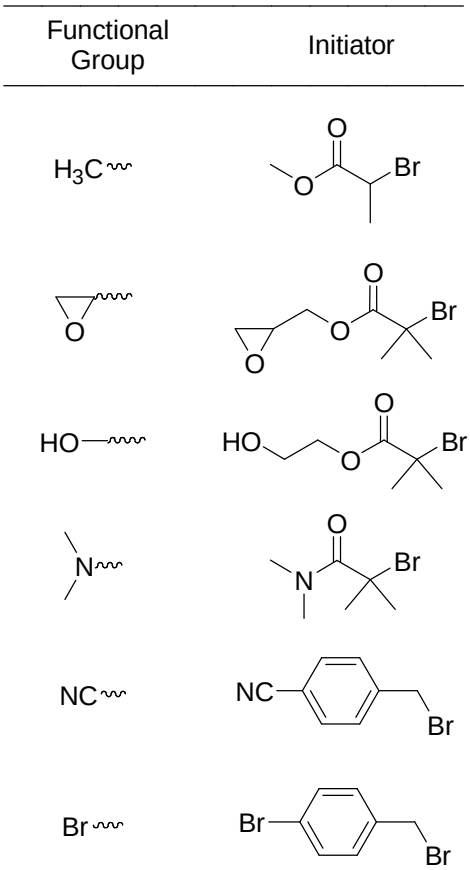

Figure 3 - Range of initiators used by Matyjaszewski *et al.* to give end functional arm first star polymers by ATRP[8]

Baek *et al.*[9, 10] further demonstrated the robustness of ATRP by using a ruthenium-based catalyst to polymerise from a variety of functional initiators. This work supported the findings of Matyjaszewski *et al.* [8] in that changing the initiator had little effect on the polymer synthesised. They confirmed the presence of the initiator functionality in the polymer using ^{1}H NMR.

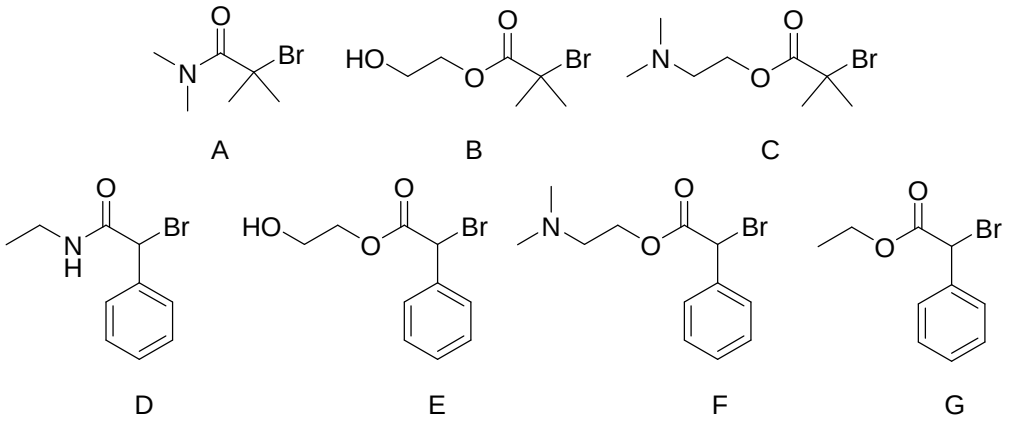

Figure 4 – The range of initiators used by Baek *et al.* to give end-functional arm-first star polymers by ATRP[9, 10]

This technique of introducing functionality at the α-end of the chain to give surface functionality in the arm-first star was subsequently used by Pan *et al.* [11] to introduce a succinimide group to the α-end of a poly(styrene) arm. They were able to use the succinimide group to react with an amine in the form of tetraaniline to give a star block-copolymer, Figure 5.

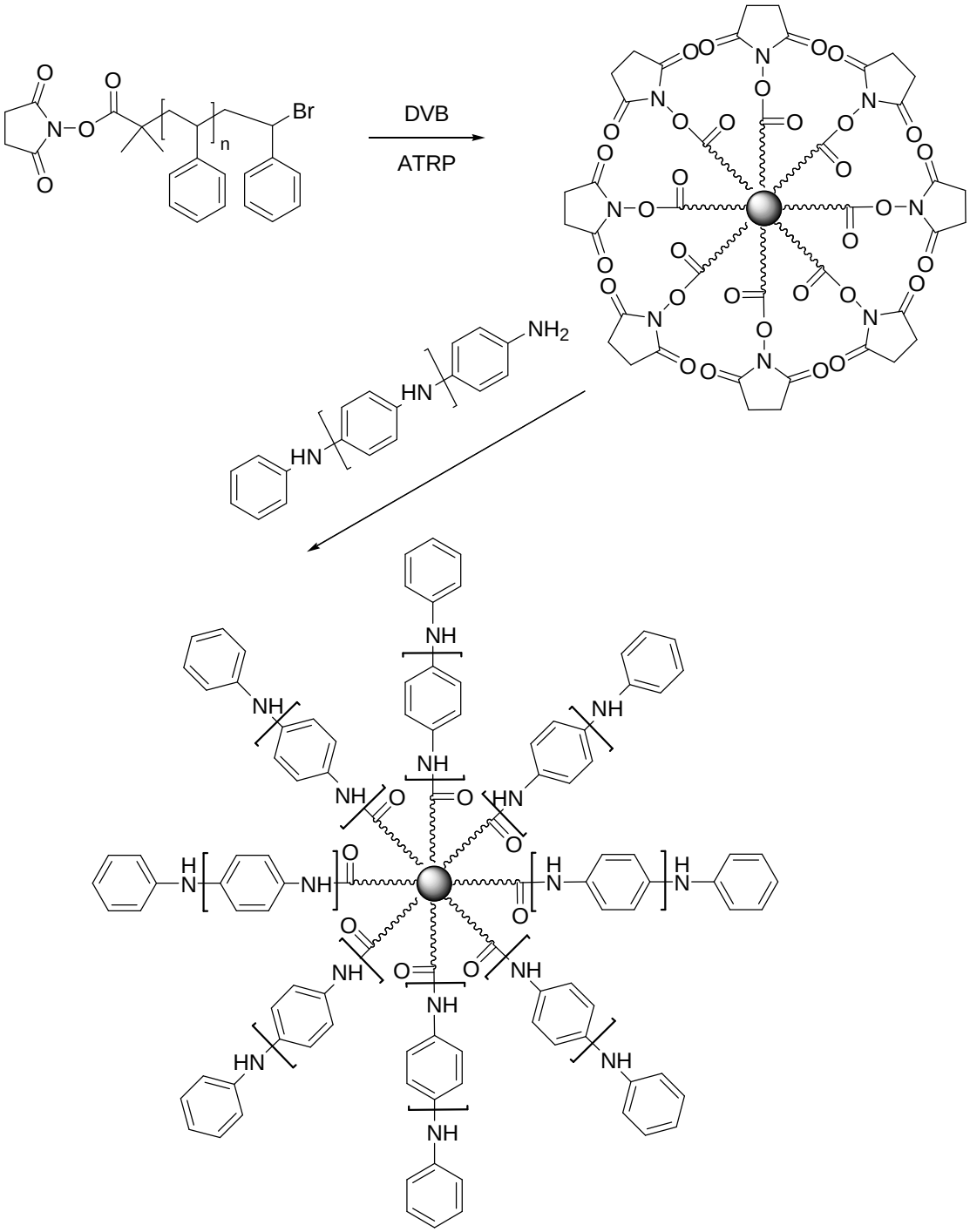

Figure 5 – Synthesis of succinimide functional arm first star polymers and the subsequent reaction with tetraaniline to form star block copolymers by Pan *et al.* [11]

This principle of introducing end functionality to polymers was further developed by Qiao *et al.*.[12] They synthesised fifth generation dendrons based on 2,2-bis(methoxy)propionic acid (bis-MPA). The dendrons were reacted with an initiator functionality suitable for ATRP, which could subsequently be used to initiate the polymerisation of styrene from the focal point of the dendron, Figure 6. The authors

then detailed how DVB was added to the polymerisation to cross-link the arms to give the arm-first star structure with dendrons at the surface of the star. The paper describes how higher generations of dendrons gave slower polymerisations of styrene under ATRP conditions. They indicate that this could be due to steric congestion around the dendron leading to a diminished rate of radical at the focal point and hence leading to a slower polymerisation.

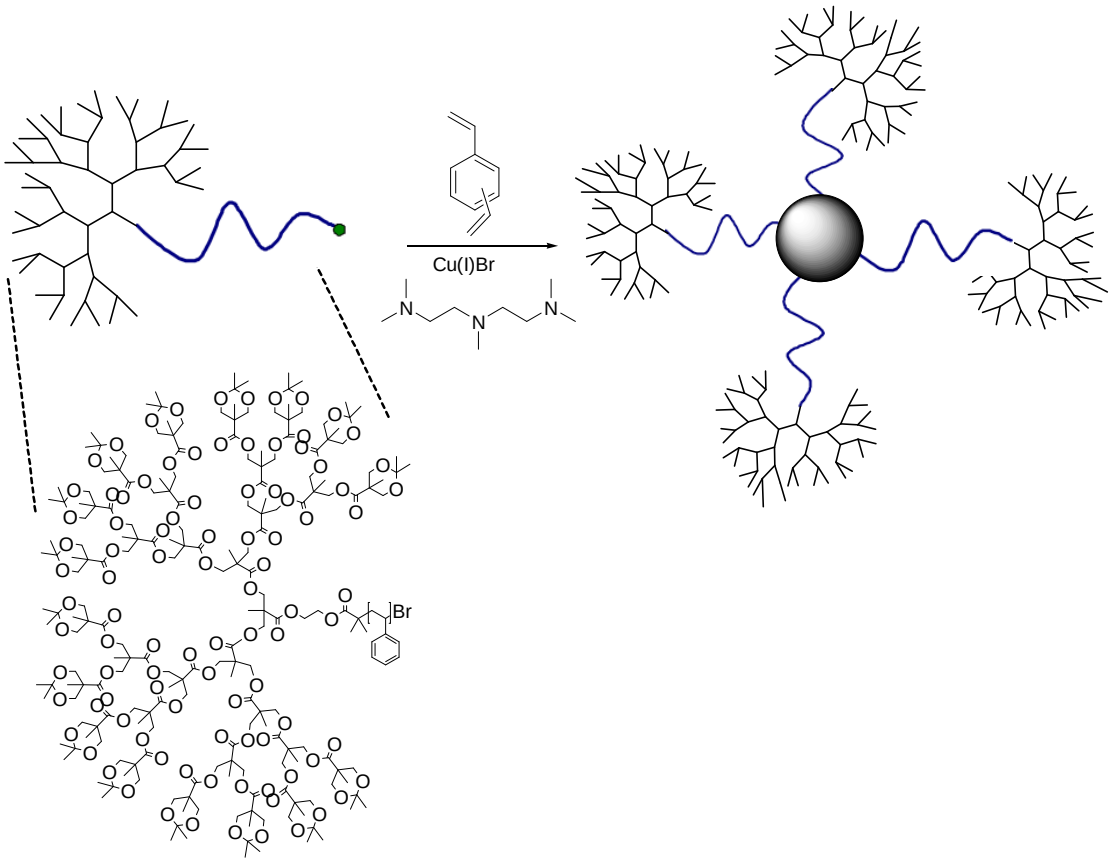

Figure 6 – The use of dendron based initiators for the arm first star polymerisation of styrene by Qiao *et al.*[12]

1.1.3 Core Functional Stars

A significant area in arm-first stars research is the introduction of functionality into the core. Here, either a co-monomer can be introduced with the cross-linking monomer and copolymerised into the core, or monomers with reactive functionalities can be copolymerised into the core and reacted with other molecules of interest post-polymerisation. An advantage of these approaches is that there is a significant density of polar groups within a small area of the polymer. This offers potential in that for a typical star the functional entities are spread throughout the arms or are located at their terminus. By having the reactive sites in the core pseudo mini-reactors can be

synthesised. The first example of introducing functionality into the core of an arm-first star polymer by ATRP was reported by Sawamoto *et al.*. [13] In this work, the authors introduced a variety of amides, esters and alcohols into the core as cross-linkers of a poly (methyl methacrylate) arm star, Figure 7. The authors were able to synthesise star polymers with 60-90% arm incorporation. Typically 5-25 hours of polymerisation were required, depending on the cross-linker used, to give sufficient time for the stars to form. The authors describe how this work is important in introducing polar functional groups into otherwise relatively non-polar polymers.[13] Sawamoto *et al.* note that with this polymerisation process the functionalities can be used unprotected which is a significant advantage over other ionic based polymerisations. The paper describes how the polar groups offer potential for host guest interactions and/or molecular recognition via these core functionalities.

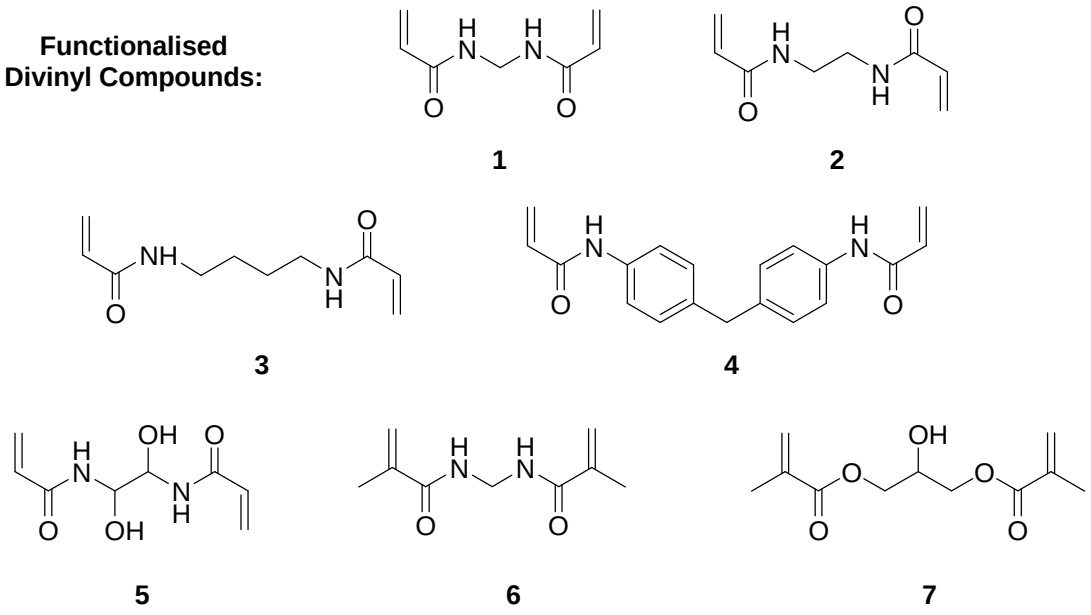

Figure 7 – The different cross-linkers used to introduce amide functionality into the cores of arm first stars by Sawamoto *et al.*[13]

Sawamoto *et al.* also described the interaction of protic guests with the polar cores of the stars synthesised.[14] They used ^{1}H NMR to study the interaction of the protic guests with the cores of the stars, Figure 8. Where the guest hydrogen bonded to the core, peak broadening was observed. Where little or no interaction was seen, the peak broadening was not observed. The authors found that for a benzoic acid moiety, the amide was best at producing a host-guest interaction, followed by an alcohol, and finally esters for which almost no interaction was seen. Interactions of other functionalities on the benzene were investigated as guests and their binding documented.

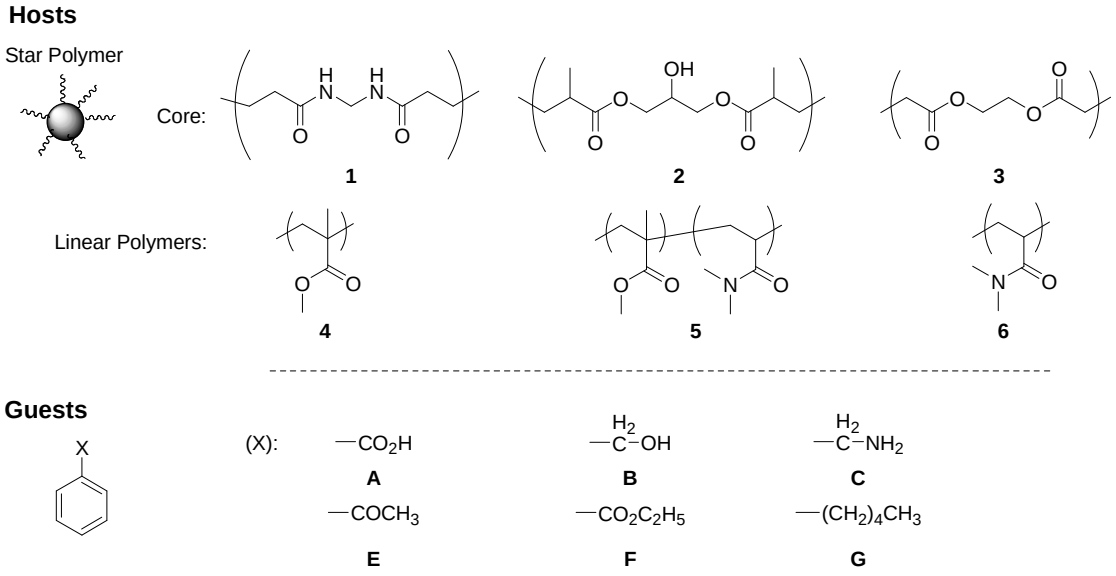

Figure 8 – The host polymers and guest substituted benzenes used by Sawamoto *et al.* [14]

This work lead to a further publication by the same group where they described the encapsulation of a ruthenium complex, in the core of the arm-first star polymer.[15] This was achieved by the copolymerisation of EGDMA as cross-linker and a monofunctional monomer with a diphenyl phosphine unit attached to it. This phosphine acted as a ligand for the ruthenium. The metal was encapsulated during the polymerisation of the star and repeated washings to remove any non-encapsulated metal allowed them to confirm that it was held in place by ligand interactions via a variety of techniques. The metal-polymer complex was then used to catalyse the transformation of 1-phenylethanol to acetophenone. The authors found that by decreasing catalyst loading in the polymer core they were able to increase the conversion to the ketone while reducing the reaction time.

The incorporation of a ligand moiety in a stars microgel core was further utilised by Sawamoto *et al.*. [16] They used PEGMA, which is thermoresponsive with an lower critical solution temperature, LCST, between 27 °C and 90 °C, with the length of the PEG chain controlling the LCST; short PEG chains with only a few repeat units give polymers with a low LCST while longer PEG chains with a significant number of repeat units give a high LCST. This principle was developed from the original work in the area by Lutz who first polymerised thermoresponsive PEG polymers by ATRP and demonstrated their temperature tenability.[17, 18] The thermoresponsive nature of the PEG methacrylate produced an amphiphilic star polymer. The star had hydrophilic arms and a hydrophobic core which contained the ligand monomer. However, unlike Lutz's work, these polymers were synthesised to have a UCST to allow the cooling of a solvent

to cause the precipitation of the polymer. The tuneable UCST allowed the authors to selectively precipitate the polymer by elevating the temperature of the solvent; potentially leading towards a catalyst that could be easily removed from a reaction.

Other work on core-functional arm-first stars was primarily reported by Qiao and coworkers. Along similar lines to Sawamoto's thermoresponsive stars, Qiao *et al.* synthesised poly(*t*-butyl acrylate) arm first stars, cross-linked by DVB, and then removal of the t-butyl group to give poly(acrylic acid) stars.[19] The hydrodynamic volumes of the stars were measured and it was found that at low pH the stars were small and contracted, while at high pH the arms were fully elongated, as could be shown by a large hydrodynamic volume. Stars with these different conformations were cast into films, which were subsequently analysed by AFM. The authors found that the fully elongated polymers gave a smooth film, while the contracted polymer gave a rough surface. Qiao *et al.* also published on the introduction of fluorescent labels into the cores of arm first stars.[20]

1.1.4 Miktoarm Star Polymers

The first example of a miktoarm star polymer was by Chen *et al.*, [21] Figure 9. A Miktoarm polymer is a block copolymers, where the blocks are different arms on the star. They modified poly(ethylene oxide) into macroinitiator for ATRP and then used this to polymerise DVB to form the arm first star. This PEO-DVB star was then used as a macroinitiator in its own right for the polymerisation of styrene to give the miktoarm star polymer. The PEO arms could then be hydrolyzed to give the DVB core on its own to investigate the cores structure and the authors comment that this core had a broad PDI.

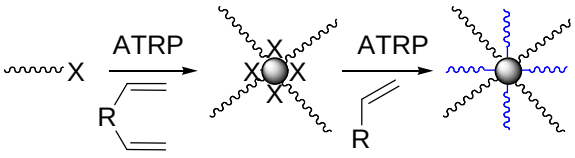

Figure 9 – The synthesis of PEO-DVB-Styrene miktoarm stars using ATRP by Chen *et al.*[21]

The authors then developed their work by first synthesising poly(caprolactone) and transforming it into a macroinitiator and again polymerised DVB to form an arm first star polymer.[22] They then again polymerised styrene to form the miktoarm star. The degradation of the caprolactone again demonstrated the broad nature of the core of the star.

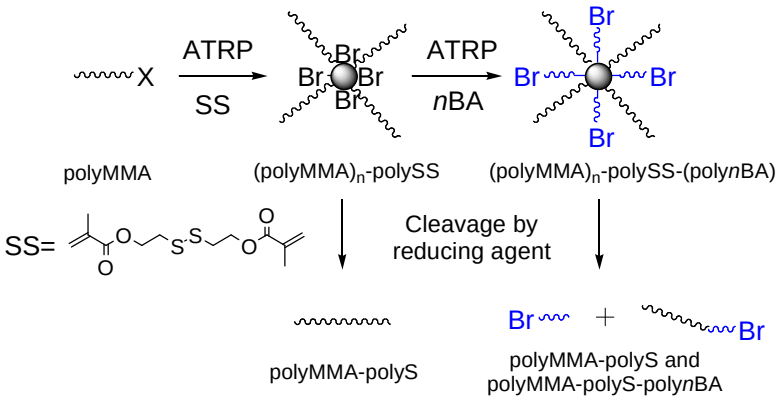

Figure 10 – Synthesis of degradable miktoarm stars by Matyjaszewski *et al.*[23]

The idea of degradable arm-first star polymers was built upon by Matyjaszewski *et al.* using a cross-linker that could be degraded after synthesis.[23] This cross-linker was based on 2,2'-dithiodiethanol which is esterified to form the dimethacrylate. This S-S bond is broken by the use of a reducing agent such as tributyl phosphine. The authors detailed how DVB was replaced with the dithio cross-linker and used to cross-link arms of *n*-butyl acrylate, MMA or styrene. These star structures were then subsequently used to form miktoarm stars by arm extension from the cores with any of the above monomers, Figure 10. After reduction of the S-S bond to remove the cross-linking in the cores, the remaining arms were analysed and found to have a broader PDI than the initial arms.

The same authors further investigated miktoarm stars in particular the initiation efficiency of the cores for chain extension of the miktoarms themselves.[24] They found that the initiation efficiency was affected by a number of parameters such as: the arm length of the macroinitiating star, the structural compactness of the macroinitiator and the chemical compatibility of the second generation arms to the preformed first generation arms.[24]

Amongst all this work, Fu *et al.*[25] synthesised poly (styrene)-co-DVB arm first star polymers. They then converted all the remaining unreacted DVB vinyl groups to initiating sites via hydroboration and then subsequently polymerised ethyl acrylate from the multitude of initiating sites in the core to form a heteroarm star polymer.

1.1.5 Polymerisation of macromonomers to give arm first stars

The pre-existing method of synthesising arm first star polymers by adding a divinyl monomer to the polymerisation at a given conversion to link the growing chains

together, results in a broad molecular weight distribution for the polymer. Unfortunately, for certain applications, particularly in the biomedical area, the need for a narrow PDI is significant. By having mono-disperse polymers, the properties of them are more uniform; this cannot be said for a polymer with a broad PDI, since there is a significant distribution in the chain length and hence its properties.

In order to synthesise an arm first star with a narrow PDI, Matyjaszewski *et al*. synthesised poly(*n*-BA) arms and then transformed the bromine end group into an acrylate functionality suitable for ATRP.[26] This macromonomer was then polymerised with a DVB into narrow PDI arm first stars. Typically, they had a PDI of 1.2, Figure 11. The authors also detailed how they could use poly(ethylene oxide) macromonomers to the same end also making low PDI arm first stars.

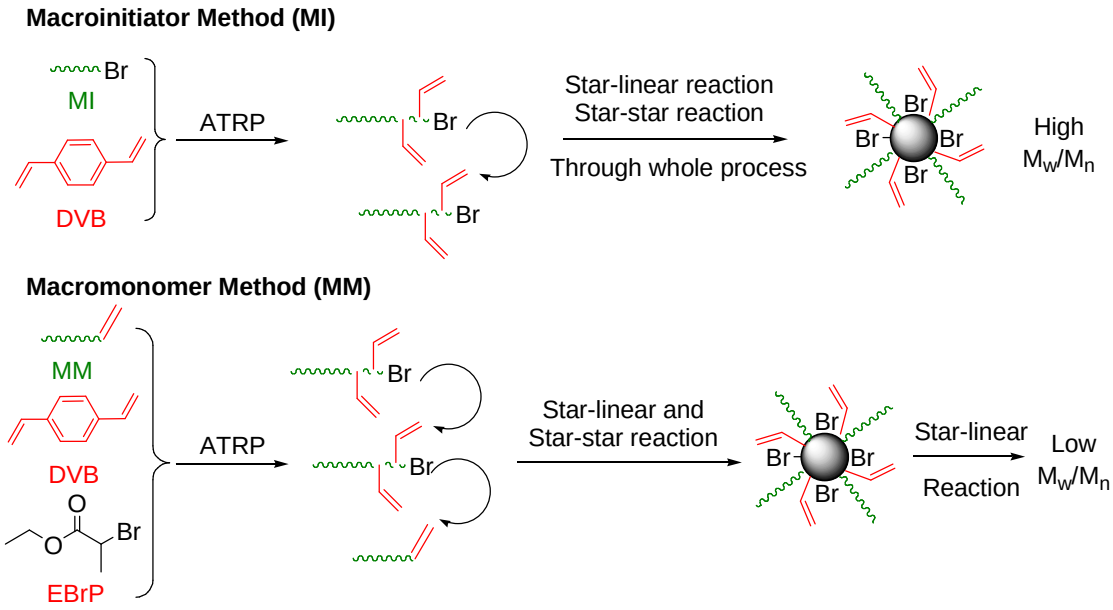

Figure 11 – A comparison of two ways arm first stars can be synthesised [26]. Firstly, the macroinitiator (MI) method which results in high PDI. Secondly, the macromonomer (MM) method which results in low PDI.

This method of synthesising low PDI arm first stars was further expanded by the introduction of functionality into the cores of the stars.[27] By using a functional initiator, a wide range of groups could be introduced into the cores. The authors chose pyrene as a model initiator as it has strong UV absorption peaks at 300 and 360 nm. This introduction of functionality produced polymers that are similar in structure to that detailed in the section 1.1.3 although these are of much narrower PDI.

Matyjaszewski *et al*. further extended this work by copolymerising two different macromonomers, or one macromonomer with another macroinitiator.[28] They

copolymerised poly(n-BA) with poly(MA) PEO macromonomers and used them all as macroinitiators, Figure 11.

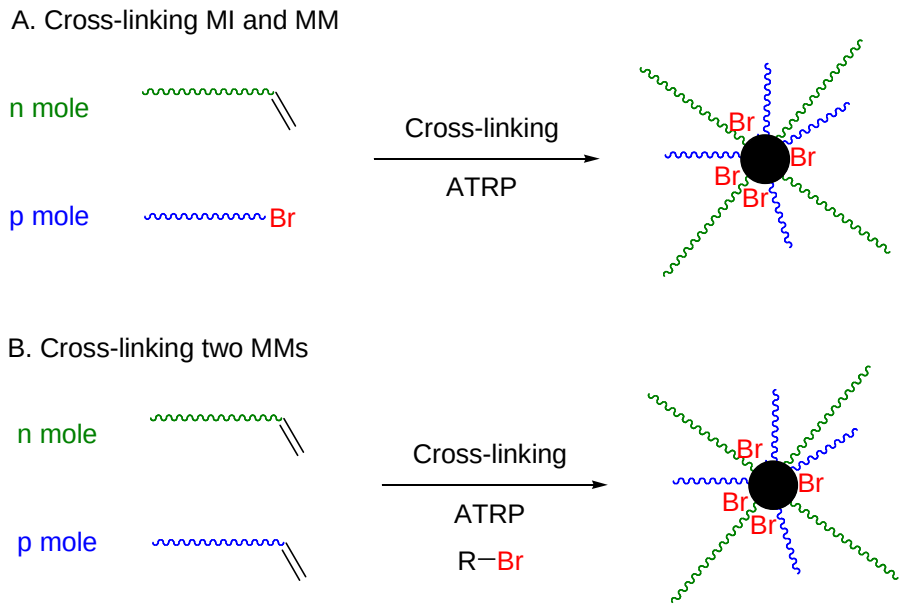

Figure 12 – Synthesis of miktoarm arm first stars from macromonomers by Matyjaszewski *et al.*[28]

1.1.6 Arm first stars by Click Chemistry

The use of click chemistry to functionalise polymers is well known in the literature and is described in detail by a number of authors in a number of reviews.[29, 30] The principle is that a polymer arm is synthesised and then either the initiator contains a reactive functionality suitable for click chemistry or the halogen end group is synthesised into the reactive group for click. In this case the use of copper-catalyzed 1,3 Huisgen dipolar cycloaddition reaction between an azide and an alkyne leading to 1,2,3-triazole is of interest as it is the most widely used for the post-reaction of polymers, Figure 13.

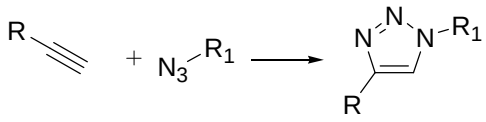

Figure 13 – Click chemistry - copper-catalyzed 1,3 Huisgen dipolar cycloaddition reaction

There were a number of publications regarding star formation by click chemistry in 2006 by three different groups. The first of which by Turro *et al.* [29] where they detailed the formation of degradable networks with a star-like nature. This work involved the synthesis of a difunctional ATRP initiator which had a degradable link between the initiating sites. This was subsequently used to polymerise *t*-BA and then the bromine

end group was reacted to form an azide. The azo functionality was reacted with a multi-alkyne core to form the star structure.

Later that year, Matyjaszewski *et al.* describe the synthesis of three- and four-arm polystyrene stars via click chemistry.[30] Again, the Br end group was transformed into an azide and reacted with a multi-alkyne core to give the star structure. The stars made had low PDI's and a predictable molecular weight based on the arm length.

At the same time, Monterio *et al.* also demonstrated the synthesis of three arm stars via ATRP and click chemistry.[31] Here, they polymerised a single polymer arm and then reacted it with a trifunctional alkyne to form the star. They also showed how it was possible to synthesise a first generation miktoarm dendritic arm first star. They achieved this by synthesising polystyrene from a difunctional initiator. The end group was then reacted with sodium azide to give the azide functionality needed for further reaction to give a difucntional alkyne suitable for further reaction with another azide functional polymer such as poly(t-BA), (MA), (AA) or (Sty).

1.2 Experimental Design

1.2.1 Why use Experimental Design?

Without experimental design, the usual approach to solving complex reactions and optimising them for yield (or other desired property) was to optimise one factor at a time and once all maximums were found for each factor, the maximum output should have been found. This is known as the One-Variable-at-a-Time approach, or *OVAT*. Taking a hypothetical reaction where we wish to optimise the conditions for reaction temperature and time, the first optimisation experiments would be to vary the reaction temperature while keeping the reaction time constant. The maximum yield is therefore found at a given temperature, Figure 14 A, which is carried forward and used as a constant while the reaction time is varied, Figure 14 B. The maximum yield is thus found at a given reaction temperature and time.

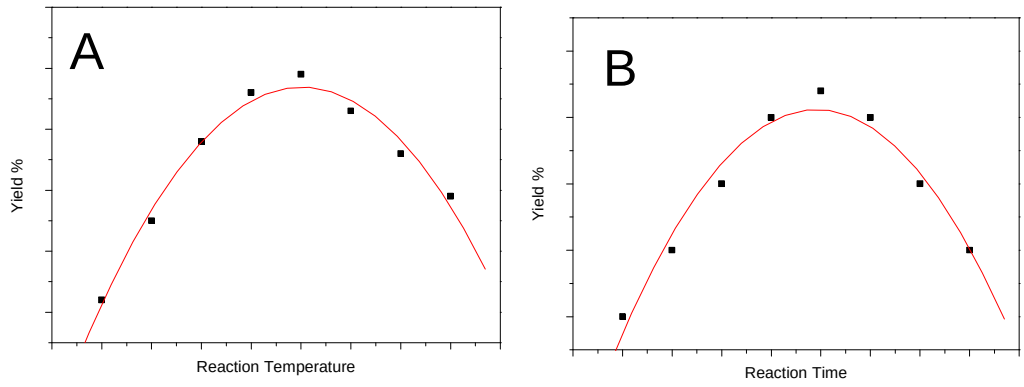

Figure 14 - The OVAT approach where temperature is varied first (A) and the maximum yield found at a given temperature is then used to vary the reaction time (B)

However, this maximum is often not the true optimal yield. OVAT can often miss the maximum output, as the optimal yield may well be at a temperature/reaction time combination that has not been tested. Therefore, the true picture may well be something like shown in Figure 15; where the series of experiments miss the true area of maximum yield.

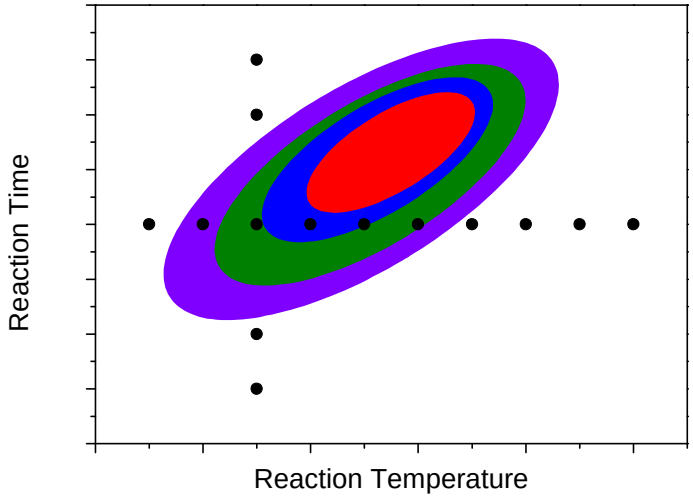

Figure 15 – A typical response from an OVAT approach – missing the actual maximum yield. The purple region is low yield, red the highest.

In order to overcome this difficulty, experimental design can be implemented. This allows the correlation of a significant number of input factors (such as reaction time, temperature and stoichiometry) and any synergistic effects there maybe between them and output factors (such as yield, cost and reaction time).

The pioneering work on experimental design was conducted by Sir Ronald Fisher in the 1920s. At that time, he worked at the Rothamsted Agricultural Experimental Station

near London. Fisher was responsible for statistics and data analysis; during his work he recognised flaws in the way the experiment that generated the data had been performed often hampering the analysis. The result of his work was the introduction of statistical thinking and principles into designing experimental investigations such as factorial design and analysis of variance, with particular interest in the agricultural field.

The three main principles Fisher introduced were:

1. Randomisation
2. Replication
3. Blocking

In his book *The Design of Experiments,* Fisher gave a specific example to explain the above effects.[32] He chose to investigate whether a person could just by taste differentiate between tea which had had milk or the tea infusion first added to the cup. In his example the tester was asked to taste 8 cups of tea, of which 4 had been made with either method and identify them. Fisher describes the above three principles in detail.

1.2.2 Randomisation

In his example, Fisher discusses the frivolous use of time in eliminating all possible variables; in this case such things as the cup – whether they were of uniform size, colouration and weight, the colour of the tea/milk mixture, the strength of the tea infusion and lastly the temperature of the resulting mixture. Obviously all the above factors could be almost completely eliminated from the study by increased labour or expense.

However, Fisher suggests that by randomising the order of the experiments, or the order in which they are presented for tasting, these factors can be eliminated. By doing so there would be no intended pattern to the combinations of cups/strength of tea/temperature leaving the intended information on whether the milk or the tea had been added to the cup first to be found. This randomisation process aims to average out all of the extraneous factors (such as listed above) from the experiment and as such remove them from being a contributory factor.

1.2.3 Replication

One probable objection was noted by Fisher; the subject may suggest that although they may mistakenly identify a single cup incorrectly, over a number of samples they would invariably give the correct result the majority of the time. This would lead to the suggestion that the study should be enlarged to allow for this. By enlarging the experiment its sensitivity would go up, in that subtle differences in detection rate could be observed. When only a small number of experiments are carried out, the rate of detection (including errors) could only go to prove the person unable to tell the difference in the way the tea was made.

Therefore, by introducing replica experiments where each factor combination is re-run a more quantitative approximation of the error(s) in the measurements can be obtained. The estimation of the error allows the determination of whether the observed differences in the data are really statistically different.

1.2.4 Blocking

This design technique is used to improve the precision with which comparisons between factors of interest are made. It is often used to remove nuisance factors (factors which may influence the experimental output in some way but in which there is no direct interest). For example, in Fisher's tea making test a significant quantity of milk may be required to complete all the necessary experiments. Therefore, the experiment may be broken down into two parts or blocks. In each block, one container of milk should be used as it would be expected that the change in taste of the milk from one container would vary less than between containers. Typically, additional blocks would be introduced for each nuisance factor such as additional tea being required.

1.2.5 Further Development of DoE

After Fishers initial work in this area, other researchers expanded the methodology for use in other areas. Box and Wilson[33] developed the response surface methodology (RSM) for an industrial application. Since their experiments took significantly less time than Fisher's in the agricultural field, they were able to show that the response variable can usually be observed immediately and also that a small number of runs can give vital information for the planning of further experiments.

Taguchi also contributed widely to the development of DoE.[34] He focused on experiments that estimated the main effects of factors with a minimum number of experimental runs, without placing a priority on interactions. A method of assessing the 'signal to noise' ratio was also a brainchild of Taguchi. He observed that Fishers work sought to optimise the mean output of an experiment such as yield of a particular crop. Although this is important for industrial applications Taguchi wanted to optimise a process with reference to the end *cost to society*. Processes may produce a part for a machine which has to have a particular hole and given size. The variation of the size of this hole may cause the part to fail and therefore replacements made. By optimising a process to produce the part with as little variation as possible even with initial increased costs Taguchi argued that the costs later would be lower and that brand reputation would be increased.

1.2.6 The use of computer based software for DOE

With the rapid increase in computer processing power it became possible for correctly designed software to quickly produce a number of potential designs. The software also is able to analyse the results to give interactions or optimal outputs for example. Typically the most widely used software products are Minitab[35] or Modde.[36] For this work Minitab was used.

2 Results and Discussion

LRP to give arm-first stars has attracted significant interest; however, an OVAT approach for optimisation has been used. Their work does identify some key factors in the synthesis of arm first stars, such as the cross-linker: initiator ratio,[1] the type of cross-linker,[1] when the cross-linker is added to the reaction as a function of monomer conversion.[1-3] In the work, there seemed to be little correlation of variance in the factors and the effect it had on the polymers molecular weight and number of arms. For this reason, this study has attempted to apply an experimental design to the area to disseminate between the factors and how much their co-variance changes the end polymer.

Prior to the use of experimental design, a few experiments were carried out to attempt to synthesise the desired arm-first stars. From previous work by Lubrizol using RAFT polymerisation, a cross-linker-to-initiator ratio was calculated as 4:1 and this used for the initial experiments. The monomer composition was as described in the introduction, 70wt% C_{12-15} methacrylate, 30wt% *n*-butyl methacrylate.

The cross-linker was added to all the reactions without additional solvent. This increased the monomer concentration and therefore sped up the polymerisation. The increase in rate of the polymerisation promoted the desired star formation.

2.1 Synthesis of an Arm First star using EGDMA as cross-linker

This first attempt at synthesising an arm first star was based on Lubrizol's previous work and work in the literature described above. The targeted molecular weight of the arm was M_n = 5000 g mol^{-1}. The cross-linker was added at 90% original monomer conversion and the polymerisation resulted in a polymer being formed with M_n = 42000 g mol^{-1}, M_w = 163700 g mol^{-1} and a PDI = 3.90. Approximately 93% of the arms were incorporated into the arms. The incorporation of the arms into the star was measured by GPC. The peaks of the arms and the star overlap and therefore the peaks were deconvoluted using a Gaussian fit in Microcal Origin. The outputs from the Gaussian fit allow the M_n, M_w and PDI to be calculated for each deconvoluted peak. This experiment was considered a success based on the high arm incorporation and the overall monomer conversion being close to 100%. Polymerisation proceeded with a living nature until the addition of the cross-linker at 90% conversion of monomer,

Figure 16. The molecular weight increased linearly with conversion prior to cross-linker addition at which time the molecular weight and PDI increased rapidly to give the highly cross-linked star, Figure 17. The drop in the first order kinetic plot is caused by the addition of the EGDMA cross-linker. This is a more polar molecule than the other reactants and caused the increase in the rate of polymerisation observed after cross-linker addition. This is observed in all cases where EDGMA is added to a polymerisation.

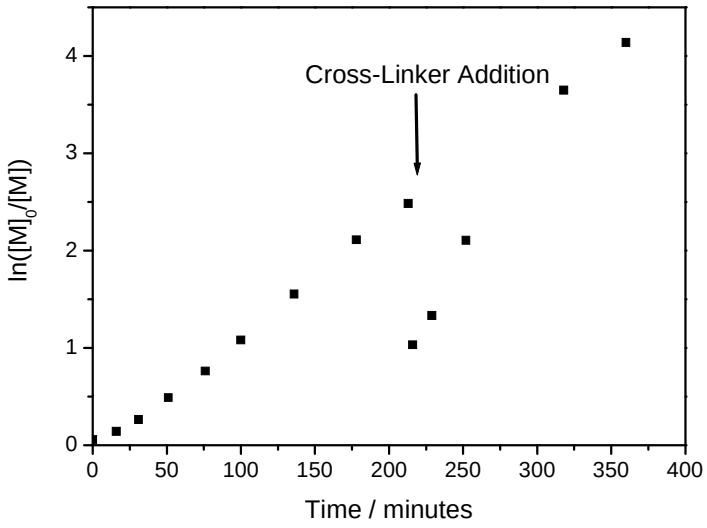

Figure 16 – First order kinetic plot of the synthesis of an arm first star using; [Monomer]:[Cu(I)Br]:[n-propyl pyridylmethanamine]:[ethyl-2-bromisobuyrate]:[EGMDA] – [23]:[1]:[2.1]:[1]:[4] in toluene at 50% solids (by volume) at 90°C.

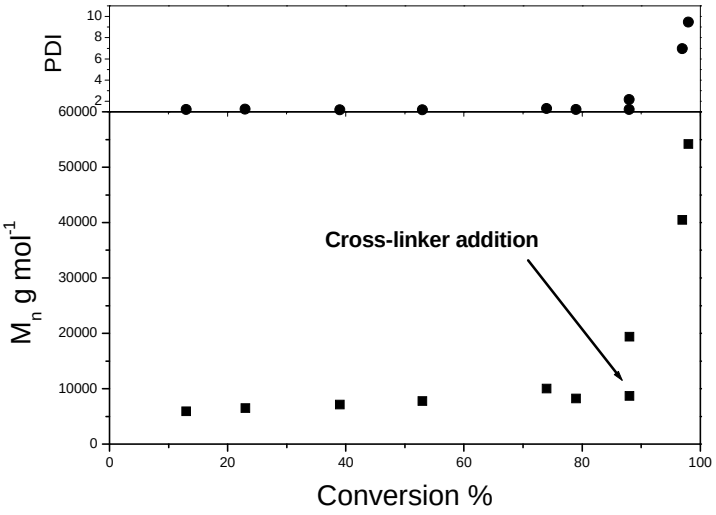

Figure 17 – Molecular weight plot for the synthesis of an arm first star using ratios; [Monomer]:[Cu(I)Br]:[n-propyl pyridylmethanamine]:[ethyl-2-bromisobuyrate]:[EGMDA] – [23]:[1]:[2.1]:[1]:[4] in toluene at 50% solids (by volume) at 90°C.

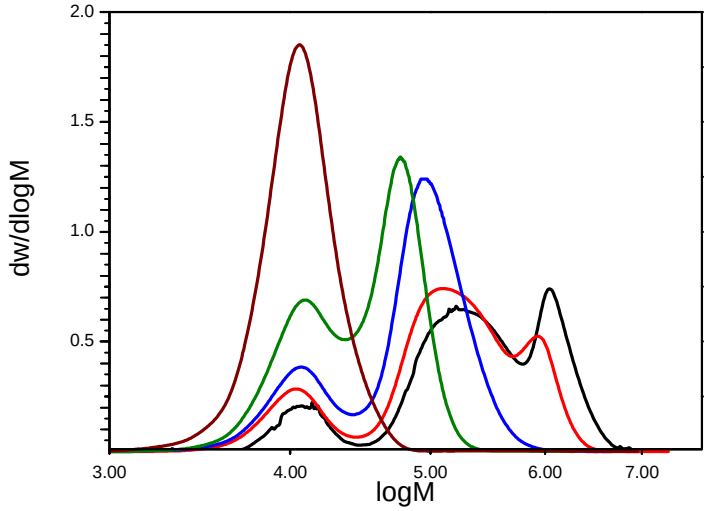

Figure 18 – The evolution of the molecular weight of the polymer shown by GPC with the arm just prior to cross-linker addition on the left, with some evidence of star-star coupling on the right.

2.2 Synthesis of an Arm First star using triethylene glycol dimethacrylate as cross-linker

The existing work by Lubrizol had almost exclusively used EGDMA as cross-linker. Therefore, a longer chain was used to confirm whether Sawamoto's observations that increasing the length of the linking groups between the reactive methacrylates causes intramolecular cyclisation of the cross-linker to dramatically increase.[2] The reaction was carried out to compare the percentage star formation with when EGDMA was used. The first order kinetic was close to the linear plot expected prior to triethylene glycol dimethacrylate (TEGDMA) addition, Figure 19, and the molecular weight also increased linearly with conversion, Figure 20. However, there was a significant amount of the arm left at the end of the polymerisation unreacted into star.

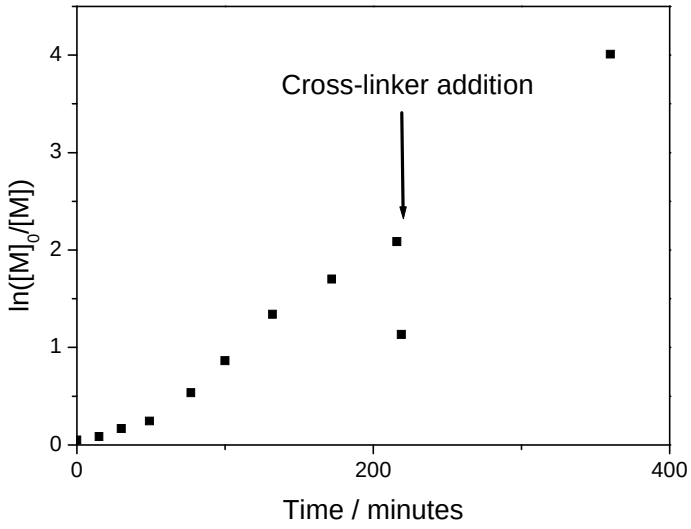

Figure 19 - First order kinetic plot of the synthesis of an arm first star using ratios; [Monomer]:[Cu(I)Br]:[n-propyl pyridylmethanamine]:[ethyl-2-bromisobuyrate]:[triethylene glycol dimethacrylate] – [23]:[1]:[2.1]:[1]:[4] in toluene at 50% solids (by volume) at 90°C.

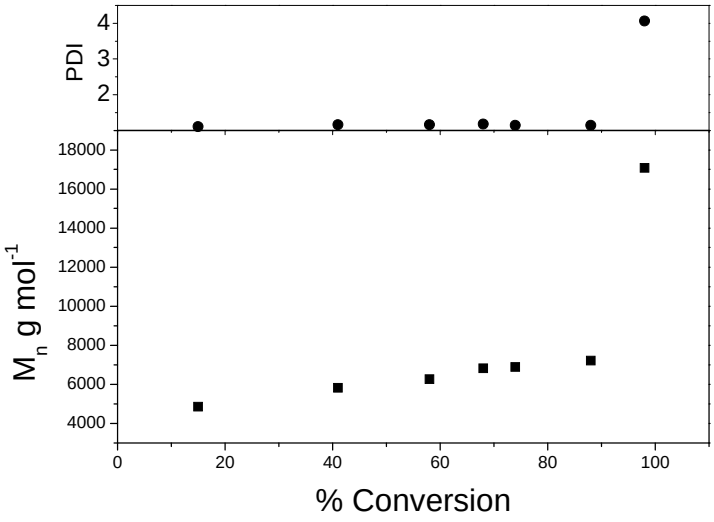

Figure 20 - Molecular weight plot for the synthesis of an arm first star using ratios; [Monomer]:[Cu(I)Br]:[n-propyl pyridylmethanamine]:[ethyl-2-bromisobuyrate]:[triethylene glycol dimethacrylate] – [23]:[1]:[2.1]:[1]:[4] in toluene at 50% solids (by volume) at 90°C.

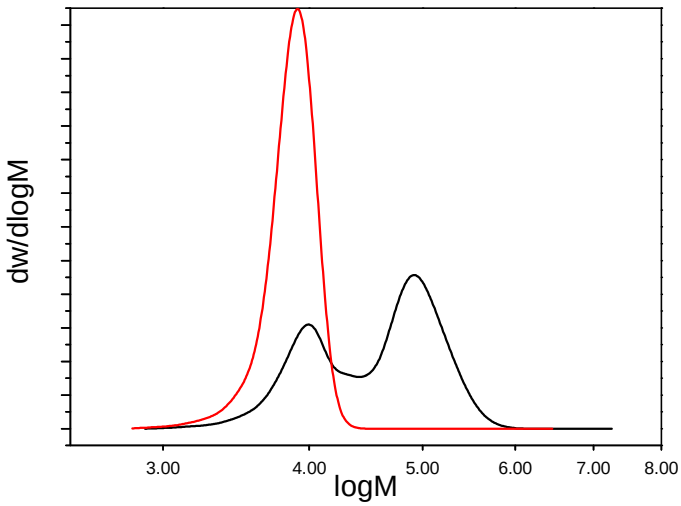

Figure 21 - The difference in the molecular weight of the polymer shown by GPC with the arm just prior to cross-linker addition on the left and the resulting polymer formed on the right.

If the two reactions are compared directly, the difference is more easily seen, Figure 22. When using the EGDMA a significant amount of arms were incorporated into stars, about 90%. However, only 70% was incorporated into stars when using the TEGDMA as cross-linker. This result is in agreement with Sawamoto's original observations; the triethylene glycol spacer between the reactive methacrylate groups is not suitable for use as a cross-linker to produce high arm incorporation into star.

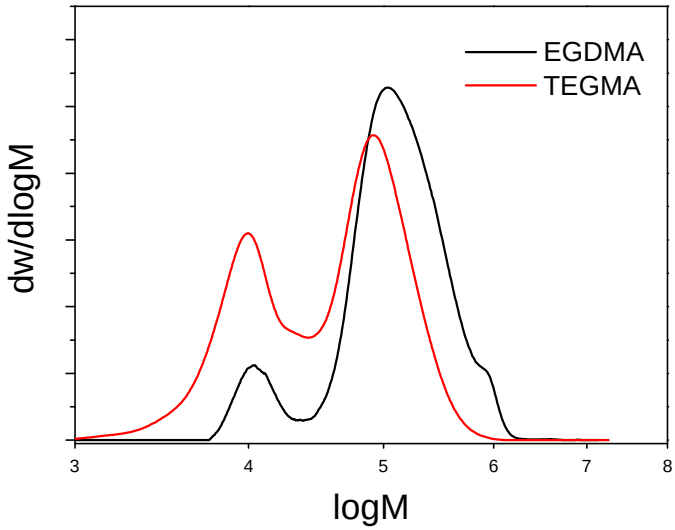

Figure 22 – Comparison of the different amount of arm incorporation using two different cross-linkers.

2.3 Synthesis of a lower molecular weight Arm First star polymer

After the initial success of polymerising an arm first star when targeting a M_n = 5000 g mol^{-1} arm, the next step was to attempt the polymerisation of a shorter arm, in this case

M_n = 2500 g mol^{-1}. The reaction conditions were kept the same where possible and not knowing the optimal ratio of cross-linker to initiator, the amount of cross-linker with respect to the initiator was halved from 4:1 to 2:1. The cross-linker was again added at 90% original monomer conversion.

The resulting polymerisation was again of a living nature prior to the addition of the cross-linker, Figure 23, after this it deviated from the expected linear plot. The molecular weight also increased linearly with conversion before the addition of cross-linker, Figure 24.

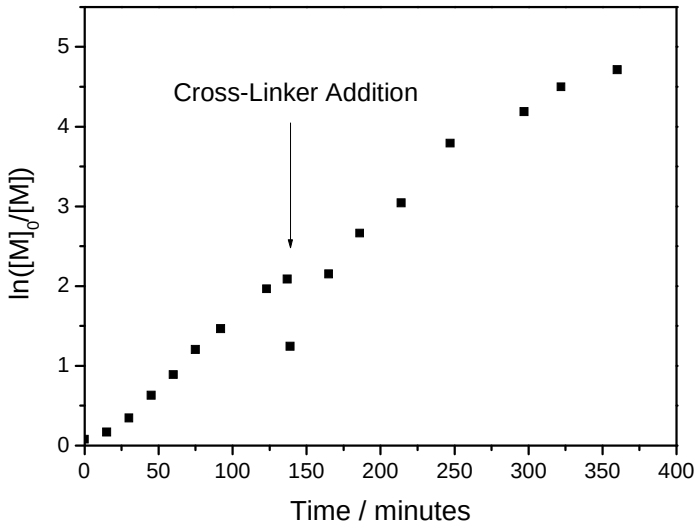

Figure 23 - First order kinetic plot of the synthesis of an arm first star using ratios; [Monomer]:[Cu(I)Br]:[*n*-propyl pyridylmethanamine]:[ethyl-2-bromisobuyrate]:[EGMDA] – [11]:[1]:[2.1]:[1]:[2] in toluene at 50% solids (by volume) at 90°C.

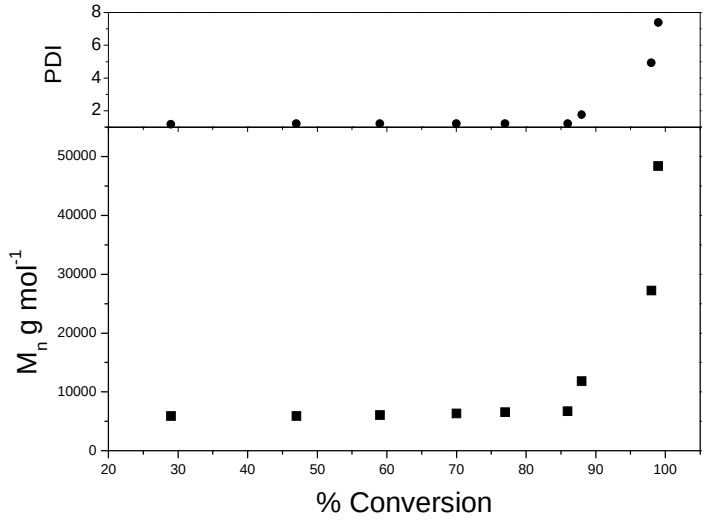

Figure 24 - Molecular weight plot for the synthesis of an arm first star using ratios; [Monomer]:[Cu(I)Br]:[*n*-propyl pyridylmethanamine]:[ethyl-2-bromisobuyrate]:[EGMDA] – [11]:[1]:[2.1]:[1]:[2] in toluene at 50% solids (by volume) at 90°C.

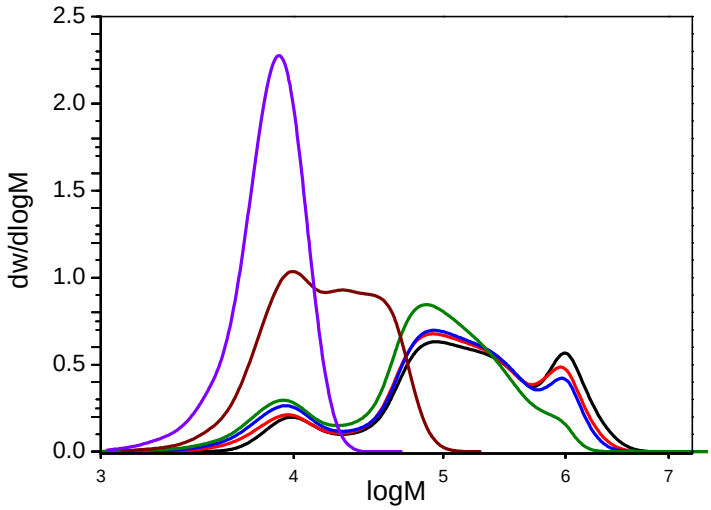

Figure 25 - The evolution of the molecular weight of the polymer shown by GPC with the arm just prior to cross-linker addition on the left, with some evidence of star-star coupling on the right.

The polymer once again formed a star very quickly after the addition of the cross-linker. It was left to react for a further 250 minutes after which a third peak had appeared on the GPC trace which can be attributed to that of star-star coupling, similar to that in the M_n = 5000 g mol^{-1}, Figure 25.

2.4 Synthesis of a higher molecular weight arm first star polymer

The length of the chain targeted was doubled from M_n = 5000 g mol^{-1} to M_n = 10000 g mol^{-1} with the cross-linker-to-initiator ratio kept the same as for the M_n=5000 g mol^{-1} reaction at 4:1 as it was suspected that addition of more cross-linker would cause gelation.

The polymerisation was as for previous experiments of a living nature prior to cross-linker addition. It had a linear first order kinetic plot, Figure 26, and the molecular weight increased linearly with conversion, Figure 27. However, these suspicions about the amount of cross-linker were incorrect and the 4:1 ratio used was demonstrated to promote <90% conversion of arm into star. This is demonstrated in Figure 28 where a large proportion of the arm remains at the end of the reaction.

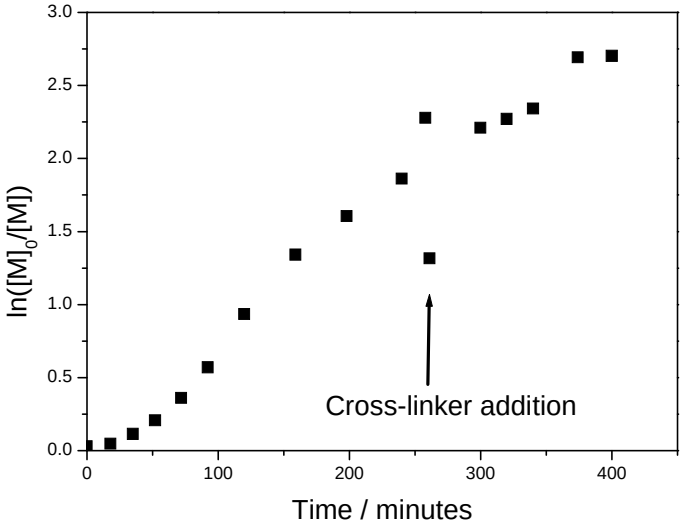

Figure 26 - First order kinetic plot of the synthesis of an arm first star using ratios; [Monomer]:[Cu(I)Br]:[*n*-propyl pyridylmethanamine]:[ethyl-2-bromisobuyrate]:[EGMDA] – [46]:[1]:[2.1]:[1]:[4] in toluene at 50% solids (by volume) at 90°C.

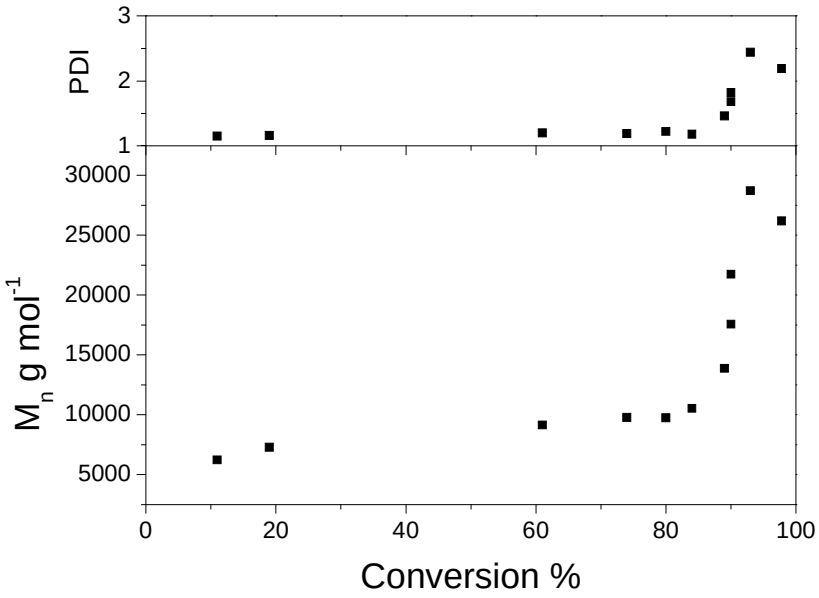

Figure 27- Molecular weight plot for the synthesis of an arm first star using ratios; [Monomer]:[Cu(I)Br]:[*n*-propyl pyridylmethanamine]:[ethyl-2-bromisobuyrate]:[EGMDA] – [46]:[1]:[2.1]:[1]:[4] in toluene at 50% solids (by volume) at 90°C.

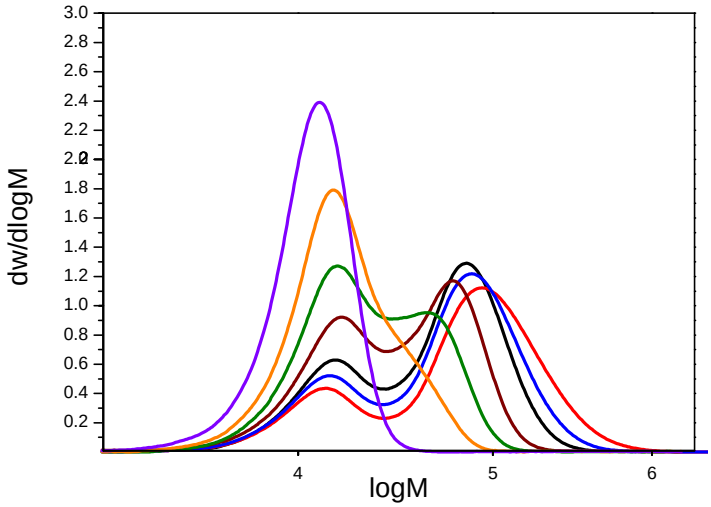

Figure 28 - The evolution of the molecular weight of the polymer shown by GPC with the arm just prior to cross-linker addition on the left. Here a large proportion of the arm remains at the end of the reaction with no star-star coupling observed.

2.5 Synthesis of a higher molecular weight Arm First star polymer with more cross-linker

The observation can be made here that the ratio between cross-linker and the length of the chain has a dramatic effect on the resulting polymer. When sufficient cross-linker is added, about 90% of the arms are reacted to form the desired star as shown in the first two reaction examples. However, when insufficient cross-linker is used, only 70% of the arms are converted to star. Therefore, the previous reaction was repeated and more cross-linker was added to the reaction, at an 8:1 crosslinker-to-initiator ratio.

In this reaction the polymerisation was once again of a living nature prior to cross-linker addition with a linear first order kinetic plot, Figure 29, and a linear growth of molecular weight with conversion of monomer, Figure 30. With the increased amount of cross-linker, the polymerisation formed a greater amount of star, approximately 88%, Figure 31.

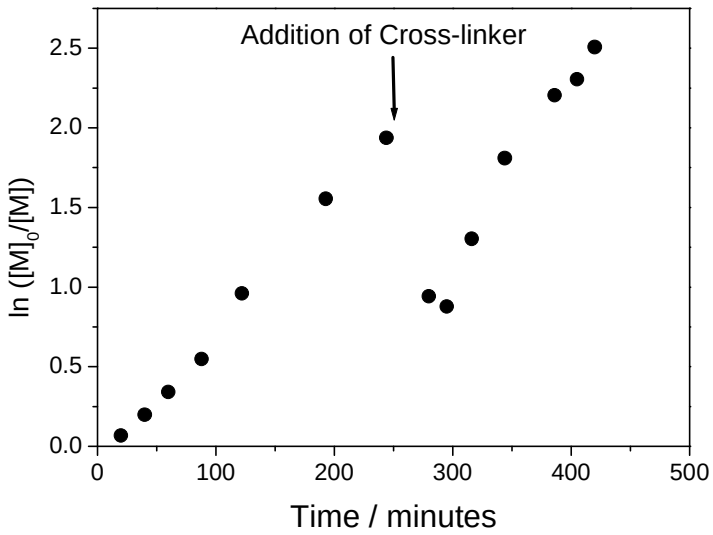

Figure 29 - First order kinetic plot of the synthesis of an arm first star using ratios; [Monomer]:[Cu(I)Br]:[*n*-propyl pyridylmethanamine]:[ethyl-2-bromisobuyrate]:[EGMDA] – [46]:[1]:[2.1]:[1]:[8] in toluene at 50% solids (by volume) at 90°C.

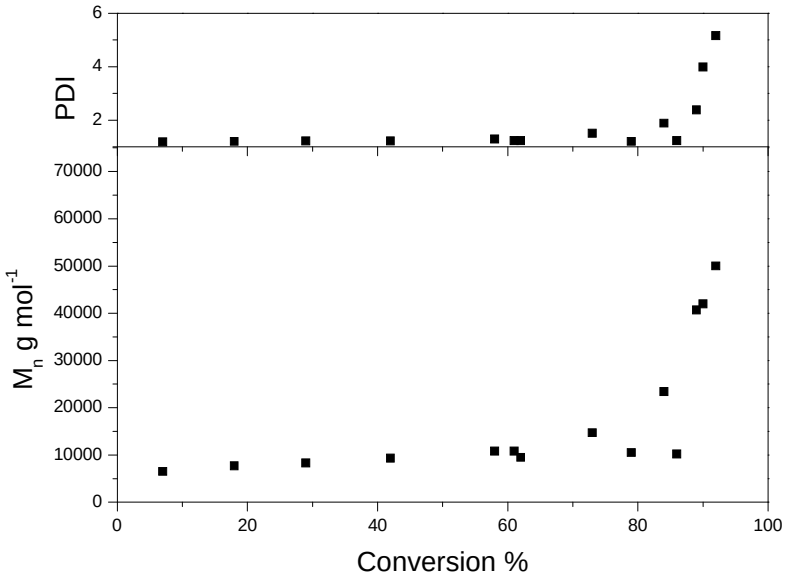

Figure 30 - Molecular weight plot for the synthesis of an arm first star using ratios; [Monomer]:[Cu(I)Br]:[*n*-propyl pyridylmethanamine]:[ethyl-2-bromisobuyrate]:[EGMDA] – [46]:[1]:[2.1]:[1]:[8] in toluene at 50% solids (by volume) at 90°C.

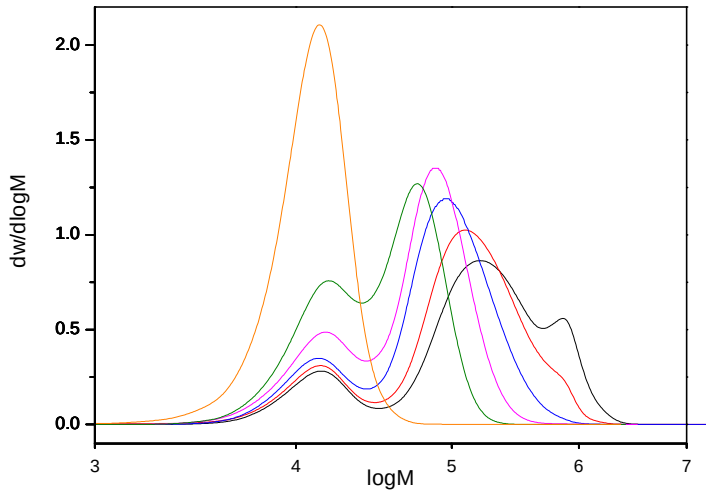

Figure 31 - The evolution of the molecular weight of the polymer shown by GPC with the arm just prior to cross-linker addition on the left, with some evidence of star-star coupling on the right.

2.6 Summary of initial results

The initial polymerisation carried out to synthesise arm first star polymers were mostly highly successful. The reactions demonstrated that it is possible, using this system and combination of monomers and cross-linker, that stars will form and with a high degree of incorporation of the original arm. The results are summarised in Table 1. The results show that the amount of cross-linker relative to the length of the chain targeted is key to give the high arm-incorporation into star.

Target arm M_n g mol^{-1}	Amount X-link	Time / min	% Conversion	M_n g mol^{-1}	M_w g mol^{-1}	PDI	% Arms in Star
5	4	360	98	54200	513400	9.47	93
2.5	2	360	99	48400	357800	7.37	93
10	4	474	98	26200	57400	2.19	70
10	8	420	92	50000	258400	5.16	87

Table 1 – Summary of the initial polymerisation data for the synthesis of arm first stars.

2.7 The use of Experimental Design to optimise the synthesis of Arm First stars

Results from work by Lubrizol suggested that the percentage conversion of the polymerisation when the cross-linker is added is the key to obtaining the desired high arm incorporation into star. This is also demonstrated by a number of authors who use this factor to vary the structure of their arm first stars.[13, 37] With this in mind, a full list of potential input factors was drawn up.

2.8 Input Factors

The input factors were first listed in full to attempt to choose between them. They were:

1. Reaction temperature

   Although this factor could be varied, ATRP has a significant body of literature where the polymerisations are carried out at 90°C and therefore in this study this temperature was be used in all experiments
2. Reaction time

   This factor can be used both as an input or an output. In order to simplify the design this kept constant.
3. Type of initiator

   The initiator can be used to introduce a wide range of functionality into the polymer. However, for this study a commercially viable initiator is being used to keep cost down and make the process as industrially applicable as possible.
4. Type of monomer ($C_{12/15}$ MA with either *n*-BMA or 2-ethyl,hexyl methacrylate)

   n-BMA was chosen as it was used in the test reactions and therefore, to minimise the number of further test reactions no changes were made here.
5. Type of cross-linker (e.g. acrylate, methacrylate, styrenic)

   A methacrylate cross-linker, ethylene glycol dimethacrylate, was selected as it is widely used in the literature and so its relative reactivites with other monomers are known.
6. The length of the chain between the vinyl groups in the cross-linker

   The spacer between methacrylate groups could prove crucial in forming stars and therefore ideally would be varied. Theoretically a longer spacer would give greater chance that the pendant methacrylate group is not hindered by the other monomers and therefore should have a higher chance of reacting.
7. Percentage conversion of original monomer when cross-linker is added

   Existing literature suggests varying this factor has a dramatic effect on the end polymer and therefore it was selected as an input factor.
8. Amount of cross-linker (cross-linker:initiator e.g. 2:1)

   Existing literature also suggests varying this factor has a dramatic effect on the end polymer and therefore it was selected as an input factor.
9. Target length of the polymer chain (DP)

   Existing literature also suggests varying this factor has a dramatic effect on the end polymer and therefore it was selected as an input factor.

Out of this initial process three input factors were chosen:

1. Target length of the polymer chain (DP)
2. Amount of cross-linker (cross-linker:initiator e.g. 2:1)
3. Percentage conversion of original monomer when cross-linker is added

2.9 Output Factors or Responses

The full list of output factors are:

1. Molecular weight of the polymer
2. Percentage conversion of all of the monomer in the reaction pot
3. Percentage conversion of polymer arms into stars
4. Viscosity data (inc VI, low temp and SSI)

The factors 1-3 are immediately available by simple testing in the laboratory; however, factor 4 requires the samples to be sent off for testing at Lubrizol and therefore this data will be added to the design at a later date should it be possible.

2.10 The initial design

Now that the input factors were set, the maximum and minimum values needed to be set. These values would represent the upper and lower extremities of the design and provide the boundaries within which it would operate.

1. Target length of the polymer chain (DP)
   Lower = 12, Upper = 46
2. Amount of cross-linker (cross-linker:initiator e.g. 2:1)
   Lower = 2:1, Upper = 8:1
3. Percentage conversion of original monomer when cross-linker is added
   Lower = 60%, Upper = 90%

The values were based on the initial experiments and the previous related work described in the introduction and shown graphically in Figure 32. A full factorial design with a full set of repeats was initially chosen to give the best potential for validating results and giving some predictability from the design.

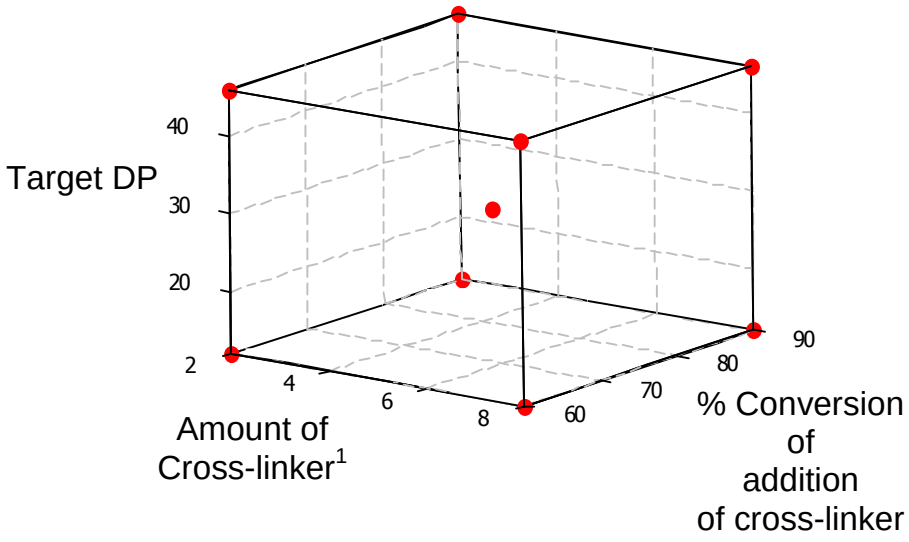

Figure 32 – The initial design space with centre point to be investigated, [1] with respect to initiator, e.g. 2:1, cross-linker:initiator

These nine experiments were carried out and the results, Table 2, the tenth experiment is commented upon later. The initial thing to note is that four experiments produced an insoluble polymer gel. Three of these experiments all had high cross-linker:initiator ratios (8:1) while experiment 9 was 5:1, while the conversion of addition changed from 60% to 75% to 90% and the DP varied from 12 to 29 to 46. The mid point was also a reaction that produced a gel, again with a relatively high amount of cross-linker.

Two other experiments produced a soluble polymer at the end of the reaction but with very little cross-linking observed, experiments 2 and 4. For both of these, the amount of cross-linker was 2 and the target DP = 46. These two results indicate alone that there was insufficient cross-linker in these reactions to give cross-linking of the polymer chains to produce a star architecture.

Exp No.	Input factors			Output factors					
	Target DP	% Conversion	Amount X-link[1]	Time / min	% Conversion	M_n g mol^{-1}	M_w g mol^{-1}	PDI	% Arms in Star
1	12	60	2	360	98	36800	297700	8.09	90.9
2	46	60	2	396	95	18100	30100	1.7	33.0
3	12	90	2	360	99	35700	120300	3.37	86.2
4	46	90	2	390	91	14600	20200	1.38	16.4
5	12	60	8	78	-	-	-	-	-
6	46	60	8	245	-	-	-	-	-
7	12	90	8	140	-	-	-	-	-
8	46	90	8	359	92	59300	354400	5.98	86.1
9	29	75	5	269	-	-	-	-	-
10	29	85	5	360	96	77200	494000	6.39	87.2

[1] with respect to initiator, e.g. 2:1, cross-linker:initiator

Table 2 – A summary of the nine initial experiments carried out for the experimental design. Where results show -, the reaction gelled and therefore no end point result for the polymer was obtainable due to its total insolubility in any solvent

There were, however, three reactions that produced polymers that were close to the targets of the design, experiments numbers 1, 3 and 8. They all have close to 90% conversion of arm into star, high overall monomer conversion with a range of molecular weights.

Of particular interest here are reactions 9 and 10. When attempting to carry out experiment 9 the cross-linker was added 10% monomer conversion late, at 85% monomer conversion. This resulted in experiment 10 which was not part of the initial run list. This reaction did not gel; producing polymer with high monomer conversion and excellent conversion of arm into star. When the reaction was repeated with the cross-linker being added at 75% conversion, the reaction gave an insoluble gel. These two reactions indicate that the conversion of addition of the cross-linker is indeed key to obtaining high arm incorporation into star and that gelation can be suppressed by adding the cross-linker later on in the reaction.

However, other than these initial generic observations, no firm conclusions were drawn due to the large proportion of experiments that produced no results. Therefore, the repeat run was abandoned and further experiments added to the design to fill in the gaps between the experiments that gelled and those that did not. The region of gelation is best shown in Figure 33. The blue dots show that the reactions that gelled were in a similar reaction space and therefore there must be a relationship between the factors that describes this phenomenon

The additional experiments were aimed to discover where the region of gelation stops and where the region of soluble polymeric material starts. To this end eight further experiments were carried out.

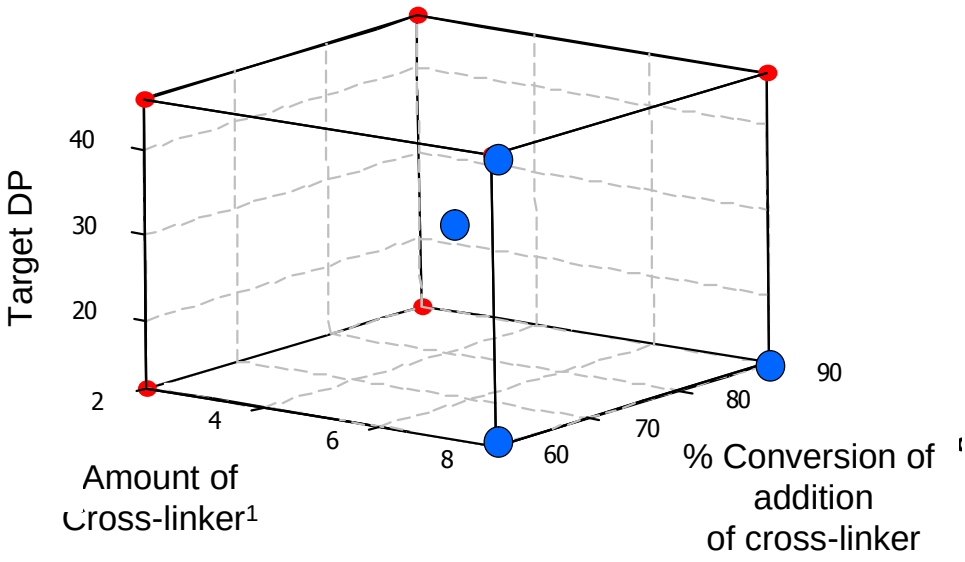

Figure 33 - The initial design space with centre point that was investigated. The blue dots show the reactions that gelled. [1] with respect to initiator, e.g. 2:1, cross-linker:initiator

2.11 Additional Experimental Design Runs

The eight reactions were placed to further define the region of gelation Figure 34 and Table 3. In this series three out of eight reactions produced no results due to formation of gel. Those reactions, experiment numbers 12, 13 and 14, all had a medium or high amount of cross-linker with respect to initiator, targeting a full range of DPs.

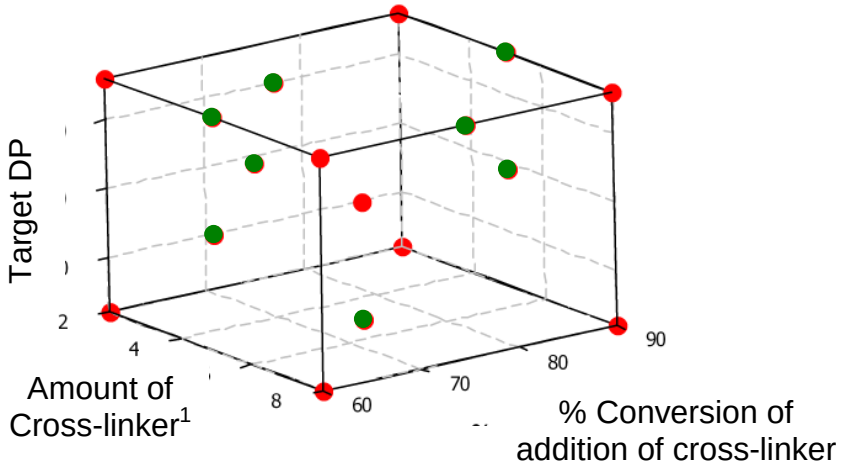

Figure 34 The design space with the original reaction shown in read and the eight additional reactions shown in green.[1] with respect to initiator, e.g. 2:1, cross-linker:initiator

Exp No.	Input factors			Output factors					
	Target DP	% Conversion	Amount X-link[1]	Time / min	% Conversion	M_n g mol^{-1}	M_w g mol^{-1}	PDI	% Arms in Star
11	46	70	4	380	93	32600	80200	2.46	78.2
12	46	75	8	320	-	-		-	-
13	29	60	5	105	-	-	-	-	-
14	12	75	5	178	-	-	-	-	-
15	29	90	5	352	97	61600	576000	9.34	90.0
16	29	75	2	355	98	21900	39900	1.82	54.3
17	46	60	5	397	95	37000	95000	2.56	75.7
18	46	90	5	392	94	35900	73000	2.38	72.5

[1] with respect to initiator, e.g. 2:1, cross-linker:initiator

Table 3 - Summary of additional experiments carried out for the experimental design. Where results show -, the reaction gelled and therefore no end point result for the polymer was obtainable due to its total insolubility in any solvent

A single experiment produced a very good result, 15, with 90% arm incorporation into star. That polymerisation also had high overall monomer conversion. The other four reactions did not form enough star polymer to be considered a good output, all having < 80% star formed.

2.12 Analysis of the Non-Gelled Polymerisations

When all the results are tabulated and compared, the relationship between the amount of the cross-linker added and the target DP of the polymer chain can be more clearly observed, Table 4. All the results which produced a gel had a large amount of cross-linker compared to the target DP. The results which did not form a large percentage of star had a low amount of cross-linker compared to the target DP. Therefore, by dividing the target DP by the amount of cross-linker a more defined relationship can be observed.

The samples that gelled, 5, 6, 7, 9, 12, 13 and 14, all had a ratio of target DP to amount of cross-linker of < 6. For the majority of those samples which did not gel, this ratio of target DP to amount of cross-linker was > 6. This observation suggests that the reason for the gelation was an excessive amount of cross-linker in the system for the length of chain being formed. In the reactions which had a small amount of cross-linker relative to the targeted degree of polymerisations all had little arm incorporation into star. This was due to insufficient reactive sites on the polymer backbone to promote star formation, Figure 35.

An alternative analysis is if the dp/xlink is multiplied by the % conversion of addition. This suggests that the reactions where this number is below 4.4 (except reaction 1) they gel, while those above do not. The accuracy of this method find would need to be further explored by repeating experiment 1 and several points around it to examine why it did not gel.

Exp No.	Input factors: Target DP	Input factors: % Conversion	Input factors: Amount X-link[1]	Time / min	Output factors: % Conversion	Output factors: M_n g mol^{-1}	Output factors: M_w g mol^{-1}	Output factors: PDI	Output factors: % Arms in Star	- $\frac{T\ \arg et\ DP}{Amount\ \ of\ X\ -\ link}$	$\frac{T\ \arg et\ DP}{Amount\ \ of\ X\ -\ link} * \%Conv$
1	12	60	2	360	98	36800	297700	8.09	91	6.00	3.60
2	46	60	2	396	95	18100	30100	1.7	33	23.00	13.80
3	12	90	2	360	99	35700	120300	3.37	86	6.00	5.40
4	46	90	2	390	91	14600	20200	1.38	16	23.00	20.70
5	12	60	8	78	-	-		-	-	1.50	0.90
6	46	60	8	245	-	-		-	-	5.75	3.45
7	12	90	8	140	-	-		-	-	1.50	1.35
8	46	90	8	359	92	59300	354400	5.98	86	5.75	5.17
9	29	75	5	269	-	-		-	-	5.80	4.35
10	29	85	5	360	96	77200	494000	6.39	87	5.80	4.93
11	46	70	4	380	93	32600	80200	2.46	78	11.50	8.05
12	46	75	8	320	-	-		-	-	5.75	4.31
13	29	60	5	105	-	-		-	-	5.80	3.48
14	12	75	5	178	-	-		-	-	2.40	1.80
15	29	90	5	352	97	61600	576000	9.34	90	5.80	5.22
16	29	75	2	355	98	21900	39900	1.82	54	14.50	10.87
17	46	60	5	397	95	37000	95000	2.56	76	9.20	5.52
18	46	90	5	392	94	35900	73000	2.38	73	9.20	8.28

[1] with respect to initiator, e.g. 2:1, cross-linker:initiator

Table 4 - A summary of all of the experiments carried out for the experimental design. Where results show -, the reaction gelled and therefore no end point result for the polymer was obtainable due to its total insolubility in any solvent

When the Target DP is increased from 12 to 46, in order to keep the arm incorporation into star above 85%, the amount of cross-linker must also be increased, Figure 36. The results circled in red produced exclusively gels where there was an excess of cross-linker for the length of chain. The results circled in green produced polymer with very high arm incorporation into star. As the target ratio of DP to amount of cross-linker increased the amount of arm incorporation decreased almost linearly.

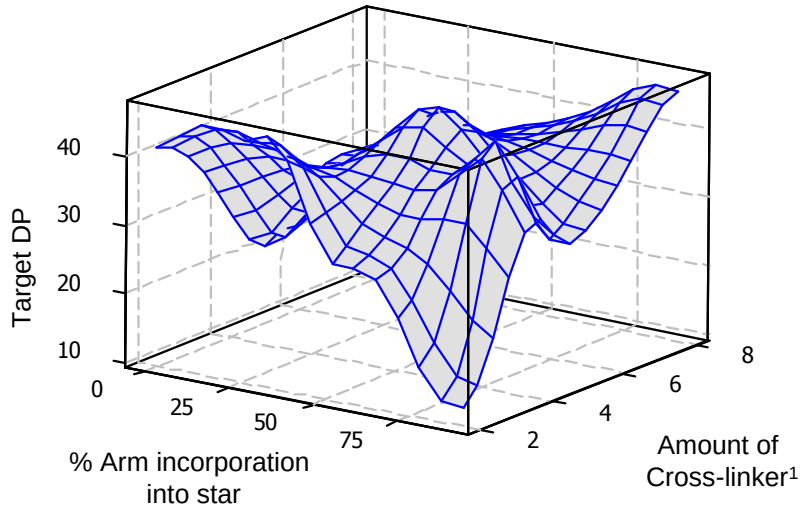

Figure 35 – The relationship between the target DP and the amount of cross-linker added to the polymerisation can be seen here. As the length of chain targeted increases more cross-linker must be added to form a large proportion of star.

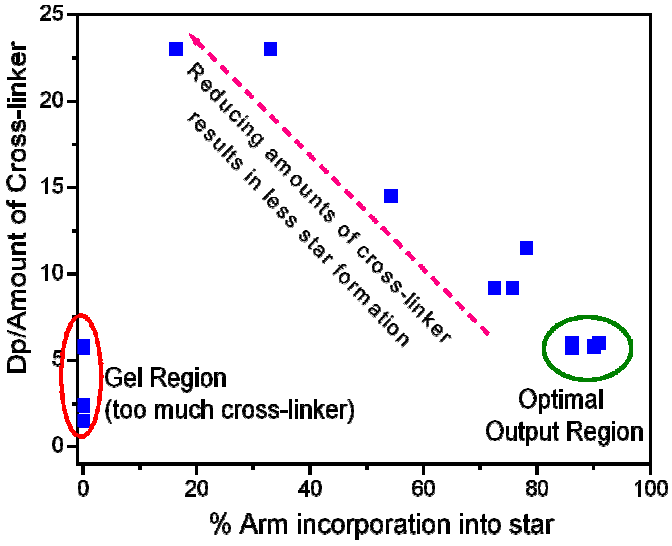

Figure 36 – This graph demonstrates the relationship between the target Dp/amount of cross-linker and how much arm is incorporated into the star polymer.

There are a few anomalies with experiments 8, 10 and 15 all have a target DP/amount of cross-linker of < 6 and therefore, according to the proposed hypothesis, should gel, however, they did not. Experiments 9 and 10 allow a potential explanation for this with

Exp. 9 gelling when a 5:1 ratio of cross-linker to initiator was used when targeting a DP = 29 and adding the cross-linker at 75% conversion, corresponding to 4 hours 29 minutes of polymerisation time. The only difference between this and exp. 10 is that the cross-linker was added at 85% conversion. This lead to a polymer being formed with 87% arm incorporation into star.

These two polymerisations suggest that although for certain polymerisations there might be too much cross-linker added for the length of chain being targeted, simply adding the cross-linker to the reaction later will suppress gelation.

3 Conclusions

The use of experimental design has allowed the successful optimisation of the synthesis of arm first star polymers via ATRP. The design demonstrated a key ratio between the factors *Target DP* and *Amount of cross-linker*, where by dividing the former by the later a key relationship is found. The ideal number here was *Target DP*/*Amount of cross-linker = 6.* This produced polymers with high arm incorporation into star. By moving much above or below this number, either the reaction gelled (< 6) or did not form much star (> 6). The point at which the cross-linker was added to the reaction was also found to influence the resulting polymer. However, this was less quantifiable. As a rule of thumb; the reactions which gelled and had a *Target DP*/*Amount of cross-linker<6,* addition of the cross-linker to the reaction later could in some cases suppress gelation. Typically, by delaying the addition by 10% monomer conversion was found to be sufficient in a number of cases.

This was found to be easily calculated by multiplying the above ratio by the % conversion. The resulting output suggested that if the calculated value was below 4.4, the reaction gelled, when it was above this value they did not. This ratio results in a similar predictive output in that the closer this output is to 4.4, the higher the conversion of polymeric arms into star polymers.

4 Experimental

4.1 Materials and Instrumentation.

All reagents were purchased from Aldrich and used without further purification unless otherwise stated, with the exception of $C_{12\text{-}15}$ methacrylate which was provided by the Lubrizol Corporation (based on Neodol 25). All solvents were purchased from Fisher Chemicals. Monomers were deoxygenated with N_2 for 45 minutes prior to use. Toluene was also degoxygenated with N_2 for 45 minutes prior to use.

Gel Permeation chromatography (GPC) was carried out using a Polymer Laboratories (PL) modular system equipped with a differential refractive index (DRI) detector calibrated with linear poly (methyl methacrylate) (PMMA) standards (M_p = 200–1.577×10^6 g mol^{-1}), obtained from Polymer Laboratories, except for the methyl methacrylate dimer, trimer and tetramer which were prepared by catalytic chain transfer polymerisation at the University of Warwick. The mobile phase used was 95% $CHCl_3$, 5% triethylamine and the elution time was standardised against toluene with a flow rate of 1.0 mL min^{-1}. The system was equipped with a PL-gel 5 μm (50 · 7.5 mm) guard column and two PL-gel 5 μm (300 · 7.5 mm) mixed C columns. ^1H and ^{13}C NMR spectra were recorded on a Bruker DPX400 spectrometer using deuterated solvents from Aldrich. Infra red absorption spectra were recorded on a Brucker Vector 22 spectrometer equipped with a Golden Gate diamond attenuated total reflection (ATR) sample platform.

4.2 Standard Procedure for Peak Deconvolution of a Multi-modal GPC trace

The relative arm incorporation into the stars was found by deconvoluting the multimodal GPC traces. Figure 37 is an example of a multimodal GPC trace which has had a multi-peak Gaussian analysis carried out on it using Microcal Origin. From the resulting deconvoluted peaks, the M_n, M_w and PDI can be calculated along with the relative areas of the peaks.

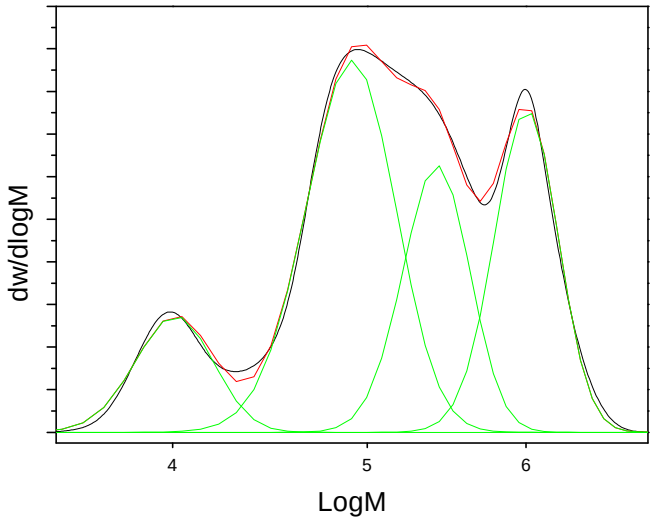

Figure 37 – A multimodal GPC trace showing the Gaussian fit in green for 4 peaks.

4.3 Copper mediated living radical polymerisation – General procedure for Arm First stars

All polymerisation were carried out using either Schlenk apparatus or a 3 necked round bottomed flask – whichever was more appropriate – under dry nitrogen. The monomer mixture used was 70wt% $C_{12\text{-}15}$ MA 30wt% *n*-butyl methacrylate. Typically all solids were added to the pre-dried reaction vessel prior to sealing with a rubber septum. The vessel was then either purged with nitrogen, in the case of the rbf, or evacuated and flushed with nitrogen three times, in the case of the Schlenk tubes, so as to remove oxygen. All remaining liquid reagents, apart from the ligand, which has been deoxygenated with nitrogen were added to the reaction vessel via dried, degassed syringes and the mixture further deoxygenated by three freeze-pump-thaw cycles, where practical. The reaction vessel was brought up to reaction temperature in a stirred, thermostated oil bath and the deoxygenated ligand added. Samples for kinetic data were taken using degassed syringes and polymer conversion data obtained by ^{1}H NMR. Molecular weight data was obtained from GPC. The samples were monitored for monomer conversion and at a given predetermined point a cross-linker such as EGDMA added to cause star formation. No additional solvent was added. Reactions were stopped by exposure to air and by further dilution in the reaction solvent. Polymers were typically purified by stirring with basic alumina to remove the copper and then filtered over a bed of celite to remove the solids. The dilute polymer-solvent mixture was concentrated *in vacuo* and precipitated by stirring in IPA:methanol (9:1) for 1 hour before cooling using a dry-ice acetone mixture to cause precipitation of the polymer. The IPA-methanol mixture was decanted off and the viscous polymer and washed with

cold IPA (approximately 100 ml × 3) Polymers were collected after precipitation as a viscous liquid and dried in a vacuum oven at 40°C overnight.

4.4 Purification of copper (I) bromide

Copper (I) bromide was purified by a method based on that of Keller and Wycoff.[38] Typcially copper (I) bromide (50 g, 0.35 mol) was placed in a large beaker and the solid washed with glacial acetic acid (300 ml), absolute ethanol (300 ml) and anhydrous diethyl ether (300 ml) ensuring that the copper species was exposed to oxygen for the minimum time possible. 38.2 g of an off-white coloured powder was obtained and dried at 100°C under vacuum overnight.

4.5 Synthesis of *N*-propyl-2-pyridiylmethanamine

N-Propyl amine (126 g, 1.77 mol) was slowly added drop wise to a stirred solution of pyridine-2-carboxaldehyde (190 g, 2.15 mol) in diethyl ether (ca. 600 ml) at 0 °C and stirred for four hours. Anhydrous magnesium sulphate (ca. 100 g) was added and the solution stirred at ambient temperature for two hours. The solution was filtered and the solvent removed *in vacuo* to yield an orange oil. This oil was distilled under reduced pressure to yield N-n-propyl-2-pyridyl-methanimne as a clear yellow liquid (boiling range 77-79 °C at 10^{-1} Torr). Obtained 158.21 g (60%).

^{1}H NMR δ (ppm) - 8.63 (d, 1H, J=3.5 Hz, Pyr-H), 8.39 (s, 1H, Pyr-CH=N-), 8.00 (d, 1H, J=7.8 Hz, Pyr-H), 7.69 (t, 1H, J=7.8 Hz, Pyr-H), 7.27 (t, 1H, J=4.6 Hz, Pyr-H), 3.64 (t, 2H, J = 7.6 Hz, -C=N-C$\underline{H}_2$-), 1.76 (sextet, 2H, J = 7.3 Hz, -CH_2-C$\underline{H}_2$-CH_3-), 0.70 (t, 3H, J = 7.5 Hz, -CH_2-C$\underline{H}_3$).

^{13}C NMR δ (ppm) -161.0 (Pyr-$\underline{C}$H=N-), 154.1, 148.7, 135.8, 123.9, 120.5 (Pyr), 62.6 (-C=N-$\underline{C}H_2$-), 22.3 (-CH_2-$\underline{C}H_2$-CH_3-), 11.3 (-CH_2-$\underline{C}H_3$).

IR (solid, ATR cell) υ (cm^{-1}) 3054, 3009 (Ar C-H str.), 2961-2834 (Alkyl C-H str.), 1651
(C=N str.), 1587, 1568, 1468, 1436 (Ar ring str.).

CHN Analysis: Theoretical C-72.9%, H-8.2%, N=18.9%, Found C-71.1%, H-8.0%, N-18.5%

5 References

1. J. Xia, X. Zhang and K. Matyjaszewski, *Macromolecules*, 1999, **32**, 4482-84.
2. K.-Y. Baek, M. Kamigaito and M. Sawamoto, *Macromolecules*, 2001, **34**, 215-21.
3. K.-Y. Baek, M. Kamigaito and M. Sawamoto, *J. Polym. Sci., Part A: Polym. Chem.*, 2002, **40**, 633-41.
4. L. A. Connal, P. A. Gurr, G. G. Qiao and D. H. Solomon, *J. Mater. Chem.*, 2005, **15**, 1286-92.
5. M. Kamigaito, T. Ando and M. Sawamoto, *Chem. Rev.*, 2001, **101**, 3689-745.
6. K. Matyjaszewski and J. Xia, *Chem. Rev.*, 2001, **101**, 2921-90.
7. A. Limer and D. M. Haddleton, *Prog. React. Kinet. Mech.*, 2004, **29**, 187-241.
8. X. Zhang, J. Xia and K. Matyjaszewski, *Macromolecules*, 2000, **33**, 2340-45.
9. K.-Y. Baek, M. Kamigaito and M. Sawamoto, *J. Polym. Sci., Part A: Polym. Chem.*, 2002, **40**, 1972-82.
10. K.-Y. Baek, M. Kamigaito and M. Sawamoto, *J. Polym. Sci., Part A: Polym. Chem.*, 2002, **40**, 1937-44.
11. D.-H. Han and C.-Y. Pan, *Polymer*, 2006, **47**, 6956-62.
12. L. A. Connal, R. Vestberg, C. J. Hawker and G. G. Qiao, *Macromolecules*, 2007, **40**, 7855-63.
13. K.-Y. Baek, M. Kamigaito and M. Sawamoto, *Macromolecules*, 2001, **34**, 7629-35.
14. K.-Y. Baek, M. Kamigaito and M. Sawamoto, *Macromolecules*, 2002, **35**, 1493-98.
15. T. Terashima, M. Kamigaito, K.-Y. Baek, T. Ando and M. Sawamoto, *J. Am. Chem. Soc.*, 2003, **125**, 5288-89.
16. T. Terashima, M. Ouchi, T. Ando, M. Kamigaito and M. Sawamoto, *Macromolecules*, 2007, **40**, 3581-88.
17. J.-F. Lutz and A. Hoth, *Macromolecules*, 2006, **39**, 893-96.
18. J.-F. Lutz, O. Akdemir and A. Hoth, *J. Am. Chem. Soc.*, 2006, **128**, 13046-47.
19. L. A. Connal, Q. Li, J. F. Quinn, E. Tjipto, F. Caruso and G. G. Qiao, *Macromolecules*, 2008, **41**, 2620-26.
20. M. Spiniello, A. Blencowe and G. G. Qiao, *J. Polym. Sci., Part A: Polym. Chem.*, 2008, **46**, 2422-32.
21. J. Du and Y. Chen, *J. Polym. Sci., Part A: Polym. Chem.*, 2004, **42**, 2263-71.
22. J. Du and Y. Chen, *Macromolecules*, 2004, **37**, 3588-94.
23. H. Gao, N. V. Tsarevsky and K. Matyjaszewski, *Macromolecules*, 2005, **38**, 5995-6004.
24. H. Gao and K. Matyjaszewski, *Macromolecules*, 2006, **39**, 7216-23.
25. Y. Wu, Y. Shi and Z. Fu, *Polymer*, 2005, **46**, 12722-28.
26. H. Gao, S. Ohno and K. Matyjaszewski, *J. Am. Chem. Soc.*, 2006, **128**, 15111-13.
27. H. Gao and K. Matyjaszewski, *Macromolecules*, 2007, **40**, 399-401.
28. H. Gao and K. Matyjaszewski, *Macromolecules*, 2008, **41**, 4250-57.

29. J. A. Johnson, D. R. Lewis, D. D. Diaz, M. G. Finn, J. T. Koberstein and N. J. Turro, *J. Am. Chem. Soc.*, 2006, **128**, 6564-65.
30. H. Gao and K. Matyjaszewski, *Macromolecules*, 2006, **39**, 4960-65.
31. M. R. Whittaker, C. N. Urbani and M. J. Monteiro, *J. Am. Chem. Soc.*, 2006, **128**, 11360-61.
32. S. R. A. Fisher, *The design of experiments*, Oliver and Boyd, London, 1960.
33. G. E. P. Box and K. B. Wilson, *Journal of the Royal Statistical Society* 1951, **13**, 1-45.
34. G. Taguchi, *Introduction to quality engineering : designing quality into products and processes*, Asian Productivity Organization, Tokyo, 1986.
35. www.minitab.com, Accessed 8th December 2008.
36. http://www.umetrics.com/default.asp/pagename/software_modde/c/2.
37. K. Matyjaszewski, P. J. Miller, J. Pyun, G. Kickelbick and S. Diamanti, *Macromolecules*, 1999, **32**, 6526-35.
38. R. N. Keller and H. D. Wycoff, *Inorganic syntheses. 1. Copper(I) chloride*, 1946.

Chapter 4

-

Phenols as accelerators for SET-LRP

Table of Contents

List of Figures

List of Tables

1 Introduction[ϕ]

Living radical polymerization catalyzed by transition metal complexes was first introduced using a Ru(II) catalyst in conjunction with activated halogen initiators, for the polymerization of MMA. The process was described to involve the reversible formal oxidation of the metal during propagation.[1] This was the first documented case of the use of additives in atom transfer living radical polymerisation when $MeAl(ODBP)_2$ was added to a ruthenium catalysed polymerisation of MMA.[1] Their roles are not well known; however they usual promote either acceleration in the rate or give better control of the polymerisation. Sawamoto states that "These additives probably can effectively reduce the metal species in higher oxidation states or form more efficient catalysts via coordination".[1]

Since this original use of $MeAl(ODBP)_2$, a number of other additives have been identified. $MeAl(ODBP)_2$ was found to be a more active additive than $Al(O\text{-}i\text{-}Pr)_3$ in that it achieved a faster and more quantitative polymerisation in toluene with CCl_4 at 60°C. However this increase in rate came along with an increase in PDI and a lower degree of control over molecular weights.[2] A number of other metal complexes were tested in this system including: $Ti(O\text{-}i\text{-}Pr)_4$, $Sn(O\text{-}i\text{-}Pr)_4$ and $[Al(acac)_3]$ and all found to give rate enhancement with differing degrees of control.[4, 5]

The exact role of the aluminium compounds was initially attributed to its coordination to the carbonyl of the monomer increasing its reactivity or by coordination to the terminal carbonyl of the growing polymer chain.[1] The type of transition metal complex was extended to copper(I) using nitrogen donor ligands in conjunction with copper(I) chloride and/or bromide in a process that has become widely known as atom transfer radical polymerization (ATRP).[3-6] An extensive range of initiators have been described including arene sulfonyl halides as efficient "*universal initiators*" with a range of low valent late transition metals employed.[7-10] The chemistry is extremely powerful for the synthesis of many complex polymer architectures with narrow molecular weight distribution, block copolymers, star copolymers, end functional polymers, polymers grown from surfaces and all types of complex polymer architecture.[11] The process has been shown to be inert to most chemical functionalities allowing many functional monomers to be utilized.[12] This use of a range of monomers has necessitated the use of

[ϕ] This work has been published: Peter M. Wright, Giuseppe Mantovani, David M, Haddleton, *J. Pol. Sci, Pol. Chem*, 2008, **46**, 7376.

a range of solvents including hydrophobic and hydrophilic fluids. In an early paper Armes showed the effectiveness of the Cu(I)Br/bpy system in water where he noted a massive acceleration of the rate.[13, 14] Subsequent research has shown that whenever polar solvents (or coordinating solvents) are employed the rate can be considerably enhanced.[15, 16] This increase in rate is partly explained by an increase in k_p due to the increase in the polarity of the polymerization medium, however, this accounts for only a small part of the rate enhancement. We have reported that the coordination of polar/coordinating monomers to copper(I) as competing ligands for the ligands employed and when the monomer can coordinate to the metal it is noted that even though the monomers might be poor coordinators they are generally present in very high concentrations relative to the ligands.[17, 18] Monomer coordination has been reported to change the reactivity ratio of the monomer pair when monomers of different coordinating ability are employed. Percec has reported that under many ATRP polymerization conditions Cu(I) salts spontaneously disproportionate to Cu(0) and Cu(II) at ambient temperature.[19] This occurs in water, alcohols, DMSO and other dipolar aprotic and protic solvents in the presence of good σ-donor ligands such as tris(2-aminoethyl)amine (TREN), tris(2-dimethylamioethyl)amine Me_6TREN and pentamethyldiethyl tetraamine(PMDETA).[19] This new system has been used for the synthesis of poly(methyl acrylate)s, poly(ethyl acrylate)s, and poly(butyl acrylate)s with α,ω-di(bromo) chain ends with M_n = 8500 to 35,000 g mol^{-1} with reported perfect bifunctionality.[20] Simulation experiments have suggested a heterolytic outersphere single-electron transfer process where the activation of the initiator and of the propagating dormant species is faster than of the homolytic inner-sphere electron-transfer process responsible for ATRP.[21, 22] Observation of polymerizations using copper(I) salts in coordinating solvents often reveal blue or green solutions, characteristic of copper(II) solutions which often passes without remark in the literature as the synthetic chemist isolates polymers with narrow PDI and structures as targeted.

This discovery led Percec to replace Cu(I) with Cu(0) as the source of copper in the form of wire and/or powder to facilitate polymerisation; a process that has been shown to work remarkably well. A mechanism has been proposed, Scheme 1, supported by computer simulations and quantum chemical calculations giving a deactivation rate constant for SET-LRP similar to ATRP but with a higher rate constant of activation.

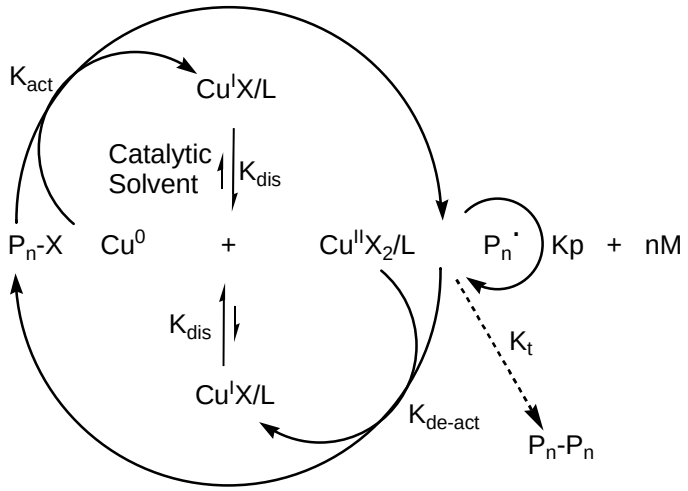

Scheme 1. Proposed mechanism for SET-LRP [19]

A further observation is that the SET mechanism allows a greater range of initiators to be used as tested with reference to Bond Dissociation Energies (BDE).[23] For this reason amide initiators have been investigated in this present work as there are not many examples for their use as initiators in ATRP or other transition metal mediated polymerization. Although some groups have had some success,[24-26] the majority of papers relating to amides show them to have low initiator efficiencies leading to higher than predicted molecular weights and often broader PDI's than is usually associated with efficient LRP.[27 28 29] Previous work by our group has shown that by optimising the conditions it was possible to obtain polymers of narrow PDI with controlled molecular weights using amide based initiators.[24]

The use of copper(II) with reducing agents present can also be used with both organic [30] and inorganic reducing agents [31 32] which will reduce the copper(II) to either copper(0) or a mixture of oxidation states. Thus the oxidation state of copper in a typical ATRP/polymerisation reaction is variable and complex.[33]

Copper(II) has also been shown to be an excellent source of copper in the presence of a reducing agent such as a sugar,[30] ascorbic acid or tin(II) reagent where the role of the reducing agent is described as reversibly generating the desired copper(I) which is in turn oxidized be reaction with alkyl halide, [31 32 34] Scheme 2.

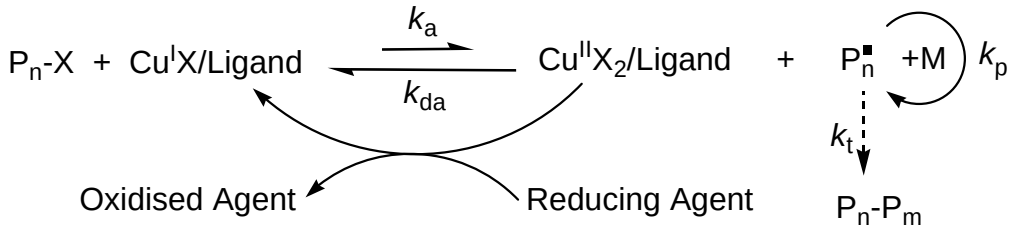

Scheme 2. Proposed mechanism of ARGET ATRP

Percec showed that the use of 10 mol% phenol in THF with Me_6Tren as ligand promoted spontaneous disproportionation of Cu(I) to Cu(0) + Cu(II).[19] Of particular interest was extending SET-LRP to non polar monomers and for application in non polar media. Previously it has been demonstrated that non sterically hindered phenols can coordinate to copper complexes with interesting results and this led us to investigate toluene as a solvent with a range of phenols as additives as a polymerisation medium for ambient temperature SET-LRP. In addition phenols have been used as reducing agents for Cu(II) in the presence of air to catalyze ATRP type reactions.[19]

The primary focus of this current work is to investigate the use of phenolic additives as accelerators for copper mediated SET-LRP in hydrophobic solvents leading toward the polymerization of hydrophobic monomers. The secondary focus is to show the versatility of the technique for the use of amide initiators.

Error! Objects cannot be created from editing field codes.

Figure 1. Initiators used for phenol accelerated copper mediated - LRP

2 Results and Discussion

In September 2006 Percec *et. al*.[35] published work using a Cu(0) based catalyst for a low temperature living radical polymerisation they termed 'SET-LRP' or single electron transfer living radical polymerisation. Their work allowed the ultra-fast polymerisation of methacrylates and acrylates in polar solvents at 25°C. The system also showed promise in the use of different initiators from ATRP, such as amides, which displayed higher efficiencies than previously reported.[36-38] However, Percec's work did not address the polymerisation of highly non-polar monomers such as the C12/15 methacrylate used for the VMs in this work. This section of work sets out to address this issue and provide a simple way of polymerising non-polar monomers via this SET-LRP method.

A second driving force for this work was the use of amide initiators such as **12**/**13**. Typically, this type of initiators are associated with low initiator efficiency and hence much higher than targeted molecular weights. A significant benefit of being able to polymerise off an amide initiator is that a wide range of them are highly efficient at absorbing to soot particles and therefore preventing them from flocculating. Several of the amides are highly coloured which also may be of interest to certain industries such as in the area of personal care products. Examples of such compounds are *N*-phenyl-1,4-phenylenediamine (ADPA) and disperse orange which are known as good dispersants. Polymers with such a head group would be best described as a polymeric dispersant and given the correct monomer composition could be used to prevent flocculating in a range of systems such as paints, automotive applications e.g. gear oils, household cleaning fluids and personal care products.

2.1 Synthesis of a polymer from an amide based initiator

2.1.1 Synthesis of 2-bromo-2-methyl-*N*-(4-phenylamino-phenyl)-propionamide-I1

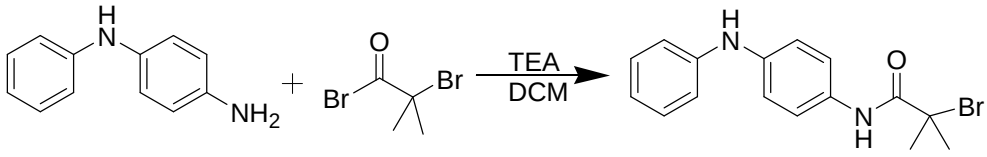

Figure 2 - Synthesis of an amide initiator for CM LRP

Phenyl-1,4-phenylenediamine is a very good polar head group which is able to adsorb onto surfaces. The introduction of it into the initiator structure was paramount so the simple amidation above was carried out. The synthesis proceeded via the slow addition of the acid bromide into the amine solution in DCM in the presence of TEA. The initiator was obtained with satisfactory purity and high yields after re-crystallisation.

2.1.2 Polymerisation of a long chain alkylmethacrylate using I1

Linear α-functional polymers were prepared via the polymerisation of C_{12-15} MA in toluene at a range of temperatures from 70-90°C employing 2-bromo-2-methyl-*N*-(4-phenylamino-phenyl)-propionamide as initiator. Cu(I)Br and n-propyl-2-pyridylmethanimine were initially used as the catalyst system. The polymers made using this catalyst system were found to have a molecular weight much higher than anticipated as detailed in Table 1. Although the molecular weights were higher than desired, the polymerisations can still be described as 'living' because the first order kinetic plot is linear and the molecular weight grows linearly with respect to monomer concentration. The high molecular weights were found to be caused by exceptionally low initiating efficiencies, in the range of 10-28% in the majority of cases, which was attributed to a very fast initiation step that meant that there were too many radicals present causing termination to occur very early in the polymerisation. The fast initiation step can be characterised by the significant molecular weight increase from 300-9000 g mol^{-1} which is often seen for amide initiators.

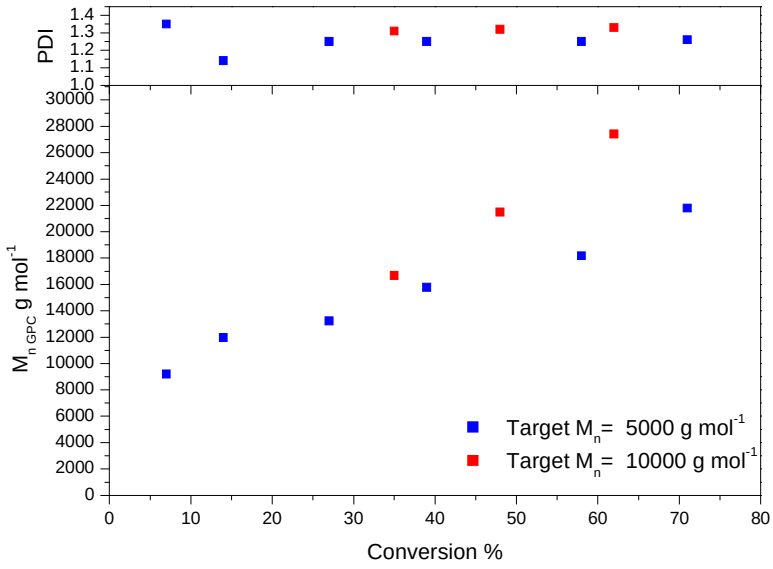

Figure 3 - Graph showing the evolution of molecular weight and MWD with conversion of monomer using 2-bromo-2-methyl-*N*-(4-phenylamino-phenyl)-propionamide (I1) as initiator.

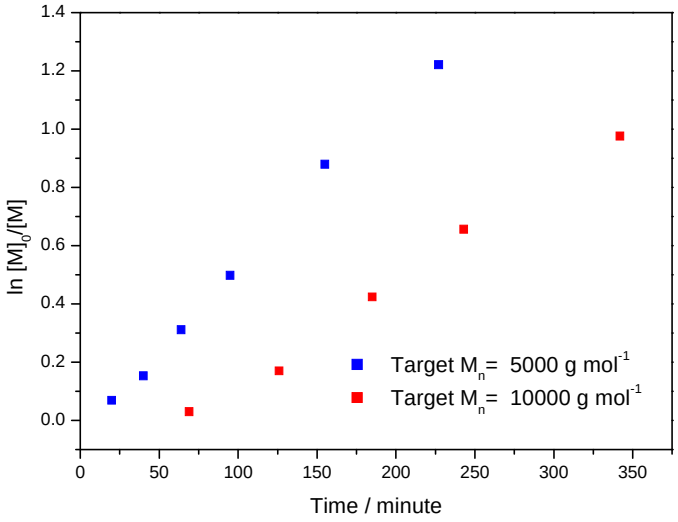

Figure 4 First order kinetic plot of polymerisations using 2-bromo-2-methyl-*N*-(4-phenylamino-phenyl)-propionamide (I1) as the initiator.

Attempts were made to reduce the rate of initiation, and hence rate of termination early on in the polymerisation, using several techniques detailed by Haddleton et. al..[24] The authors described how by reducing the temperature of the polymerisation at the start, the rate of initiation could be reduced allowing the initiator to react with a monomer unit, while minimising the rate of bi-molecular termination of the initiator. Following this period at reduced temperatures, the reaction could be warmed and the polymerisation rate increased. Firstly, Cu(I)Cl was used in conjunction with *n*-propyl-2-

pyridylmethanimine with an induction period, usually 30 minutes at ambient temperature before heating to reaction temperature (90°C). This was found to have no effect on the initiation efficiency although the rate of polymerisation did slow as is common with the use of Cu(I)Cl. This technique of using an induction period was also used for Cu(I)Br. It was found that this also had no positive effect on the initiation efficiency. Several polymerisations were carried out using a variety of induction periods to ascertain whether 30 minutes was sufficient to allow the initiation step to proceed. It was found that increasing the induction time had a small effect on the initiating efficiency, Table 1.

Copper Halide	$M_{n\ Target}$ g mol $^{-1}$	Induction time (at 25°C) / min	Conversion %	$M_{n\ Theo}$ g mol^{-1}	PDI	$M_{n\ NMR}$ g mol^{-1}	Initiator Eff. %
CuBr	5000	0	71	3550	1.26	28000	13
CuBr	5000	30	71	3550	1.32	25000	14
CuBr	10000	3970	79	7900	1.26	28600	28
CuCl	5000	30	75	3750	1.51	26000	15
CuCl	5000	0	69	3450	1.51	28000	12

Table 1 - A summary of the opimisation techniques used in the polymerisations of $C_{12\text{-}15}$ methacrylate

Since induction time was found to not affect the initiation efficiency within a reasonable timescale, the reaction temperature was next examined for any affect it may have. A polymerisation was carried out at 70°C with a 30 minute induction period. The polymerisation at this temperature failed and no further polymerisations were carried out at reduced temperature.

2.1.3 Synthesis of poly(methylacrylate) using a *N*-phenyl-1,4-phenylene diamine based initiator

First attempts at using this initiator were made in DMSO using methyl acrylate repeating Percec's conditions as much as possible.[35] The initial polymerisation was carried out at 66% solids which resulted in an ultra-fast polymerisation which reached 89% conversion after 40 minutes. Therefore the concentration was reduced to 50% solids to slow the reaction down to allow more samples to be taken, Figure 5, Figure 6.

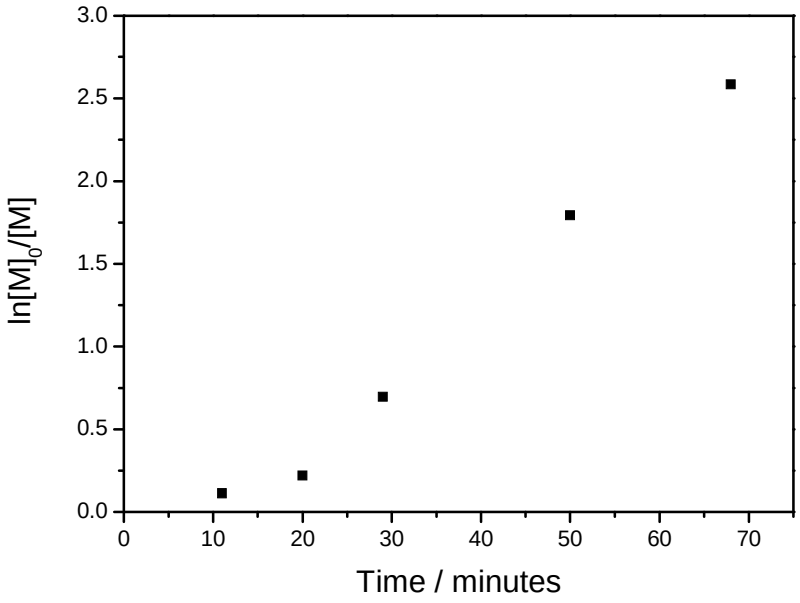

Figure 5 - First order kinetic plot for the SET-LRP of MA in DMSO, using Cu(0)/Me_6Tren as catalyst at 25°C. [Cu(0)]:[Me_6Tren]:[Initiator]:[MA] – [1]:[1]:[1]:[116], 50% solids.

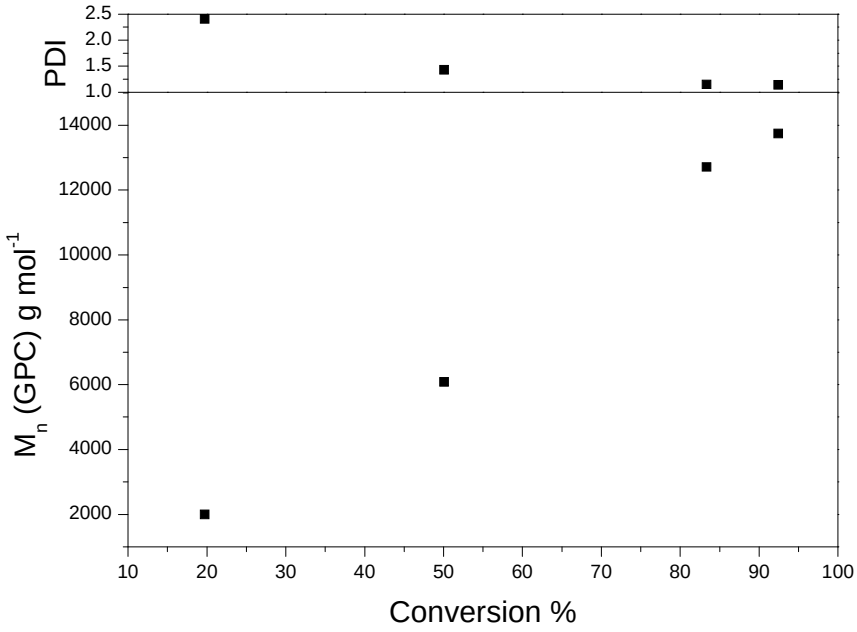

Figure 6 -Dependence of $M_{n,(GPC)}$ and PDI on monomer conversion for the polymerization of MA in DMSO, using Cu(0)/Me_6Tren at 25°C.
[Cu(0)]:[Me_6Tren]:[Initiator]:[MA] – [1]:[1]:[1]:[116], 50% solids.

The polymerisation gave a high degree over control with narrow PDI and linear first order kinetics. The PDI also remains narrow up to >90% conversion with no termination effects observed indicating a highly controlled polymerisation even at high conversions. The molecular weight is also much closer to the targeted value when

compared to using a Cu(I)Br/pyridineimine catalyst system. These results indicated that the ADPA based initiator was indeed suitable for use in SET-LRP and polymerised with a much higher initiator efficiency than in ATRP. However, the monomer composition needed for the end application is highly non-polar and therefore insoluble in DMSO. This resulted in other solvent systems being explored for use in SET-LRP.

2.1.4 Synthesis of PMA using Cu(0) in the presence of an accelerating agent.

Following this confirmation of the results reported by Percec[19] it was decided to investigate the use of Cu(0) in toluene as a non-polar solvent with coordinating/accelerating additives. The supplementary information of Percec's paper[35] notes that the use of phenol (10 mol%) in THF allowed the disproportionation of Cu(I)Br. It is observed here that Haddleton *et. al*.[39] previously used phenol as an additive for ATRP to discover whether phenolic inhibitors needed removing from monomers prior to polymerisation and what, if any, effect they might have. Therefore phenol was used as an additive to accelerate SET-LRP of various monomers in toluene.

2.1.5 The disproportionation of Cu(I)Br in the presence of phenol

Copper complexes have characteristic UV/Vis spectra with copper(I) compounds usually colorless (d^{10}) in the absence of ligand-metal charge transfer and copper(II) usually green or blue (d^9), depending upon the complex shape and nature of ligand/solvent. It is noted here that both $CuBr_2$ and CuBr are soluble in DMSO without additional ligands. UV/Vis spectra were recorded in mixtures of deoxygenated toluene/phenol and Me_6Tren in airtight cuvettes containing the relevant Cu salt after leaving to stand for 10 minutes. It was observed that spontaneous disproportionation of Cu(I) happened in toluene and phenol (30 mol%) in agreement with Percec [19]. Thus unless the ligand is chosen to specifically stabilize Cu(I), as is the case for pyridine imine and diazabutadiene ligands, disproportionation takes rapidly at rates that depend largely on the coordinating ability of the solvent and/or species present in the solution. This reaction is on the same time scale as polymerization such that the copper species present in solution and thus the nature of the catalyst will/can be changing throughout the polymerization.

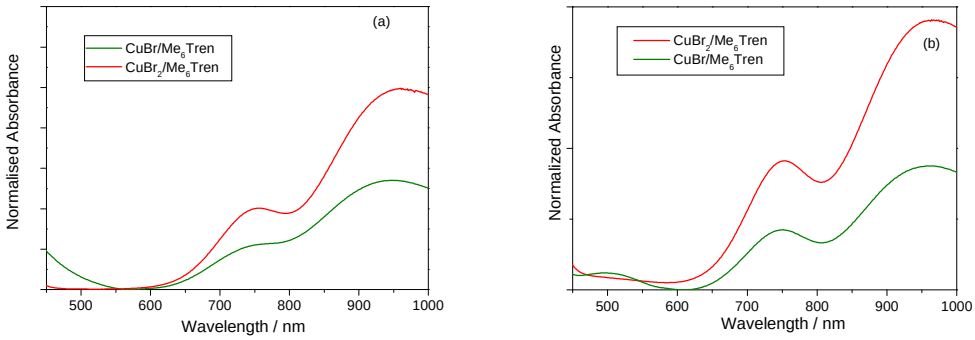

Figure 7. UV-Vis spectra of (a) $CuBr_2$ (red) and CuBr (green) in DMSO, (b) $CuBr_2/Me_6$-TREN (red) and CuBr/Me_6-TREN (green) in toluene and phenol (30 mol%).

2.1.6 The synthesis of PMA in the presence of phenol

Thus, polymerization of methyl acrylate initiated by **12** was carried out in the presence of varying amounts of phenol. The rate of polymerization was found to depend on concentration of phenol relative to the initiator, Figure 8.

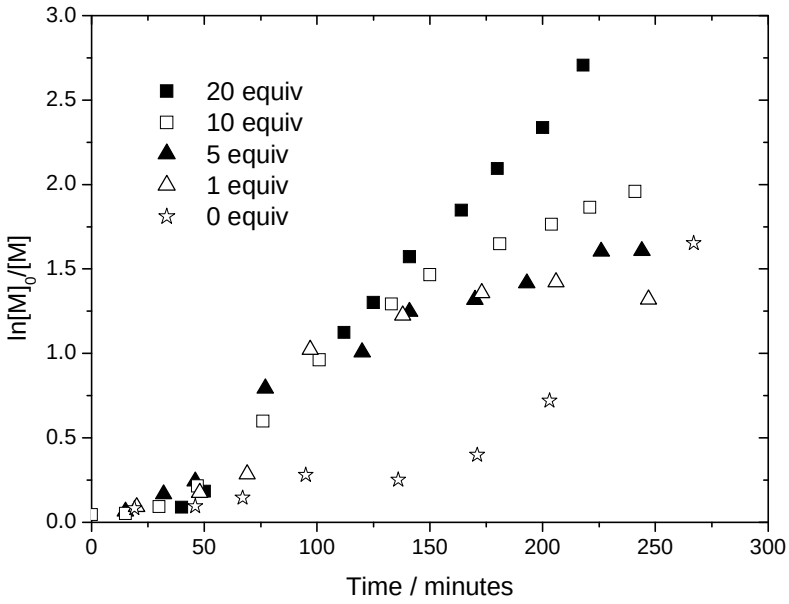

Figure 8. - First order kinetic plots for the polymerization of MA, in toluene, using Cu(0)/Me_6Tren as catalyst in the presence of varying amounts of phenol with respect to initiator at 25°C, [methyl acrylate]/[Cu(0)]/[Me_6TREN]/[**13**]/[Phenol] = 116/1/1/1/X.

When 20 equivalents of phenol with respect to initiator are used, a constant concentration of propagating species is observed after a short induction period with linear first order kinetics, Figure 8. However, with lower amounts of phenol, 10, 5 and 1

equivalents, the rates plateau after polymerising at a similar initial rate. This indicates that there is an increased amount of termination occurring or that the catalyst is being deactivated. However, the PDI's remain fairly narrow, <1.25, suggesting catalyst deactivation is affecting the polymerisation as opposed to excessive termination. The M_n increases linearly with respect to monomer conversion and the PDI's are narrow in all cases, suggesting controlled polymerisations, Figure 9. On lowering the amount of phenol the PDI at the beginning of the polymerisation is much broader suggesting that the rate of initiation is slower with lower phenol concentrations. The results using **12** as initiator using Cu(0)/ Me_6Tren for the polymerisation of methyl acrylate are summarized in Table 1. On reducing the amount of phenol relative to the catalyst the rate of reaction slows such that with a 20 fold excess there is 93% conversion after 218 minutes as compared to 80% conversion with a 5 fold excess and the product has a slight broadening of PDI.

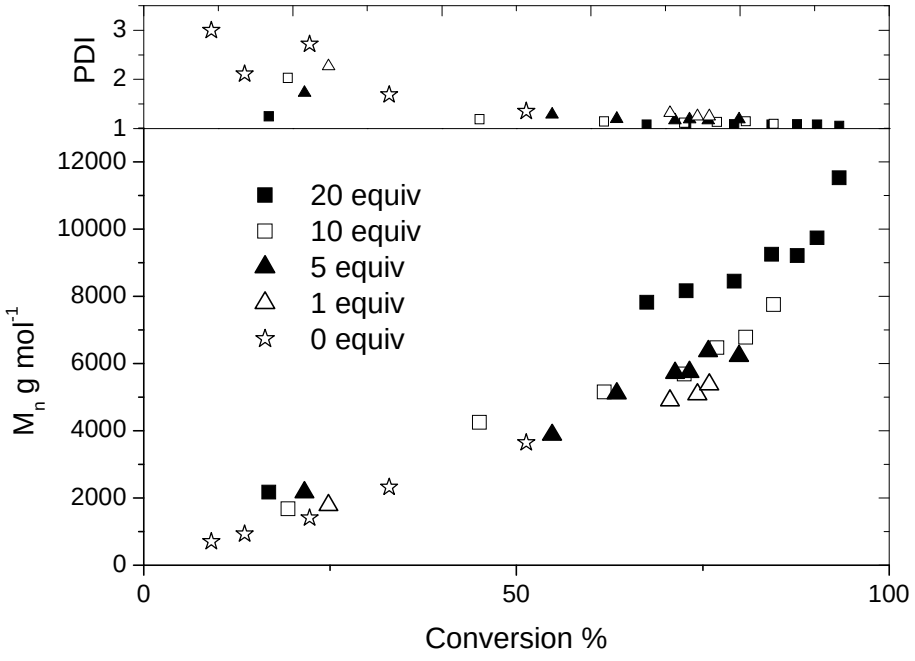

Figure 9. Dependence of $M_{n,(GPC)}$ and PDI on monomer conversion for the polymerization of MA, in toluene, using Cu(0)/Me_6Tren as catalyst in the presence of varying amounts of phenol with respect to initiator at 25°C.

[Phenol]/[Cu(0)]	Time / min	Conversion %	$M_{n,(theo)}$ / g mol^{-1}	$M_{n,GPC}$ /g mol^{-1}	PDI
20	218	93	9330	11500	1.06
10	241	86	8590	7750	1.10
5	244	80	7990	6220	1.19
1	247	73	7330	5370	1.25
0	267	81	8090	5310	1.21

Table 2. Polymerization of MA with Cu(0) and Me_6Tren; varying [phenol]/[**13**]

2.2 Synthesis of PMA using Cu(0) in the presence of different phenols

Previous work by Haddleton *et. al.* showed that for the polymerization of methyl methacrylate with Cu(I)Br/*N*-pentyl-1-pyridyl-methanimine catalyst and ethyl 2-methyl-2-bromopropionate initiator steric hindrance of the phenol had little effect on the rate of polymerization [40] . In this previous work when a 10 fold excess of **5** and **6** were added after 4 hours the conversion reached in both case was similar (75%) and higher than in the absence of phenol (54%). It might have been anticipated that if the role of the phenol is to coordinate to the copper then increasing bulkiness alpha to the phenol might prevent/reduce this, with copper(I) with pyridine imine ligands this is not the case. Thus a range of phenols were investigated for their effect on the polymerization mediated by Cu(0)/Me_6TREN, Figure 10.

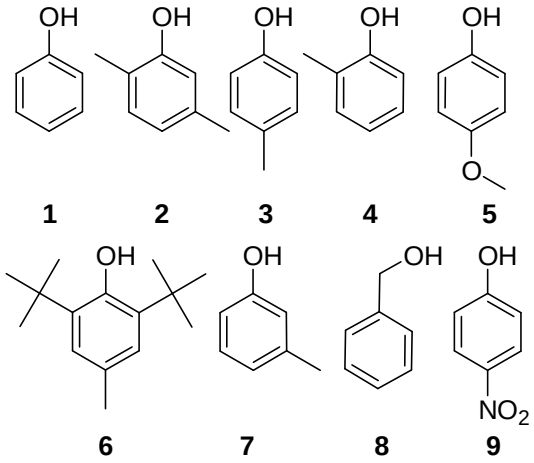

Figure 10 – The different phenols used in this work

When using non-sterically hindered phenols, **1** and **3**, in a 20 molar excess with respect to the initiator the polymerizations had good linear first order plots and polymers with narrow PDI, 1.06 and 1.16 respectively, Table 2 and Figure 11. However, when a highly hindered phenol, **6**, was employed there is a significant induction period prior to

polymerisation taking place which is similar to when using no phenol is added, Figure 8, with no enhancement in the rate of polymerisation. Less hindered phenols accelerated the polymerization when compared to polymerisations with no added phenol. Polymerisation in the presence of **4** proceeded at an acceptable rate suggesting although that the ortho-methyl group was hindered enough to slow the rate, but not enough to prevent the phenol from having an accelerating effect on the reaction. In the presence of para nitro substituted phenol, **9**, no polymerisation was observed.

Phenol	Time / min	Conversion %	$M_{n,(theo)}$ / g mol^{-1}	$M_{n,(GPC)}$ / g mol^{-1}	PDI
9		No polymerization observed			
8	237	70	7020	6970	1.24
7	254	34	3410	3500	1.12
6	212	51	5090	6180	1.17
4	240	84	8370	14290	1.20
3	240	93	9260	16210	1.16
2	246	64	6360	7910	1.07
1	218	93	9330	11520	1.06

Table 3 – SET-LRP of methyl acrylate with Cu(0) and Me_6Tren; varying the phenol structure.

The rates of propagation (k_p), taken from linear fits to the first order kinetic plots are summarized in Table 4. On increasing steric hindrance around the -OH of the phenol the rate of polymerization decreases. The induction time also increases as the rate slows indicating that the steric hindrance of the phenol might have a dual effect of both reducing the k_p and introducing an increased induction time. For example, **1** shows an induction period of approximately 30 minutes and a rate three times faster than that of **6** which has an induction time of 140 minutes.

Phenol	**8**	**7**	**6**	**4**	**3**	**2**	**1**
k_p [Pol*] min^{-1}	---	---	0.00569	0.00959	0.0133	0.00886	0.0145

Table 4. Rate of propagation when using various phenols as accelerators for the polymerisation of MA.

With both phenols **2** and **7** a significant induction time was observed, (Figure 11), similar to that of **6**; however, the polymerizations in the presence of either proceeded to lower conversions after ~4 hours than **6**. This indicates that the site(s) of substitution

give rise to an electronic effect on the aromatic ring that gives a detrimental effect on the phenols ability to accelerate the rate of polymerization. The M_n of the polymers increases linearly with monomer conversion and all polymers have narrow PDI, Figure 12. The increase in the rate is ascribed to O- coordination of the phenol at copper in an as yet undetermined oxidation state. The alternative explanation of the phenol acting as a reducing agent is considered unlikely as a similar accelerating effect is observed with aliphatic alcohols such as methanol and benzyl alcohol **8** with copper(0). Increasing steric hindrance at the –OH prevents this coordination which indicates that the role of phenol is different with either copper(0) or copper(I)[5].

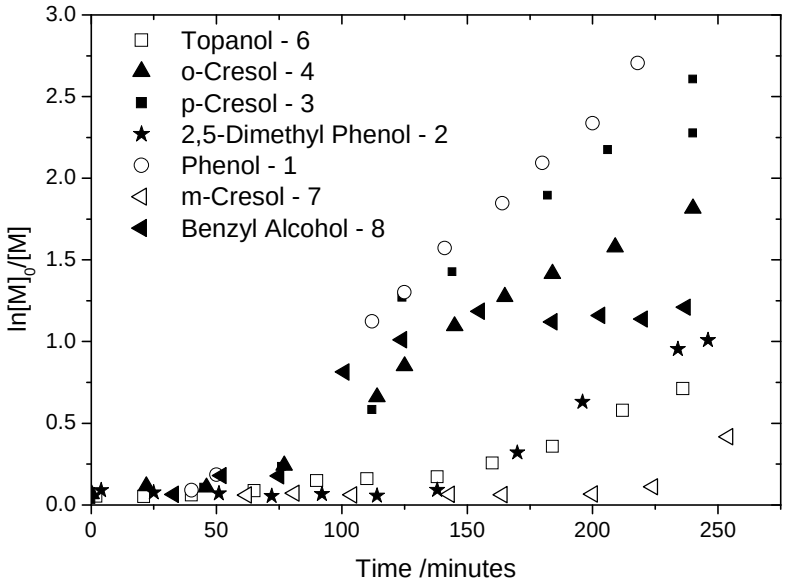

Figure 11 First order kinetic plot for the SET-LRP of MA, in toluene, using Cu(0)/Me_6Tren as catalyst in the presence of different phenols at 25°C.

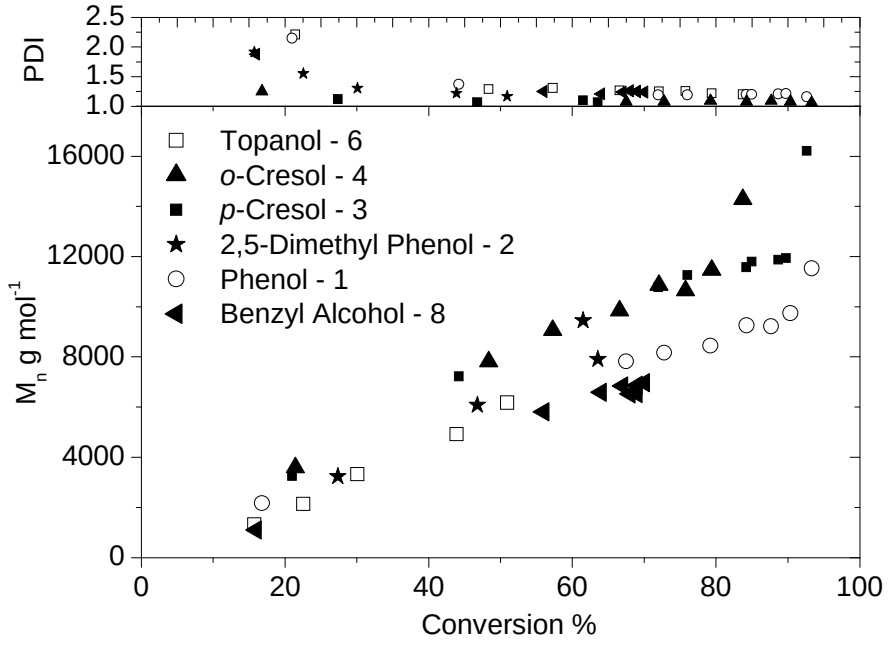

Figure 12. Dependence of $M_{n\,(GPC)}$ and PDI on monomer conversion for the SET-LRP of MA, in toluene, using Cu(0)/Me_6Tren as catalyst in the presence of different phenols at 25°C.

2.3 Synthesis of poly(methyl acrylate) using Cu(0) with different initiators

Percec *et. al.* suggested that the SET mechanism allows for a greater range of initiators to be used due to the lower BDE involved.[19 23] In order to investigate this, four initiators were chosen (Figure 9) for the polymerisation of methyl acrylate in the presence of a twenty fold excess of phenol. All four initiators gave polymers with narrow PDI, <1.22, and controlled molecular weights, Table 5. The benzyl amide initiator, **12**, showed good first order kinetics which deviate from linearity and a slightly broader PDI with controlled than polymerisation with **10**, **11**, or **13**. Conversions after ~4 hours were all similar, although polymerisation from **13** gave a slightly faster polymerisation. Figure 13 shows that there are constant concentrations of propagating species in the reaction.

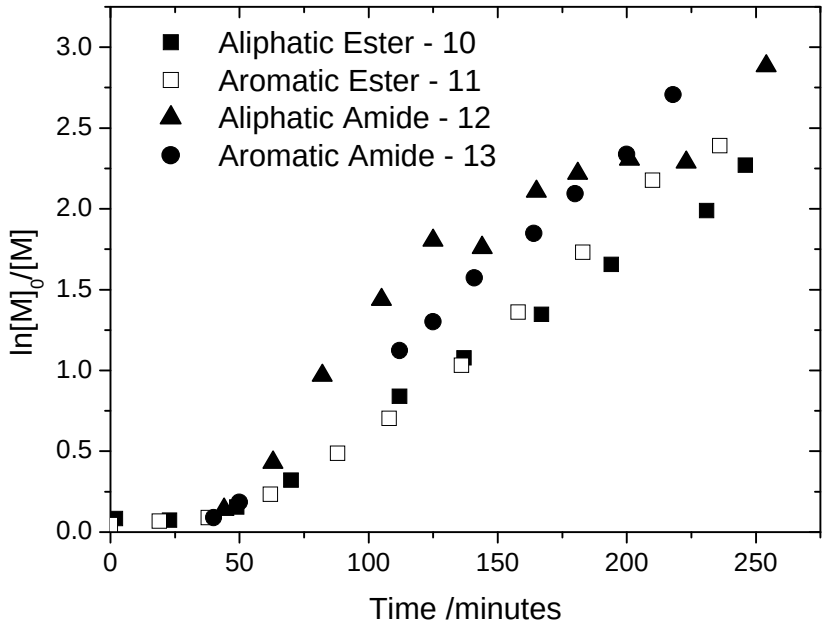

Figure 13. First order kinetic plot for the SET-LRP of MA, in toluene, using Cu(0)/Me_6Tren as catalyst in the presence of phenol using different initiators at 25°C.

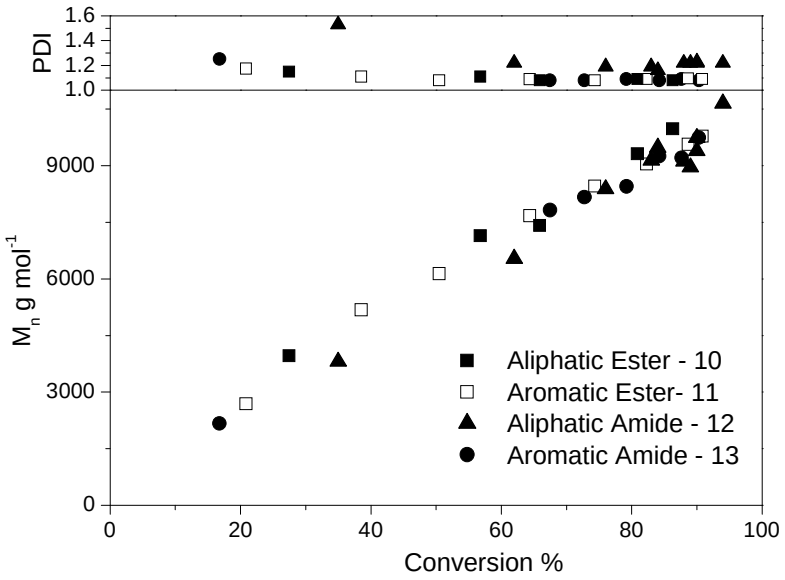

Figure 14. Dependence of M_n GPC and PDI on monomer conversion for the SET-LRP of MA, in toluene, using Cu(0)/Me_6Tren as catalyst in the presence of phenol using different initiators, 25°C.

Initiator	Time / min	Conversion %	$M_{n\ theoretical}$ / g mol^{-1}	$M_{n\ GPC}$ /g mol^{-1}	PDI
13	218	93	9330	11520	1.06
12	254	94	9440	10650	1.22
11	236	91	9080	9780	1.09
10	246	90	8970	12860	1.05

Table 5 - SET-LRP of MA with Cu(0) and Me_6Tren; varying the initiator effect on polymer

2.4 Synthesis of a linear poly(alkylacrylate)

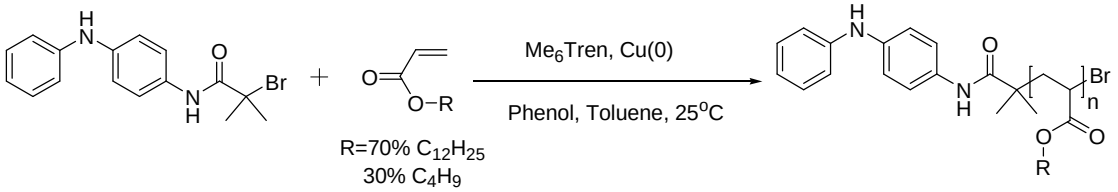

Scheme 1 - Synthesis of a poly(alkyl acrylate) with *N*-phenyl-1,4-phenylene diamine as a head group

The above polymer was made with good control over molecular weight and PDI. However, due to insufficient copper wire being added to the reaction, the polymerization

was very slow. This reaction was carried out on the 2 L scale to provide Lubrizol with a sample for viscometric tests.

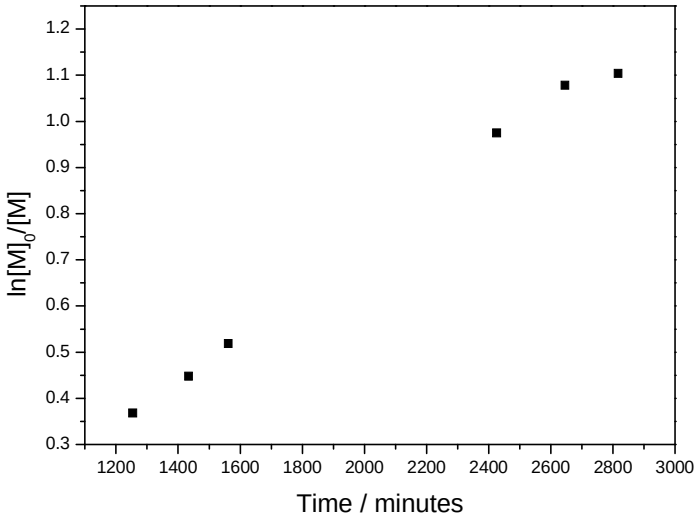

Figure 15 – The first order kinetic plot for the synthesis of a linear polyacrylate. [lauryl acrylate]:[*n*-BA]:[Ligand]:[Cu(wire)]:[Initiator] - [73]:[59]:[11]:[50 cm]:[1], 25°C, 50% solids, in toluene solution

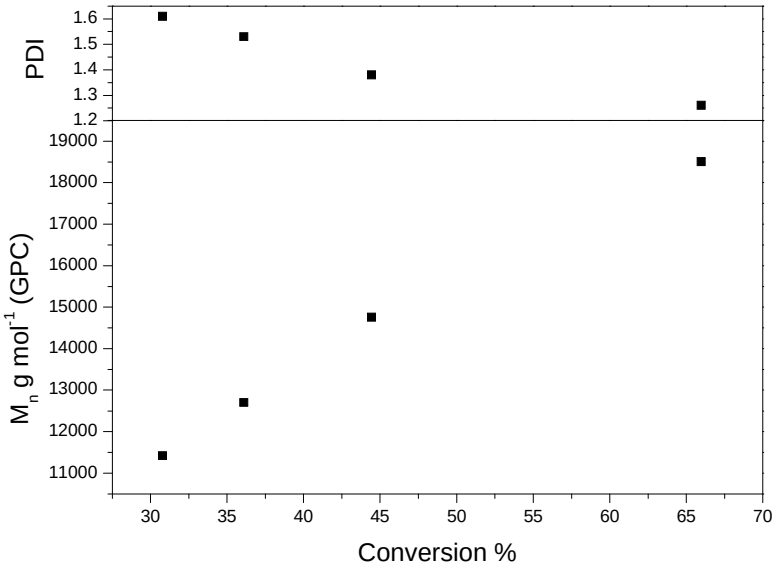

Figure 16 - M_n and PDI versus conversion for the co-polymerisation of lauryl acrylate and *n*-butyl acylate. [lauryl acrylate]:[*n*-BA]:[ligand]:[Cu(wire)]:[initiator] - [73]:[59]:[11]:[50 cm]:[1], 25°C, 50% solids, in toluene solution

3 Conclusions

The use of an ADPA based initiator with an ATRP, Cu(I)Br catalyst system was found to give very low initiator efficiencies. The polymerisations were however highly controlled with the PDIs narrow and linear first order kinetics. Despite the literature suggesting possible ways to overcome this, such as the use of low temperature induction times and Cu(I)Cl, all were unsuccessful. However, when Percec published about a SET-LRP system a new method of polymerisation was available. The use of a polar solvent and an Me6Tren/Cu(0) catalyst system showed that the ADPA based initiator could be utilised to initiate polymerisations of acrylates with molecular weights close to those predicted and with narrow PDIs.

The system was further developed to allow the polymerisation of non-polar monomer in non-polar solvents. Toluene with added phenol proved an ideal solvent system. Numerous derivatives of phenol were tested and all found to be inferior to phenol at accelerating the polymerisation. It was found that the more steric hindrance around the OH group of the lower the accelerating effect.

A range of ester and amide initiators were also polymerised and found to give high degrees of control.

4 Experimental

4.1 Synthesis of 2-bromo-2-methyl-*N*-(4-phenylamino-phenyl)-propionamide – I1

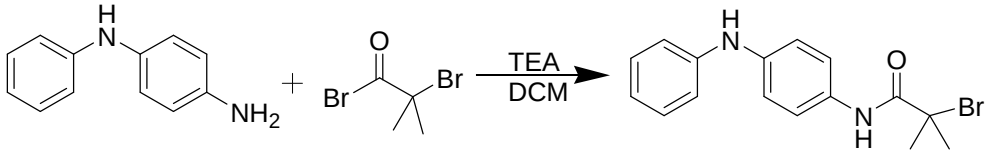

Figure 17 - Synthesis of an amide initiator for CM CLRP

N-Phenyl-1,4-phenylenediamine (10 g, 0.0448 mol) was placed in a round bottomed flask which was flushed with nitrogen for 15 minutes. Anhydrous dichloromethane (150 ml) was added and the solution left to stir for 2 minutes to allow the *N*-phenyl-1,4-phenylenediamine to dissolve fully. Triethylamine (4.98 g, 0.0492 mol) was added via a degassed syringe. 2-Bromo-2-methyl-propionyl bromide was added drop wise to this solution at 0°C with rapid stirring. The solution was left to stir for 30 minutes at ambient temperature after which it was washed with 3M NaOH (3×150 ml) and water (3×150 ml). The solution was dried with magnesium sulphate which was removed by filtration. This mixture was chromatographed (20 g silica) using 3:2, petroleum ether 40-60°C : diethyl ether (Product R_f = 0.3). Pure product was obtained as yellow crystals yielding 2.45 g, 16%. Mpt: 112.8-113.4°C uncorrected.

^{1}H NMR ($CDCl_3$) δ (ppm), 8.38 (s, 1H, -Ph-N<u>H</u>-CO-), 7.41 (m, 2H, C<u>H</u> aromatic), 7.24 (m, 2H, C<u>H</u> aromatic), 7.05 (m, 4H, C<u>H</u> aromatic), 6.91 (m, 1H, C<u>H</u> aromatic), 5.72 (s, 1H, -Ph-N<u>H</u>-Ph-), 2.04 (s, 6H, C(C<u>H</u>$_3$)$_2$).

^{13}C NMR ($CDCl_3$) δ (ppm), 170.1 (<u>C</u>O-C(CH$_3$)$_2$Br), 143.5 (CH-<u>C</u>(NH)-CH-C(NH)-CH), 140.4 (CH-<u>C</u>(NH)-CH), 131.1 (CH-C(NH)-CH-<u>C</u>(NH)-CH), 129.7 (<u>C</u>H aromatic), 121.9 (<u>C</u>H aromatic), 121.2 (<u>C</u>H aromatic), 118.9 (<u>C</u>H aromatic), 117.7 (<u>C</u>H aromatic), 63.6 (CO-<u>C</u>(CH$_3$)$_2$Br), 32.9 (CO-C(<u>C</u>H$_3$)$_2$Br).

IR (solid, ATR cell) ν (cm^{-1}): 3385 (Ph-<u>NH</u>-Ph stretching vibration), 1673 (C=O amide), 1594 (C=C stretch aromatic), 1514, 13997, 1304, 1232, 1152, 1102.

Mass Spectrometry (+EI, m/z): 333.2 (Expected 333.22)

CHN analysis: Theoretical C – 57.71%, H – 5.11%, N – 8.11%, Found: C - 57.67%, H - 5.14%, N - 8.41%.

4.2 Synthesis of 2-Bromo-2-methyl-*N*-phenyl propionamide (13)

Aniline (4.13 g, 44.4 mmol) was placed in an rbf which had been purged with N2 for 10 minutes. THF anhydrous (250 ml) was added followed by triethylamine (4.5 g, 44.4 mmol) in a degassed syringe. This mixture was cooled to 0°C and 2-bromo-isobutryrylbromide (9.3 g, 40.4 mmol) was added dropwise over 30 minutes and left to stir for a further 2 hours. After this time the mixture was filtered, the solvent removed in vacuo, the solid redissolved in DCM which was washed with 1M HCl (3 × 150 ml) and dried over magnesium sulfate. The DCM was removed in vacuo and the solid recrystallised from DCM/Petroleum Ether 40-60°C to give an off white powder (10.75 g, 85% yield, Mp 83.0-83.6°C).

^{1}H NMR ($CDCl_3$) δ (ppm), 8.45 (s, 1 H) 7.55 (d, 2 H, J=8 Hz), 7.35 (t, 2 H, J=8 Hz) 7.15 (t, 1 H, J=8 Hz), 2.05 (s, 6 H).

^{13}C NMR ($CDCl_3$) δ (ppm), 170 (C=O), 137 (C-NH-C=O), 129 (CH-CH-C(NH)), 125 (CH-CH-CH-C(NH)), 120 (CH-C(NH)), 63 ($C(CH_3)_2Br$), 32 ($C(CH_3)_2Br$).

IR (solid, ATR cell) υ (cm^{-1}) 1653 (C=C aromatic), 1596 (C=O).

CHN analysis: Theoretical C-49.61%, H-5.00%, N-5.79%. Found C-49.63%, H-4.96%, N-5.71%.

4.3 Synthesis of Me_6Tren[41]

A mixture of formaldehyde (37% (w/w)) and formic acid (90% (w/w)) was stirred at 0 °C. Over a period of an hour, a solution of TREN (20 ml, 0.13 mol) and deionized water was added dropwise. The mixture was gently refluxed overnight at 100°C. After cooling to room temperature, the volatile fractions were removed by rotary evaporation. The distinctly brown residue was treated with a saturated sodium hydroxide aqueous solution until pH > 10, producing an oil layer, which was extracted into methylene chloride. The organic phase was dried over magnesium sulphate and evaporated to produce a yellow oil. Yield 27.1g (90.6%).

^{1}H NMR ($CDCl_3$) δ (ppm), 2.53 (t, 6H, $C\underline{H}_2NMe_2$), 2.33 (t, 6H, $NC\underline{H}_2CH_2NMe_2$), 2.16 (s, 18H, $N(C\underline{H}_3)_2$)

^{13}C NMR ($CDCl_3$) δ (ppm), 57.34 ($N(\underline{C}H_2)_3$), 52.93 ($\underline{C}H_2N(CH_3)_2$), 45.74 ($N(\underline{C}H_3)_2$)

4.4 *N*-Benzyl-2-bromo-2-methylpropionamide (12) [24]

Benzylamine (30 mL, 0.27 mol), triethylamine (76.5 mL, 0.55 mol), and anhydrous THF (1000 mL) were placed in a three-neck round-bottomed flask. 2-Bromoisobutyryl bromide (50.9 mL, 0.41 mol) was added slowly at 0 °C with stirring. A white precipitate, of triethylammonium bromide, was formed, and the reaction was left for 20 h at ambient temperature with stirring. The precipitate was removed by filtration prior to removal of volatiles in vacuo to leave a brown liquid. The product was redissolved in dichloromethane and was subsequently isolated following washing with two 200 mL portions of saturated sodium carbonate solution, 0.5 M HCl(aq), and deionized water. The dichloromethane solution was dried over $MgSO_4$ and the volatiles removed in vacuo to give a light brown solid.

^{1}H NMR ($CDCl_3$) δ (ppm), (7.31 (M, 5 H, Aro), 7.02 (S, 1 H, NH), 4.46 (d, J = 5.8 Hz, 2H, Aro-CH_2-NH), 1.99 (s, 6H, C=O-CMe_2).

^{13}C NMR ($CDCl_3$) δ (ppm), 171.95($\underline{C}$=O), 137.77, 128.81, 127.55, 127.40 (Aro), 62.90 (C=O-$\underline{C}Me_2$), 44.38 (Aro-$\underline{C}H_2$-NH), 32.62 (C=O-C$\underline{Me}_2$).

IR (solid, ATR cell) ν(cm^{-1}): 3291 (amide N-H stretch), 1642 (amide -CONH stretch), 1534 (Aro -H vibration), 1354, 1293, 1102, 693, 638.

CHN analysis: Theoretical C-51.58%, H-5.51%, N-5.47%. Found C-51.60%, H-5.51%, N-5.43%.

4.5 2-Bromo-2-methyl-propionic acid benzyl ester (10) [43]

A solution of 2-bromoisobutyryl bromide (6.39 g, 27.8 mmol) in THF (20 mL) was added dropwise to a solution of benzyl alcohol (2.00 g, 18.5 mmol) and pyridine (1.58, 20 mmol) in THF (50 mL). After being stirred overnight at room temperature, the reaction mixture was poured onto aqueous HCl (50 mL, 4 M). The aqueous layer was

extracted with CH_2Cl_2 (3 × 100 mL). The combined organic layers were extracted with aqueous solution of NaOH (3 × 50 mL, 1 M). The organic layer was dried with Na_2SO_4, and the solvent was removed in vacuo. The product was purified by column chromatography on basic alumina and isolated as a colorless oil in 61% yield (2.91 g, 11.3 mmol).

^{1}H NMR ($CDCl_3$): δ7.39 (m, 5 H, Ph(*H*)), 5.23 (s, 2 H, PhCH_2O), 1.98 (s, 6 H, CMe_2).

^{13}C NMR ($CDCl_3$): δ171.6 (C(O)), 135.7 (1 C, Ar, C-CH_2), 128.8, 128.6, 128.1 (5 C, ArC), 67.8 (ArCH_2), 56.0 (CMe_2), 31.1 (CMe_2).

CHN analysis: Theoretical C-51.38%; H-5.10%. Found: C-51.41%; H-5.12%.

4.6 2-Bromo-2-methyl-propionic acid 4-methyoxyphenol ester (11)[42]

4-Methoxyphenol (24.83 g, 0.2 mol), triethylamine (30.6 mL, 0.22 mol), and THF (400 mL) were placed in a three-neck round-bottomed flask. Bromoisobutyryl bromide (27.2 mL, 0.22 mol) was added slowly with stirring. A white precipitate, of triethylammonium bromide, was formed, when the reaction was left for 6 h with stirring. The insolubles were removed by filtration prior to removal of solvent in vacuo to leave a yellow liquid. The product was isolated following washing with 2 × 200 mL portions of saturated Na_2CO_3(aq), dilute HCl(aq), and distilled water. The dichloromethane solution was dried with $MgSO_4$ and the solvent removed by rotary evaporation to give a yellow oily liquid. On overnight cooling, the product crystallized. The product was recrystallized three times from ethanol at 5 °C. Yield = 33.9 g (62%).

^{1}H NMR ($CDCl_3$) δ (ppm), 7.04 (d, *J* = 9.1 Hz 2 H), 6.90 (d, *J* = 9.1 Hz 2 H), 3.80 (s, 3H), 2.05 (s, 6H).

^{13}C ($CDCl_3$) δ (ppm), 170.45, 157.38, 144.15, 121.68, 114.38, 55.45, 30.54.

IR (solid, ATR cell): 3011, 2975, 2842, 1749, 1595, 1503, 1454, 1272, 1249, 1181, 1160, 1137, 1100, 1026, 941, 872, 816, 744 cm^{-1}.

4.7 Synthesis of poly(methyl acrylate) (PMA).

Cu(0) (1 equiv), phenol (20 equiv) were added to a Schlenk tube which was degassed by 5 vacuum/N_2 cycles. Methyl acrylate (116 equiv), Toluene (50% solids) and Me_6Tren (1 equiv) were added after being purged with N_2 for 30 minutes. This mixture was subjected to 5 freeze-pump-thaw cycles and while frozen the initiator (1 equiv) was added and the Schlenk tube was again degassed by a further 5 vacuum/N_2 cycles. After the final thaw the Schlenk tube containing the reaction mixture was placed in an oil bath at 25°C (± 0.5°C) and stirred. The polymerisation mixture was periodically sampled with an airtight degassed syringe. The samples were analyzed by both ^{1}H NMR to obtain monomer conversion and GPC to obtain molecular weight data. The polymerisation was stopped by the addition of toluene and bubbling with air for ~2 minutes. Polymers were isolated by passing through a column of basic alumina and precipitation into methanol:water (90:10) and dried in a vacuum oven at 30°C for 24 hours.

5 References

1. M. Kato, M. Kamigaito, M. Sawamoto and T. Higashimura, *Macromolecules*, 1995, **28**, 1721-3.
2. T. Ando, M. Kato, M. Kamigaito and M. Sawamoto, *Macromolecules*, 1996, **29**, 1070-2.
3. J. S. Wang and K. Matyjaszewski, *J. Am. Chem. Soc.*, 1995, **117**, 5614-15.
4. D. M. Haddleton, M. C. Crossman, B. H. Dana, D. J. Duncalf, A. M. Heming, D. Kukulj and A. J. Shooter, *Macromolecules*, 1999, **32**, 2110-19.
5. M. Kamigaito, T. Ando and M. Sawamoto, *Chem. Rev.*, 2001, **101**, 3689-745.
6. A. Limer and D. M. Haddleton, *Progress in Reaction Kinetics and Mechanism*, 2004, **29**, 187-241.
7. V. Percec, B. Barboiu and H.-J. Kim, *J. Am. Chem. Soc*, 1998, **120**, 305.
8. V. Percec, B. Barboiu, A. Neumann, J. C. Ronda and M. Y. Zhao, *Macromolecules*, 1996, **29**, 3665-68.
9. V. Percec and B. Barboiu, *Macromolecules*, 1995, **28**, 7970-72.
10. A. E. Feiring, E. R. Wonchoba, F. Davidson, V. Percec and B. Barboiu, *J. Polym. Sci. Pol. Chem.*, 2000, **38**, 3313-35.
11. W. A. Braunecker and K. Matyjaszewski, *Prog. Polym. Sci.*, 2007, **32**, 93-146.
12. A. Lecolley, C. Waterson, A. J. Carmichael, G. Mantovani, S. Harrisson, H. Chappell, A. Limer, P. Williams, K. Ohno and D. M. Haddleton, *J. Mat. Chem.*, 2003, **13**, 2689-95.
13. E. J. Ashford, V. Naldi, R. O'Dell, N. C. Billingham and S. P. Armes, *Chem. Comm.*, 1999, 1285.
14. S. Perrier, S. P. Armes, X. S. Wang, F. Malet and D. M. Haddleton, *J. Polym. Sci. Pol. Chem.*, 2001, **39**, 1696-707.
15. S. Harrisson, S. R. Mackenzie and D. M. Haddleton, *Macromolecules*, 2003, **36**, 5072-75.
16. S. Harrisson, S. R. Mackenzie and D. M. Haddleton, *Chem. Commun.*, 2002, 2850-51.
17. J. Lad, S. Harrisson, G. Mantovani and D. M. Haddleton, *Dalton Trans*, 2003, 4175-80.
18. J. Lad, S. Harrisson and D. M. Haddleton, *Advances in Controlled/Living Radical Polymerization*, 2003, **854**, 148-60.
19. V. Percec, T. Guliashvili, J. S. Ladislaw, A. Wistrand, A. Stjerndahl, M. J. Sienkowska, M. J. Monteiro and S. Sahoo, *J. Am. Chem. Soc.*, 2006, **128**, 14156-65.
20. G. Lligadas and V. Percec, *J. Polym. Sci. Pol. Chem.*, 2007, **45**, 4684-95.
21. M. J. Monteiro, T. Guliashvili and V. Percec, *J. Polym. Sci. Pol. Chem.*, 2007, **45**, 1835-47.
22. B. M. Rosen and V. Percec, *J. Polym. Sci. Pol. Chem.*, 2007, **45**, 4950-64.
23. T. Guliashvili and V. Percec, *J. Polym. Sci. Pol. Chem.*, 2007, **45**, 1607-18.
24. A. Limer and D. M. Haddleton, *Macromolecules*, 2006, **39**, 1353-58.
25. Y. Xia, N. A. D. Burke and H. D. H. Stover, *Macromolecules*, 2006, **39**, 2275-83.
26. C. L. Lin, P. H. Tung and F. C. Chang, *Polymer*, 2005, **46**, 9304-13.
27. V. B. Sadhu, J. Pionteck, D. Voigt, H. Komber and B. Voit, *Macromol. Symp.*, 2004, **210**, 147-55.
28. S. Venkataraman and K. L. Wooley, *Macromolecules*, 2006, **39**, 9661-64.
29. A. Postma, T. P. Davis, G. Moad and M. S. O'Shea, *React. Funct. Polym.*, 2006, **66**, 137-47.
30. A. de Vries, B. Klumperman, D. de Wet-Roos and R. D. Sanderson, *Macromol. Chem. Phys.*, 2001, **202**, 1645-48.

31. W. Jakubowski, K. Min and K. Matyjaszewski, *Macromolecules*, 2006, **39**, 39-45.
32. K. Matyjaszewski, W. Jakubowski, K. Min, W. Tang, J. Y. Huang, W. A. Braunecker and N. V. Tsarevsky, *Proceedings of the National Academy of Sciences of the United States of America*, 2006, **103**, 15309-14.
33. K. Matyjaszewski, N. V. Tsarevsky, W. A. Braunecker, H. Dong, J. Huang, W. Jakubowski, Y. Kwak, R. Nicolay, W. Tang and J. A. Yoon, *Macromolecules*, 2007, **40**, 7795-806.
34. K. Min, H. F. Gao and K. Matyjaszewski, *Macromolecules*, 2007, **40**, 1789-91.
35. V. Percec, T. Guliashvili, J. S. Ladislaw, A. Wistrand, A. Stjerndahl, M. J. Sienkowska, M. J. Monteiro and S. Sahoo, *J. Am. Chem. Soc.*, 2006, **128**, 14156-65.
36. Y. Xia, N. A. D. Burke and H. D. H. Stoever, *Macromolecules*, 2006, **39**, 2275-83.
37. R. M. Broyer, G. M. Quaker and H. D. Maynard, *J. Am. Chem. Soc.*, 2008, **130**, 1041-47.
38. S. Venkataraman and K. L. Wooley, *Macromolecules*, 2006, **39**, 9661-64.
39. D. M. Haddleton, A. J. Clark, M. C. Crossman, D. J. Duncalf, A. M. Heming, S. R. Morsley and A. J. Shooter, *Chem. Commun.*, 1997, 1173-74.
40. D. M. Haddleton, A. J. Clark, M. C. Crossman, D. J. Duncalf, A. M. Hemings, S. R. Morsley and A. J. Shooter, *Chem. Commun.*, 1997, 1173.
41. M. Ciampolini and N. Nardi, *Inorg. Chem.*, 1966, **5**, 41-4.
42. D. M. Haddleton and C. Waterson, *Macromolecules*, 1999, **32**, 8732-39.

Chapter 5

-

Testing of Polymer Viscosity Modifiers

Table of Contents

List of Figures

List of Tables

1 Introduction

This chapter reports on studies investigating the polymers synthesised in chapters 2 and 3 for use as VMs in gear box oils. The relationship between the number of arms in the star and the viscometric properties is of particular interest. Any core first stars that may have performed dramatically better than any other could have been targeted during arm first polymerisation. The polymers have been tested for several parameters to assess this suitability. The tests were carried out at Lubrizol's site at Hazelwood, Derbyshire by their testing engineers. The tests include:

1. Absolute viscosity

   Absolute viscosities were measured using a Brookfield Viscometer using a liquid bath at -40°C.

Figure 1 – The Brookfield viscometer used to measure the absolute viscosity at -40°C

2. Kinematic viscosity

   Kinematic viscosities were measured on a Cannon automated viscometer at both 40°C and 100°C. These values were used to calculate the VI as shown in chapter 1.

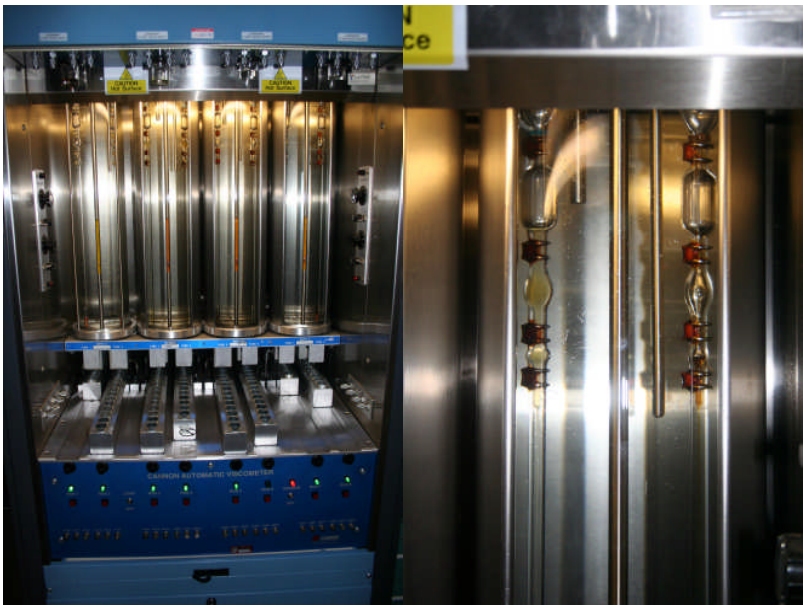

Figure 2 – The Cannon Automated Viscometer, using four parallel capillary viscometers one of which is shown on the right, used to measure the kinematic viscosities from which the VIs were calculated

3. Shear stability

   The tapered roller bearing of the KRL shear rig was spun at 1475 rpm, under a 5000 N load, at 60°C for 20 hours with the kinematic viscosity measured before and after. The calculation of SSI is shown in chapter 1.

Figure 3 – The KRL shear rig used to test the polymers shear stability. The tapered roller baring is shown on the right side.

From these tests, further information is calculated:

1. Viscosity Index (VI)
2. Thickening efficiency

The polymer samples were blended into two oil mixtures. The first series had equal amounts of the polymer in them (equal actives) at 8%. The second series was blended to an equal viscosity at 100°C of ~12.00 cSt using the data from the equal actives tests. All the samples had two pour point depressants added at 0.2 weight % each.

1.1 Literature examples of VM performance

Sanyo Chemical Industries Ltd filed a patent for *VII and Lube oil containing the same* in 2003.[1] In this patent they detail the synthesis of linear polymers by free radical polymerisation using a variety of alkyl methacrylate monomers. The polymers were a statistical mixture of different alkyl methacrylates which were found to have VIs between 218 and 263, when added to oil at 17 weight %, depending on the composition. The authors claim that the polymers had shear stabilities of 10%, they do not quote shear stability index so no direct comparison is possible.

In 2005 a group from the Egyptian Petroleum Research Institute published data on acrylate based VMs synthesised by free radical polymerisation.[2] Their research was concerned with the comparison of different alkyl chain lengths of the monomer units. They investigated chain lengths of decyl up to hexadecyl. They also investigated the effect of the addition of styrene, although this is not of interest for this work. They found that simply by changing the monomer units chain length the VI could be increased from ~125 for decyl acrylate, up to ~180 for hexadecyl acrylate. Their polymers were between M_n = 6000 to 10000 g mol^{-1}. However, their polymers were usually only giving a 20-30 point increase in VI versus the base oil VI.

Later Janovic and coworkers described the synthesis of methacrylate based VMs also by free radical polymerisation.[3] Their polymers were mixtures of MMA, Dodecyl MA and Octadecyl MA with varying compositions. Dodecyl MA was the largest percentage of the polymer chain. They found that the polymers had VIs between 148 and 172 with SSIs between 5 and 22. Their M_ns varied between 30000 and 104000 g mol^{-1}. The VI was increased by the addition of more MMA. The change in composition from MMA/dodecyl MA/octadecyl MA 8/74/18 weight % to 18/66/16 gave a 20 point increase in VI from 220 to 240. These results are in agreement with Selby's observations, described in chapter 1, since the polymer will become less soluble in oil at low temperature reducing its viscosity contribution.[4] However, below a critical

molecular weight the polymers seem to have insufficient viscosity contribution and do not increase the VI markedly with the larger % of MMA.

2 Results and Discussion

The polymers synthesised and detailed in chapter 2 were submitted for a range of tests at Lubrizol. Samples were made based on the results from chapter 3 and are documented in the arm first stars section below. These tests were the standard industrial tests for VMs. The polymer synthesised were compared with 8420 a linear baseline polymer. Ideally the stars made in this work would have a higher VI and TE, lower absolute viscosity and be more shear stable than the baseline polymer.

2.1 Core First Stars – Blended to Equal Actives Content

The polymers were first added to blends in equal amounts by weight percentage. These results allowed the calculation of the amounts of polymer to be added to produce a blend at equal viscosity. Unfortunately there was insufficient sample to test these samples for shear stability and therefore the SSI is unknown at equal actives.

2.1.1 Core First Star polymers with $M_{n\ target}$=10 K g mol^{-1}

2.1.1.1 Molecular Weight by GPC

The molecular weights of the polymers were compared across two different GPC systems. The Warwick system used chloroform with 5% TEA eluent calibrated against narrow PDi PMMA standards and the Lubrizol system using THF calibrated against narrow PDi PSty standards. The molecular weights from the two systems were similar, Table 1, good indication that the molecular weights are close to that targeted.

Sample Number	No. Arms	Composition*	GPC Data Warwick			GPC Data Lubrizol		
			M_n g mol^{-1}	M_w g mol^{-1}	PDI	M_n g mol^{-1}	M_w g mol^{-1}	PDI
2.35	3	100% $C_{12/15}$MA	14200	15300	1.08	14000	15100	1.08
2.50	3	30% BMA	16400	19700	1.20	16000	19200	1.20
2.52	5	30% BMA	12600	14100	1.12	13000	14600	1.12
3.19	1	30% BMA	7500	8800	1.17	12300	14300	1.17
3.32	3	30% BMA	8000	8800	1.10	11500	13000	1.13
3.35	5	30% BMA	7800	9000	1.15	12300	14500	1.18
3.42	4	30% BMA	8600	9900	1.14	10300	11600	1.13
3.45	8	30% BMA	10800	12400	1.14	12300	14400	1.17

Table 1 – A comparison of the molecular weights using two different GPC systems.

*The remaining monomer is $C_{12/15}$MA

2.1.1.2 Absolute and Kinematic Viscosity

The absolute and kinematic viscosities were compared with that of 8420, a linear baseline polymer. The first observation to make is regards sample 2.35 which has 100% $C_{12/15}MA$ and had a very high absolute viscosity at -40°C, >400K cP, Table 2. This was caused by the polymer/oil blend solidifying, thereby demonstrating that the BMA is needed to prevent the polymer thickening the oil too much at low temperature. However, the VI measured calculated for sample 2.35 is similar to the other polymers with 30% BMA, indicating the addition of BMA to enhance the low temperature properties does not have a negative effect on those at higher temperature.

Sample Number	BV at -40°C / cP	KV - cSt			TE
		40°C	100 °C	VI	
3.19	13360	28.10	5.90	**162**	1.38
2.35	>400K	27.36	5.78	**161**	1.26
2.50	9360	28.60	6.08	**168**	1.54
3.32	23100	28.90	5.99	**160**	1.46
3.42	16220	29.40	6.13	**164**	1.58
2.52	11500	30.61	6.56	**177**	1.95
3.35	12480	29.10	6.10	**164**	1.56
3.45	14780	29.40	6.10	**162**	1.56
8420	8710	29.92	6.13	**159**	1.58

Table 2 – A summary of the viscosity data for the $M_{n\ target}$=10 K g mol^{-1} core first star polymers

All the samples show an increased VI compared to 8420 with a maximum increase of 18 to a VI of 177 for sample 2.52. However, there is no obvious relationship between the number of arms in the star and the resulting VI of the polymer, Figure 4.

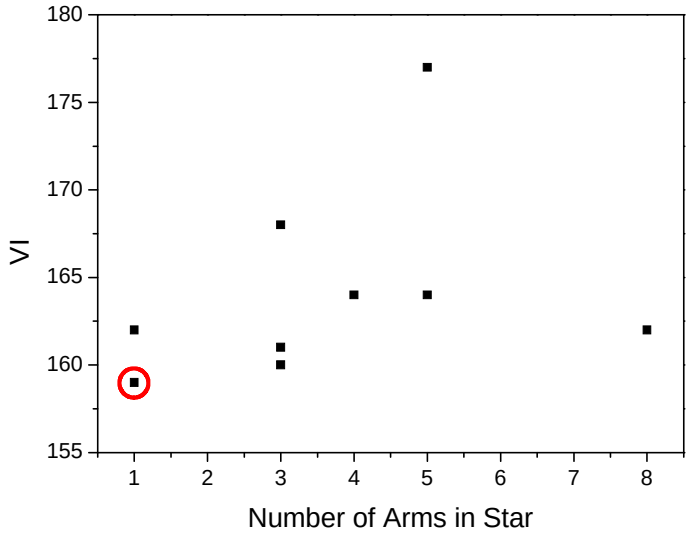

Figure 4 – A comparison of how the Viscosity Index (VI) varies with the number of arms in the star; the 8420 linear baseline is circled in red.

The low temperature properties of the stars show that they all thicken the oil more than 8420 at low temperature. This is not ideal as the absolute viscosity should be quite low at -40°C; excessive thickening of the oil at low temperature adversely affects the performance of the lubricating oil package. There is a trend in the response between the absolute viscosity of the polymers and the number of arms in the star. As the number of arms in the star is increased, the absolute viscosity at -40°C increases, Figure 5. The rise in absolute viscosity with the number of arms could point towards the core of the polymer having an increasing effect on its low temperature properties. Since the molecular weight of the polymers remains approximately constant the arms become gradually shorter as the number of them increases. Therefore the effect of the core on its properties becomes gradually more significant. The effect seen at low temperature could be exactly this core effect, indicating that there is a critical arm length to be reached before any effects of the core on the polymers overall properties are sufficiently minimised.

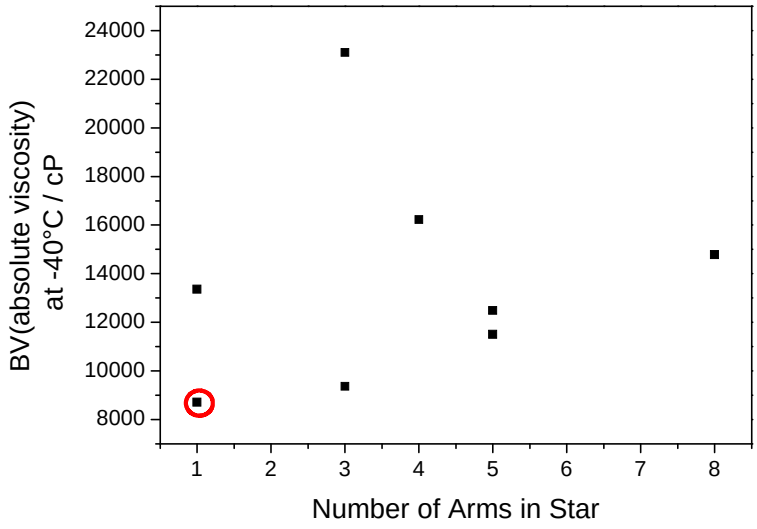

Figure 5 – A comparison of how the Absolute Viscosity measures on the Brookfield viscometer varies with the number of arms in the star. The 8420 linear baseline is circled in red.

The thickening efficiencies (TE) show that sample 2.52 gives the best thickening per weight of polymer added along with the highest VI, while sample 2.35 gives the worse TE at 1.26. There is no trend or obvious relationship between the number of arms in the stars synthesised and their TE, Figure 6.

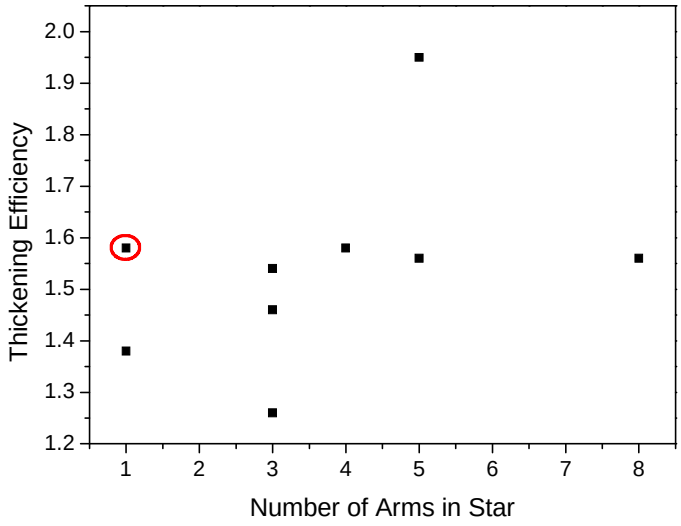

Figure 6 – A comparison of how the Thickening Efficiency changes with the number of arms in the star tested. The 8420 linear baseline is circled in red.

2.1.2 Core First Star polymers with $M_{n\ target}$=20 K g mol^{-1}

2.1.2.1 Molecular Weight by GPC

The polymers synthesised were run on two different GPC systems. The Lubrizol system uses THF calibrated with polystyrene standards, while the Warwick system uses chloroform with 5% TEA calibrated with poly methylmethacrylate standards. The agreement for the higher molecular weight polymers is also very close, baring sample 3.36. The reason this samples GPC data is so different is that it is the most highly branched sample and therefore most different from the linear standard. This would cause the resulting molecular weight data to differ considerably.

Sample Number	No. Arms	Composition*	GPC Data Warwick			GPC Data Lubrizol		
			M_n g mol^{-1}	M_w g mol^{-1}	PDI	M_n g mol^{-1}	M_w g mol^{-1}	PDI
3.20	1	30% BMA	19900	22900	1.15	17100	19700	1.15
2.46	3	100% $C_{12/15}$MA	23200	25700	1.11	23000	25500	1.11
2.51	3	30% BMA	26200	28300	1.08	26000	28000	1.08
3.34	3	30% BMA	14500	16300	1.12	19300	21500	1.11
3.44	4	30% BMA	12000	13800	1.14	16400	17900	1.09
2.53	5	30% BMA	19800	21800	1.10	20000	22000	1.10
3.36	8	30% BMA	12300	13500	1.09	20200	26000	1.29

Table 3– A comparison of the molecular weights using two different GPC systems.

*The remaining monomer is $C_{12/15}$MA

2.1.2.2 Absolute and Kinematic Viscosity

Within the $M_{n\ target}$ = 20 K g mol^{-1} bracket, the VIs are higher than with the $M_{n\ target}$=10 K g mol^{-1} samples, Table 4. This is a known effect of increasing the molecular weight.[5]

Sample Number	BV at -40°C / cP	KV - cSt			TE
		40°C	100 °C	VI	
3.20	12440	29.38	6.27	**172**	1.71
2.46	>400K	31.37	6.63	**175**	2.01
2.51	8480	30.27	6.58	**182**	1.97
3.34	10940	28.20	6.11	**173**	1.56
3.44	9980	26.60	5.86	**174**	1.34
2.53	7970	27.27	5.83	**165**	1.31
3.36	15380	30.80	6.45	**169**	1.86
8420	8710	29.92	6.13	**159**	1.58

Table 4 - A summary of the viscosity data for the $M_{n\ target}$=20 K g mol^{-1} core first star polymers

The VIs for the synthesised polymers are all greater than the VI for 8420 by at least 6 (sample 2.53) up to a maximum of 23 (sample 2.51). This is a dramatic improvement by changing the structure of the polymer. As with the $M_{n\ target}$ = 10 K g mol^{-1} samples, there is no obvious relationship between the VI and the number of arms in the star, Figure 7.

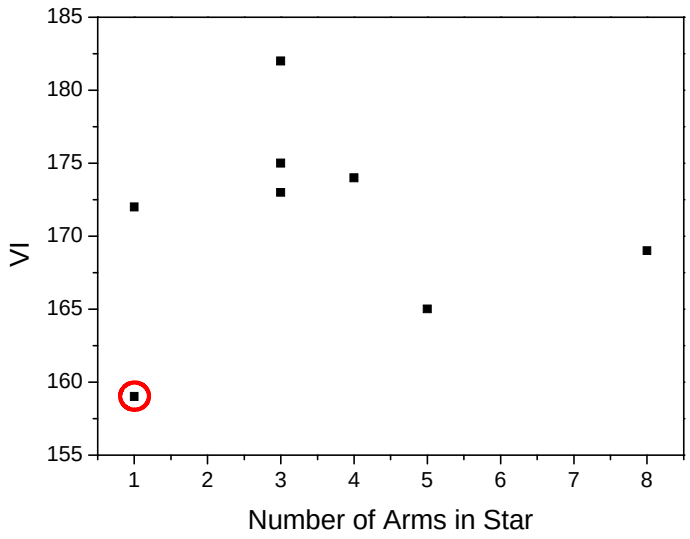

Figure 7 - A comparison of how the Viscosity Index (VI) varies with the number of arms in the star; the 8420 linear baseline is circled in red.

The low temperature properties of the higher molecular weight core first stars are on average, much better than their low molecular weight counterparts, Figure 8. However, there is no obvious trend between the absolute viscosity and the number of arms in the star.

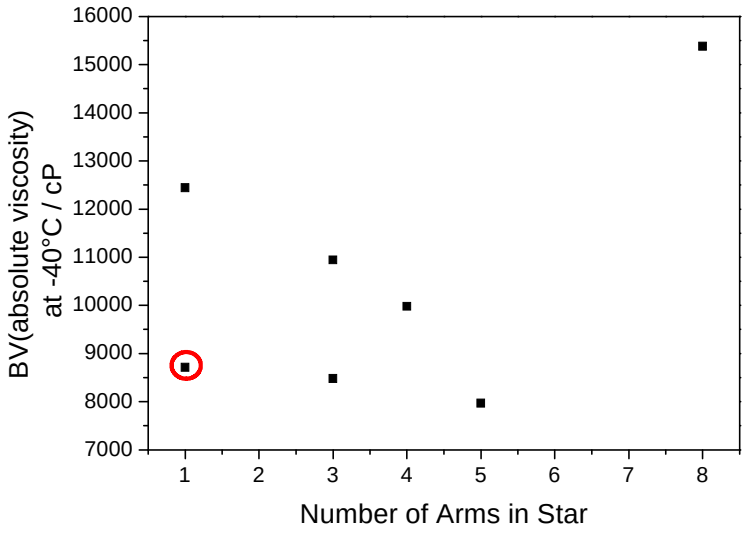

Figure 8 - A comparison of how the Absolute Viscosity measures on the Brookfield viscometer varies with the number of arms in the star; the 8420 linear baseline is circled in red.

The TEs of the polymers also show no obvious relationship with the number of arms in the star, Figure 9.

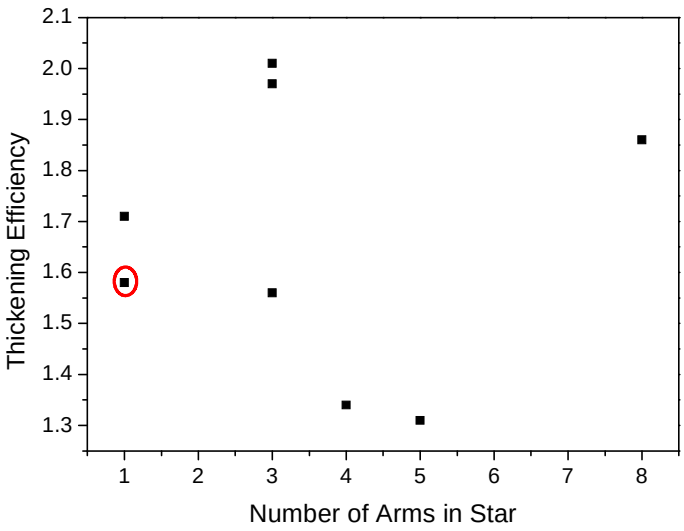

Figure 9 - A comparison of how the Thickening Efficiency changes with the number of arms in the star tested; the 8420 linear baseline is circled in red.

2.2 Core First Stars – Blended to Equal Viscosity

The tests above where the polymers were blended to equal active content allowed the calculation of the amount of polymer required to obtain a given kinematic viscosity at 100°C. These tests should give a more realistic insight as to the properties and effects of the individual VIs.

2.2.1 Core First Star polymers with $M_{n\ target}$ = 10 K g mol^{-1}

2.2.1.1 Absolute and Kinematic Viscosity

Sample Number	Treat Rate	BV at -40°C / cP	KV - cSt			TE
			40°C	100 °C	VI	
3.19	24.4	139000	58.7	10.66	**174**	1.50
2.35	25.8	Test Failed	57.26	11.01	**188**	1.48
2.50	21.7	Test Failed	60.98	11.33	**182**	1.81
3.32	25.7	324000	76.51	12.13	**163**	1.65
3.42	23.8	58790	69.08	11.35	**176**	1.66
2.52	24.7	Test Failed	60.68	11.31	**183**	1.59
3.35	24.2	65790	72.5	12.02	**175**	1.73
3.45	24.2	108000	70.69	11.83	**169**	1.70
8420	22.5	43000	64.55	11.57	**176**	1.79

Table 5 – Summary of the Kinematic Viscosity data for the $M_{n\ target}$ = 10 K g mol^{-1} core first star polymers

These polymers are again compared to the 8420 linear polymer baseline and compared to the linear baseline the core first star polymers give comparable or better VIs. However, the improvement is only small, if any at all with these low molecular weight polymers. The linear polymer by ATRP, sample 3.19, shows no improvement versus 8420 with respect to VI or TE, while its absolute viscosity is 3.5 times higher, which is not ideal. There is no apparent relationship between the VI and the number of arms in the star, Figure 10.

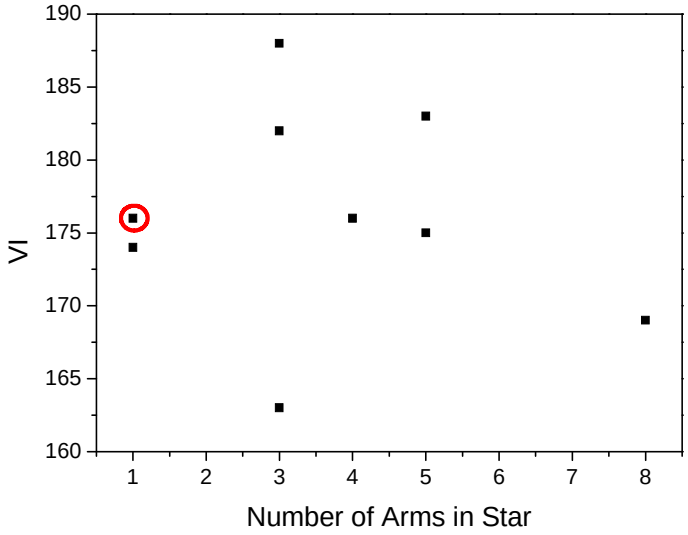

Figure 10 - A comparison of how the Viscosity Index (VI) varies with the number of arms in the star; the 8420 linear baseline is circled in red.

The majority of the samples require more polymer to be added to achieve the VIs than 8420, reflected in the lower TE values, Table 5 and Figure 12. This causes the low temperature properties to be much worse as demonstrated in the Brookfield (BV) viscosity test for absolute viscosity. The absolute viscosities of the core first stars of this molecular weight are all either just above or much higher than the 8420 baseline. This can be attributed to the increased treat rate; the more polymer that is added to the oil, the higher the absolute viscosity at low temperature. Once again, as with the sample blended to equal actives content, there is an upward trend for the absolute viscosity as the number of arms in the star increases.

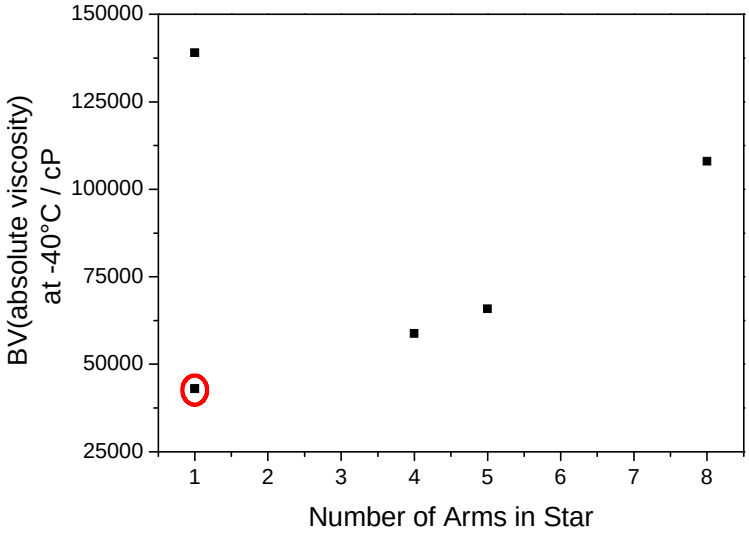

Figure 11 - Comparison of how the Absolute Viscosity measures on the Brookfield viscometer varies with the number of arms in the star; the 8420 linear baseline is circled in red.

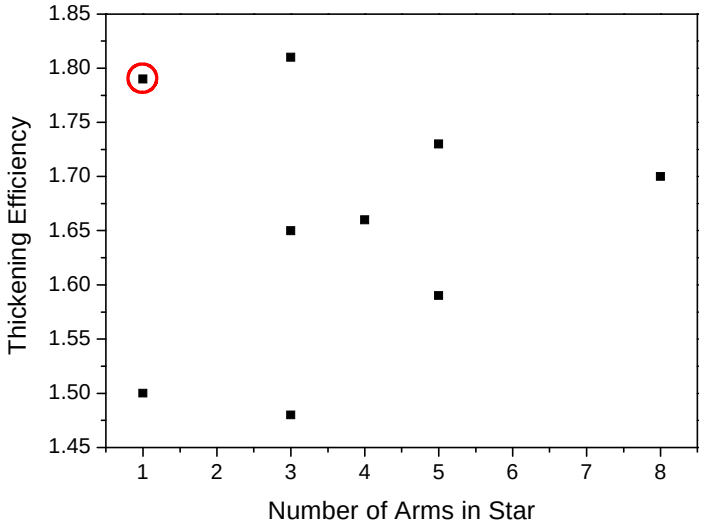

Figure 12 – Comparison of how the Thickening Efficiency changes with the number of arms in the star tested; the 8420 linear baseline is circled in red.

2.2.1.2 Shear Stability

The shear stability was measured using a KRL shear rig and ideally the polymers should be more shear stable than the 8420 baseline. In all cases, the polymers with $M_{n\ target}$ = 10 K g mol^{-1} are significantly more stable to shear than 8420, Table 6 and Figure 14. This increase in shear stability (decrease in SSI) can be attributed to the star architecture. With a star, if part of it is removed by a mechanical or chemical process the relative drop in molecular weight is much less than with a linear polymer, Figure 15. This results in a more shear stable polymer.

Sample Number	20 hr KRL			
	SOT (start of test)	EOT (end of test)	% shear loss	SSI
3.19	10.68	10.8	-1.12	**-1.9**
2.35	11.01	10.92	0.82	**1.4**
2.50	11.36	11.04	2.82	**4.7**
3.32	12.13	12.13	0.00	**0.0**
3.42	11.35	11.57	-1.94	**-3.2**
2.52	11.36	11.53	-1.50	**-2.5**
3.35	12.02	11.9	1.00	**1.6**
3.45	11.83	11.8	0.25	**0.4**
8420	11.52	10.82	6.10	**10.0**

Table 6 – Summary of the Shear Stability data from the KRL shear rig.

These samples targeting low molecular weights are uniformly more shear stable than 8420, Figure 14. The most sheared polymer had an SSI of 4.7 (sample 2.50) while three of the polymers (samples 2.52/3.19/3.42) had a higher viscosity after being subjected to the shear test. This was most unexpected.

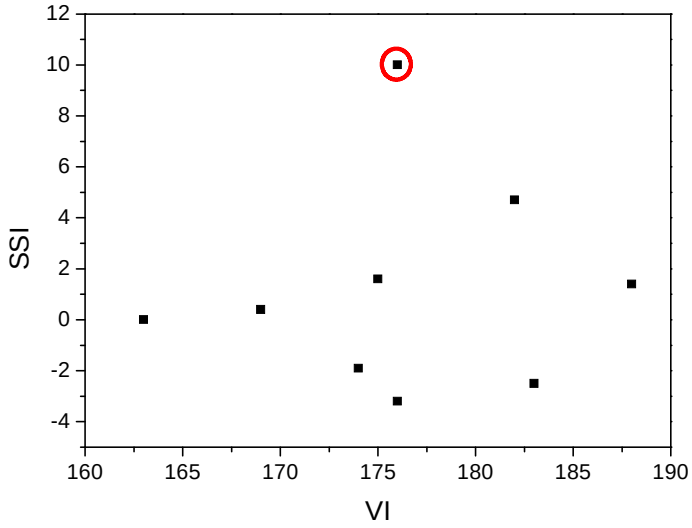

Figure 13 – Comparison of how the shear stability of the stars vary with their viscosity indexes (VI); the 8420 linear baseline is circled in red.

When comparing the SSI with the VI the samples are all more shear stable than 8420 for equal VI, Figure 13. Only three samples have a higher VI than 8420 and no clear trend in the relationship between these two factors is apparent.

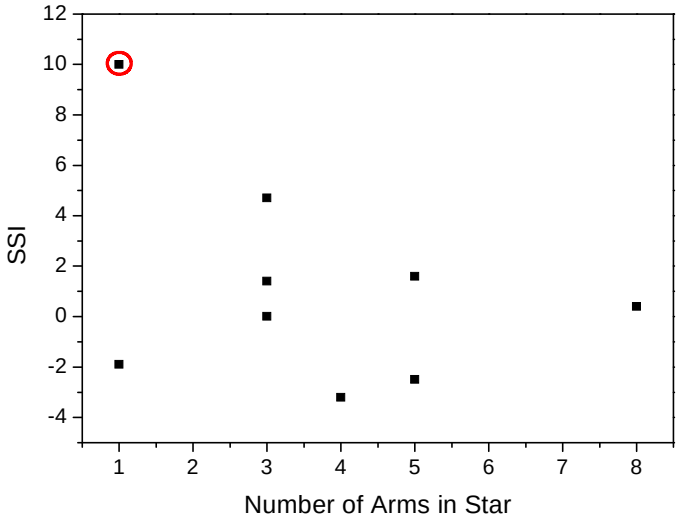

Figure 14 – The change in shear stability as the number of arms in the star is varied $M_{n\ target}$=10 K g mol^{-1}

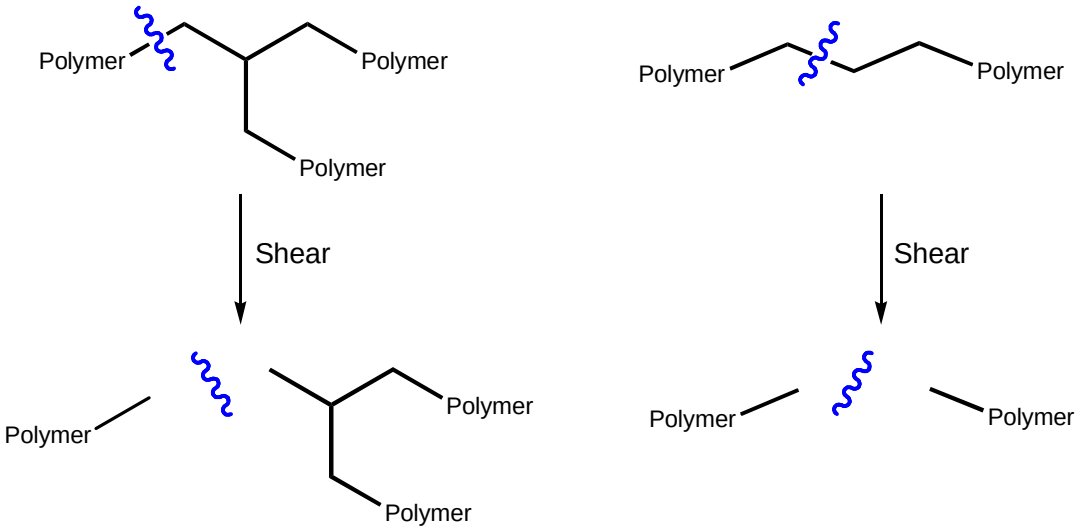

Figure 15 – Comparison of how the molecular weight can drop due to the polymer chain being broken apart. Star polymers lose less molecular weight than linear polymers.

2.2.2 Core First Star polymers with $M_{n\ target}$ = 20 K g mol^{-1}

2.2.2.1 Absolute and Kinematic Viscosity

The larger $M_{n\ target}$ = 20 K g mol^{-1} polymers show vastly improved viscometric properties. They all have VIs > 8420, with a minimum improvement of 7 (sample 3.36) up to 29 (sample 3.44); there is no trend relating the VI of these polymers with the number of arms in the star, Figure 16.

Sample Number	Treat Rate	BV at -40°C / cP	KV - cSt			TE
			40°C	100 °C	VI	
3.20	20.5	175000	59.4	11.33	**188**	1.92
2.46	17.7	Test Failed	55.06	10.92	**195**	2.13
2.51	17.6	Test Failed	55.97	11.18	**197**	2.20
3.34	24.1	27640	70.12	11.62	**188**	1.68
3.44	27.8	16240	59.03	12.00	**205**	1.50
2.53	17.8	37600	54.71	10.78	**193**	2.09
3.36	20.5	68090	63.56	11.35	**183**	1.92
8420	22.5	43000	64.55	11.57	**176**	1.79

Table 7 - Summary of the Kinematic Viscosity data for the $M_{n\ target}$=20 K g mol^{-1} core first star polymers

At this higher molecular weight the linear polymer synthesised by ATRP shows an improved VI and TE versus 8420. However, the low temperature properties are nearly four times worse than the baseline.

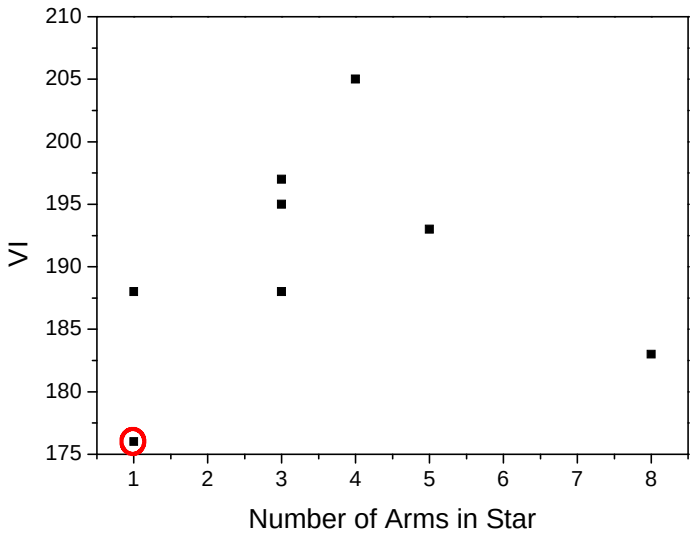

Figure 16 - Comparison of how the Viscosity Index (VI) varies with the number of arms in the star; the 8420 linear baseline is circled in red.

The low temperature properties of the core first stars are comparable to, or better than 8420, Figure 17. Samples 2.53, 3.34 and 3.44 all have lower absolute viscosities at -40°C, whilst the linear ATRP polymer (sample 3.20) had a very high absolute viscosity. As with the $M_{n\ target}$ = 10 K g mol^{-1} samples, there is an upward trend in the absolute viscosity with the number of arms in the star, Figure 17.

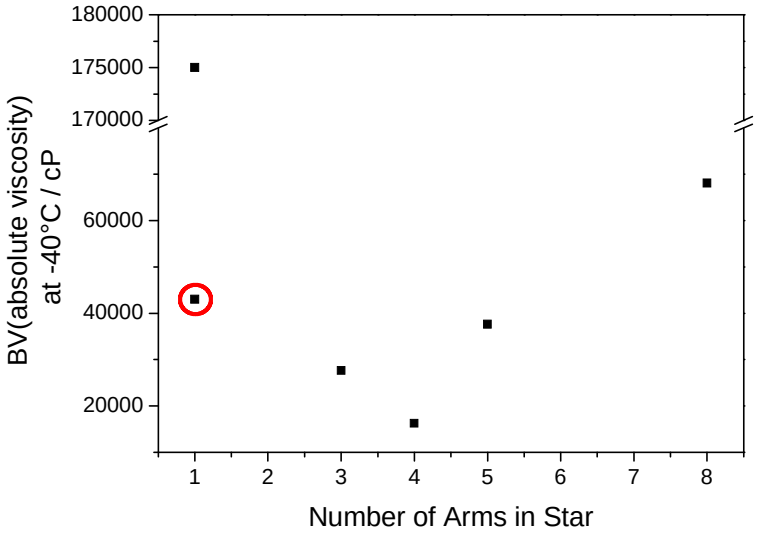

Figure 17 - Comparison of how the Absolute Viscosity measures on the Brookfield viscometer varies with the number of arms in the star; the 8420 linear baseline is circled in red.

The TE of these higher molecular weight polymers are much improved versus their lower molecular weight counterparts. All except two samples show a higher TE than the linear baseline, Figure 18. The increase in TE can be directly attributed to the lower treat rate, Table 7, required to give the desired viscosity.

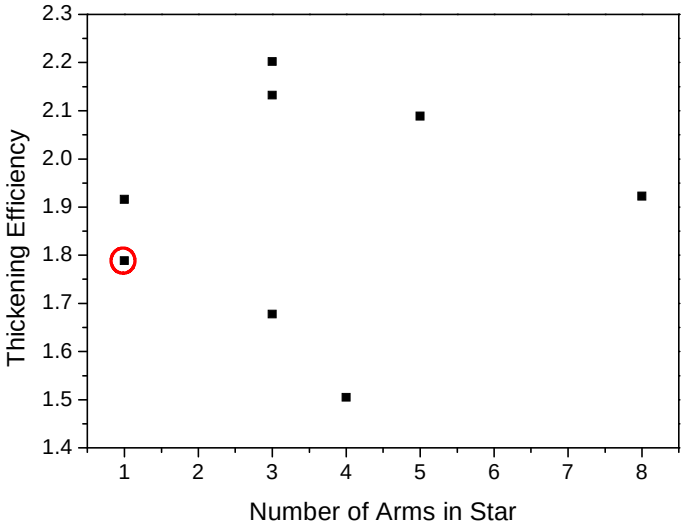

Figure 18 - Comparison of how the Thickening Efficiency changes with the number of arms in the star tested; the 8420 linear baseline is circled in red.

2.2.2.2 Shear Stability

The shear stability of the higher molecular weight $M_{n\ target}$ = 20 K g mol^{-1} samples should be lower than for $M_{n\ target}$ = 10 K g mol^{-1}. This was found to be the case, Table 8. The samples were all more shear stable than 8420, Figure 20. Unlike with the $M_{n\ target}$ = 10 K g mol^{-1} only one sample shows thickening after shear (sample 3.34).

Sample Number	20 hr KRL			
	SOT (start of test)	EOT (end of test)	% shear loss	SSI
3.20	11.29	11.2	0.80	**1.3**
2.46	10.98	10.48	4.55	**7.7**
2.51	11.22	10.57	5.79	**9.6**
3.34	11.62	11.68	-0.52	**-0.8**
3.44	failed	failed	failed	failed
2.53	10.77	10.68	0.84	**1.4**
3.36	11.35	11.11	2.11	**3.5**
8420	11.52	10.82	6.10	**10.0**

Table 8 - Summary of the Shear Stability data from the KRL shear rig data for the $M_{n\ target}$=20 K g mol^{-1} core first star polymers.

A potentially interesting observation is how the SSI changes with VI for these polymers as generally, the higher VI samples have a high molecular weight causing the samples to

have a higher SSI. This increasing SSI with VI is also observed for these samples, Figure 19, although they are still below that of 8420 for a significant increase in VI.

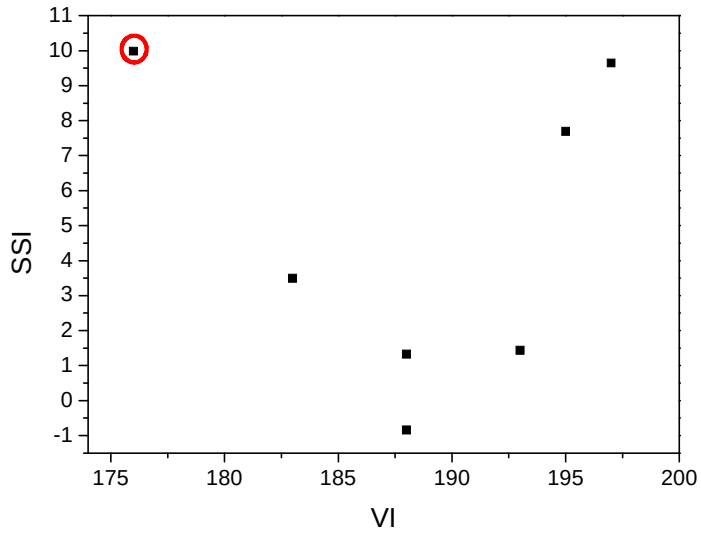

Figure 19 - Comparison of how the shear stability of the stars vary with their viscosity indexes (VI); the 8420 linear baseline is circled in red.

There seems to be a tentative relationship with these samples between the SSI and the number of arms in the star, Figure 20. The SSI rises for increasing arm number. However, this is counter-intuitive as this is the reverse to what would be expected. With increasing arm number the arms of the star get shorter. This should result in a reduced shear rate of the arms. This is the opposite of that observed with these polymers and was not the case of the lower $M_{n\ target}$ = 10 K g mol^{-1} samples.

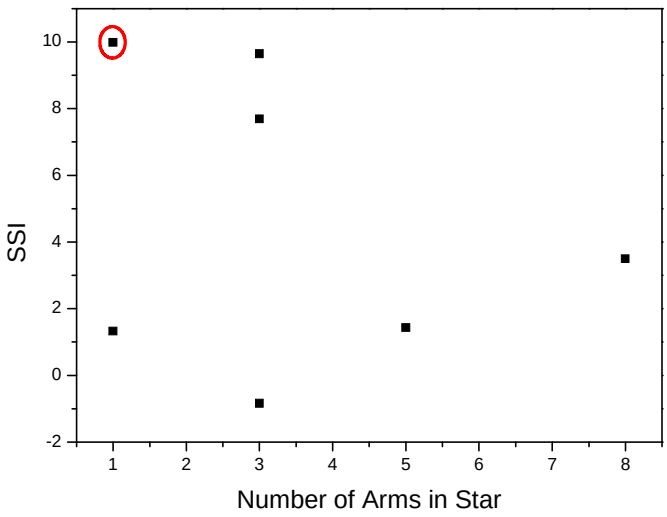

Figure 20 - Change in shear stability as the number of arms in the star is varied for $M_{n\ target}$ = 20 K g mol^{-1} samples

2.3 Core First Stars synthesised in Oil tested at Equal Treat Rate

The polymers synthesised at Warwick were representative of academic samples synthesised in optimal polymerisation conditions. To show that polymers can be synthesised in more industrially relevant conditions they were synthesised using a Tornado, six flask reactor. Oil was used as solvent. Due to the smaller reaction flasks used, approx 200 ml, there was insufficient sample to obtain testing at both equal treat rate and equal viscosity.

2.3.1 Molecular Weight by GPC

The polymers were synthesised targeting M_n = 10 K g mol^{-1} and M_n = 20 K g mol^{-1}. The molecular weights are quite close to that targeted even though the reactions were not monitored and therefore not stopped at a specific conversion to give the desired molecular weight.

Sample Number	No. Arms	Composition*	GPC Data - Lubrizol		
			M_n g mol^{-1}	M_w g mol^{-1}	PDI
Oil 1	3	30% EHMA	19200	24000	1.24
Oil 2	3	30% EHMA	11400	15000	1.31
Oil 3	5	30% EHMA	20100	34000	1.66
Oil 4	5	30% EHMA	12100	19000	1.56
Oil 5	8	30% EHMA	No data	No data	No data
Oil 6	8	30% EHMA	13600	25000	1.81

Table 9 – Summary of a series of core first star polymers synthesised in oil at Hazelwood, Lubrizol's research site in the UK. *The remaining monomer is $C_{12/15}$MA

2.3.2 Absolute and Kinematic Viscosity

The polymers were subjected to the same testing procedure as the polymers synthesised at Warwick. They all have a higher VI than 8420 with a minimum increase of 3 (Oil 2) up to a maximum of 31 (Oil 5), Figure 21 and Table 10. Their absolute viscosities are higher than 8420, giving a thicker oil blend at lower temperatures with typically a 1.5 to 2 times increase observed.

Sample Number	BV at -40°C / cP	KV - cSt			
		40°C	100°C	VI	TE
Oil 1	11620	36.69	7.51	**178**	2.68
Oil 2	17960	32.31	6.54	**162**	1.93
Oil 3	14360	38.12	7.91	**186**	2.97
Oil 4	13440	33.28	6.79	**168**	2.14
Oil 5	12800	40.48	8.39	**190**	3.29
Oil 6	16860	34.94	7.17	**175**	2.43
8420	8710	29.92	6.13	**159**	1.58

Table 10 - Summary of the Kinematic viscosity data for the core first star polymers synthesised in oil at Lubrizol, tested at equal treat rate

The TE of these polymers are very high when compared to 8420, the samples synthesised in oil give a significant increase in TE, in some cases (Oil 3 and 5) reaching close to or above a two fold increase. This increase in TE would result in less polymer being added to the oil blend to give a required viscosity. These thickening efficiencies are much higher than the samples synthesised in toluene, Table 2 and Table 4. The highest TE of the samples synthesised in toluene is sample 2.46 with TE = 2.01. This is similar to the lowest TE of sample Oil 2, TE = 1.93.

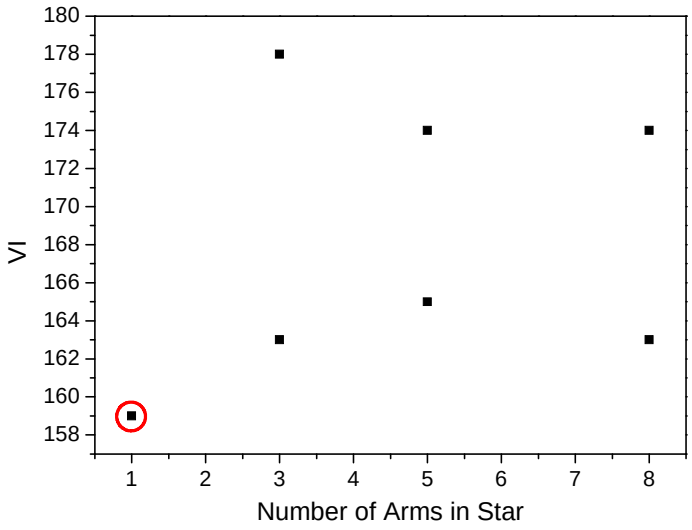

Figure 21 - Comparison of how the Viscosity Index (VI) varies with the number of arms in the star; the 8420 linear baseline is circled in red.

2.4 Arm First Stars

The information obtained from Chapter 3 on the synthesis of arm first stars was used to make three star polymer samples for testing. They were chosen to target arm lengths of M_n = 2500/6250/10000 g mol^{-1} which are samples 3.86, 3.91 and 3.92 respectively. The samples give an overview of the performance of the arm first stars synthesised by ATRP. Their syntheses were repeats of experiments 3, 10 and 8 respectively from chapter 3 and therefore and not documented further.

2.4.1 Molecular Weight data by GPC

The samples are a mixture of stars and un-reacted arms. Therefore they were subjected to peak de-convolution as described in the experimental to obtain molecular weight data for the star peak. This also allowed the calculation of the percentage incorporation of the polymer arm into the stars. The data obtained shows that the arm first stars will be comparable to the five and eight arm core first stars with one sample, 3.92, having more arms on average than the core first stars.

Sample Number	Calculated No. Arms	GPC Data Warwick (star)			
		M_n g mol^{-1}	M_w g mol^{-1}	PDI	Percentage arm incorporation into star
3.89	1	36900	43400	1.17	--
3.90	1	25500	29700	1.16	--
3.86	6	44200	55200	1.25	86
3.91	7	55500	71900	1.30	80
3.92	10	88700	129200	1.46	86

Table 11 – The molecular weight data for the arm first stars synthesised at Warwick by ATRP

2.4.2 Arm first star polymers blended to equal treat rate

As with the core first stars, the polymers were first blended to equal treat rate of 8% actives in oil. This series of tests demonstrate that the polymers are all reasonable VMs with acceptable low temperature properties. At equal treat rate the linear polymers synthesised by ATRP have comparable low temperature viscosity to the 8420 baseline but have much higher VIs and TE. There is an upward trend in the VI of the arm first stars with the number of arms, Figure 22; although at equal treat rate the stars have a lower VI than the linear ATRP samples. The increase in VI with the number of arms can be attributed to the longer polymer chain lengths targeted. Longer polymer chains are known to have higher VIs; as with samples 3.89/90.

Sample Number	Calculated No. Arms	BV at -40°C / cP	KV			TE
			40°C	100 °C	VI	
3.89	1	11320	41.11	9.187	215	3.78
3.90	1	10740	33.22	7.179	188	2.44
3.86	6	36140	28.34	6.122	172	1.58
3.91	7	32190	27.72	6.276	188	1.71
3.92	10	31320	24.79	5.961	201	1.43
8420	1	8710	29.92	6.130	159	1.58

Table 12 – The kinematic and absolute viscosity data for the arm first stars blended at equal treat rate

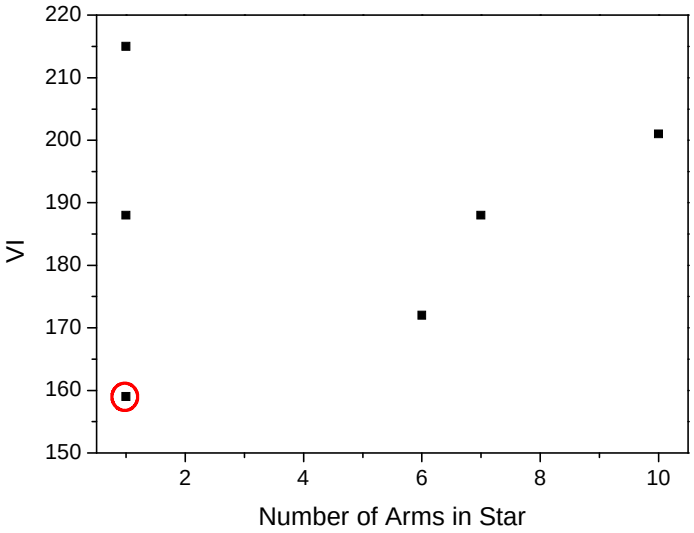

Figure 22 - Comparison of how the Viscosity Index (VI) varies with the number of arms in the star; the 8420 linear baseline is circled in red.

The low temperature viscosities of the arm first stars at equal treat rate are much higher than the 8420 baseline, in the order of four times higher, Figure 23. However, there is a trend indicated in that as the number of arms in the star increases, the absolute viscosity decreases. The linear polymers by ATRP have only slightly higher absolute viscosities than 8420.

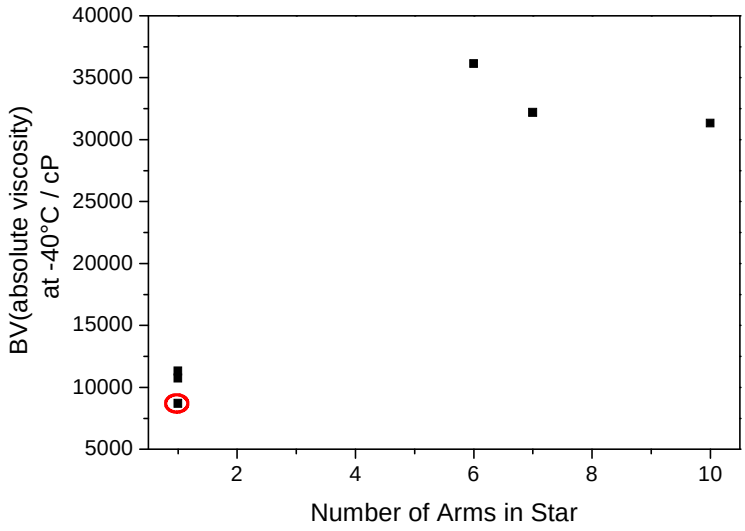

Figure 23 - Comparison of how the Absolute Viscosity measures on the Brookfield viscometer varies with the number of arms in the star; the 8420 linear baseline is circled in red.

2.4.3 Arm first star polymers blended to equal viscosity

Using the information from the equal treat rate viscosity testing further blends were made for testing at equal viscosity at 100°C. This series of tests show an interesting set of properties for the polymers. The VIs show the most dramatic change from the equal treat rate tests; the linear ATRP samples are once again give a much improved VI versus 8420 with a 29 to 44 point increase depending on the molecular weight of the sample.

Sample Number	Calculated No. Arms	Treat Rate	BV at -40°C /cP	KV			TE
				40°C	100 °C	VI	
3.89	1	10.0	13660	47.28	10.50	**220**	3.60
3.90	1	15.2	19180	51.25	10.69	**205**	2.42
3.86	6	23.0	>400000	61.37	11.76	**191**	1.78
3.91	7	21.3	340000	52.21	11.93	**233**	1.95
3.92	10	25.2	19100	48.92	13.81	**296**	1.90
8420	1	22.5	43000	64.55	11.57	**176**	1.79

Table 13 - The kinematic and absolute viscosity data for the arm first stars blended to equal viscosity at 100°C

The arm first stars show a significant upward trend in VI with the number of arms in the star, Figure 24. The core first stars are similar in the number of arms to samples 3.86 and 3.91 and have a comparable VI to sample 3.86. However, sample 3.91 has a much improved VI compared to the eight arm stars using a core first approach, Table 7. All the core first stars viscosity data together with sample 3.86 demonstrate that the star architecture gives an improvement in VI, absolute viscosity and SSI. However, from 3 to 8 arms for a core first approach no clear trend is found regarding the optimal number of arms. The arm first samples with above 7 arms show a dramatic improvement. The

VI for sample 3.92 which has ten arms is 296, a 120 improvement in VI versus 8420. Sample 3.91 has a VI 50 higher than an eight arm core first star and 57 higher than 8420.

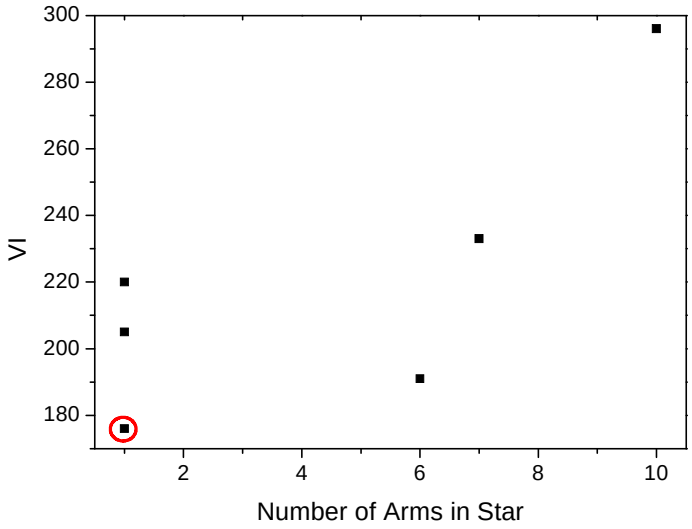

Figure 24 - Comparison of how the Viscosity Index (VI) varies with the number of arms in the star; the 8420 linear baseline is circled in red.

The low temperature properties of the arm first stars also show a trend with respect to the number of arms in the star. The absolute viscosity of the stars decreases with increasing number of arms in the star. While the linear samples synthesised by ATRP have an absolute viscosity at least half that of 8420; the 6 and 7 arm, arm first stars have a much higher absolute viscosity. These absolute viscosities are about eight times higher than 8420 for a 15 to 57 point VI increase. However, when the number of arms is increased to ten, the absolute viscosity decreases to 19000 cP.

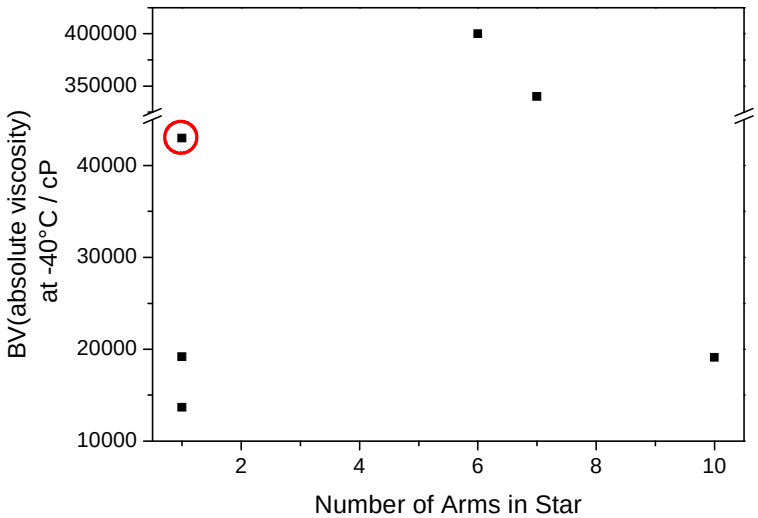

Figure 25 - Comparison of how the Absolute Viscosity measures on the Brookfield viscometer varies with the number of arms in the star; the 8420 linear baseline is circled in red.

The TEs for the arm first stars are close the value for 8420, Figure 26. The linear samples have much higher TE due to the increased molecular weight. Although the thickening efficiency is not a vast improvement compared to the baseline the significant increase in VI at the same TE is considerable progress towards an arm first star as a commercial VM.

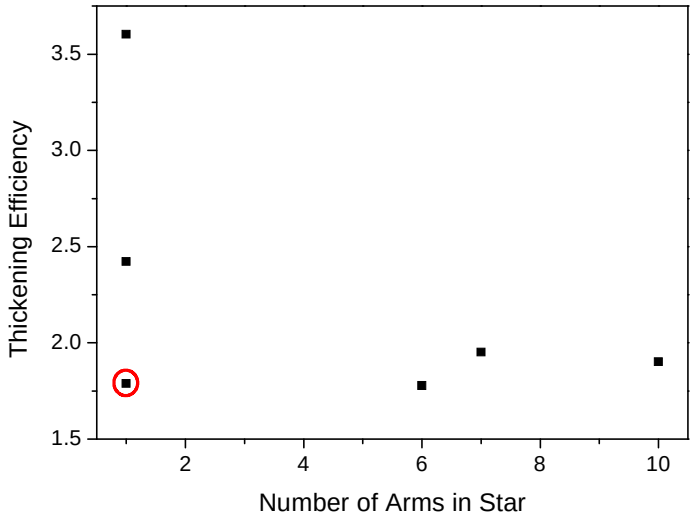

Figure 26 - Comparison of how the Thickening Efficiency changes with the number of arms in the star tested; the 8420 linear baseline is circled in red.

2.4.4 Shear Stability

The shear stability of the arm first star samples varies quite considerably with the number of arms in the star. While increasing the number of arms in the star significantly improves the viscosity properties, the shear stability of the polymers can suffer as the polymer chains get longer. This is observed with the arm first star samples.

Sample Number	20 hr KRL			
	SOT (start of test)	EOT (end of test)	% shear loss	SSI
3.89	11.74	11.25	4.17	**6.7**
3.90	10.68	10.15	4.96	**8.5**
3.86	11.74	11.25	4.17	**6.7**
3.91	12.03	11.52	4.24	**6.8**
3.92	13.97	11.40	18.40	**27.1**
8420	11.52	10.82	6.10	**10.0**

Table 14 - Summary of the shear stability data from the KRL shear rig data for the arm first star polymer

The SSI of the polymers ideally would be lower than 8420, the linear baseline. This is the case for samples 3.86 and 3.91, Table 14. However, sample 3.92 indicates that there is a critical chain length, that above which the shear stability of the polymers is

insufficient. The SSI of the polymers shows a clear trend when varying the number of arms in the star, Figure 27. As the number of arms increases, so does the SSI.

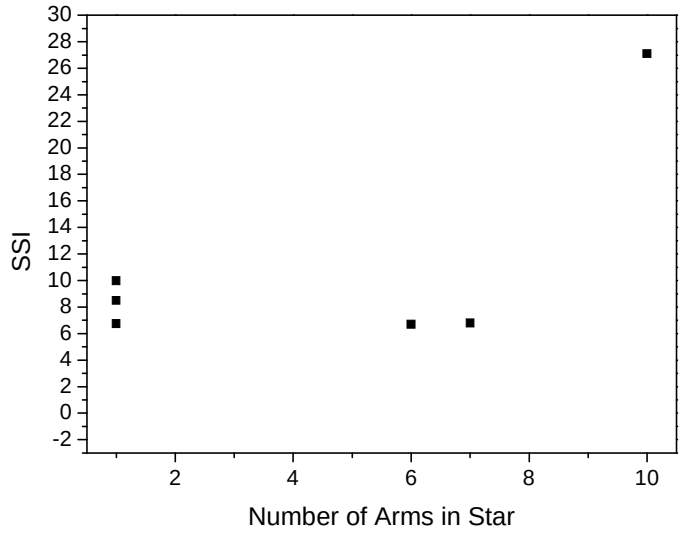

Figure 27 - Change in shear stability as the number of arms in the star is varied for $M_{n\ target}$=20 K g mol^{-1} samples

2.5 Viscosity Temperature Improvers

In chapter 1 section 1.2.5, work by Selby in 1958 was described regarding his reclassification of VMs to viscosity temperature improvers (V-TIs).[4] Selby's work pointed out that the most suitable VMs thickened the oil more at higher temperatures than at lower temperature. This lead to the reclassification to a V-TI. Having compared the polymers against the VI scale and found them to be highly effective VMs, an interesting comparison would be to see which fit Selby's definition as V-TIs. As defined by Selby if the $\mu_{sp}100/\ \mu_{sp}40$ is above 1 then the polymer is a V-TI. This is the case for only a limited number of samples – 3.89/90/91, Table 15. These samples are all arm first stars with greater than six arms. Therefore of the polymers synthesised only three are V-TIs according to Selby's definition.

Sample	Kinematic viscosity / cSt		Kinematic viscosity contribution of the additive / cSt		$\mu_{sp} = (\mu-\mu0/\mu0)$		V-T Characteristic $\mu_{sp}100/\ \mu_{sp}40$	VI
	40°C	100°C	40°C	100°C	40°C	100°C		
Base Oil	20.91	4.48	-	-	-	-		129
2.59	50.30	9.96	29.39	5.48	1.41	1.22	0.87	189
3.19	58.70	10.66	37.79	6.18	1.81	1.38	0.76	174
3.20	59.40	11.33	38.49	6.85	1.84	1.53	0.83	188
2.35	57.26	11.01	36.35	6.53	1.74	1.46	0.84	188
2.46	55.06	11.01	34.15	6.44	1.63	1.44	0.88	195
2.50	60.98	11.33	40.07	6.85	1.92	1.53	0.80	182
2.51	55.97	11.18	35.06	6.70	1.68	1.50	0.89	197
3.32	76.51	12.56	55.60	8.08	2.66	1.80	0.68	163
3.34	70.12	11.62	49.21	7.14	2.35	1.59	0.68	188
3.42	69.08	11.35	48.17	6.87	2.30	1.53	0.67	176
3.44	*59.03*	*12.00*	*38.12*	*7.52*	*1.82*	*1.68*	*0.92*	*205*
2.52	60.68	11.31	39.77	6.83	1.90	1.52	0.80	183
2.53	54.71	10.78	33.80	6.30	1.62	1.41	0.87	193
3.35	72.50	12.02	51.59	7.54	2.47	1.68	0.68	175
3.36	63.56	11.35	42.65	6.87	2.04	1.53	0.75	183
3.45	70.69	11.83	49.78	7.35	2.38	1.64	0.69	169
3.89	*47.28*	*10.5*	*26.366*	*6.02*	*1.26*	*1.34*	*1.07*	*220*
3.90	51.25	10.69	30.336	6.21	1.45	1.39	0.96	205
3.86	61.37	11.76	40.456	7.28	1.93	1.63	0.84	191
3.91	*52.21*	*11.93*	*31.296*	*7.45*	*1.50*	*1.66*	*1.11*	*233*
3.92	*48.92*	*13.81*	*28.006*	*9.33*	*1.34*	*2.08*	*1.56*	*296*
8420	64.55	11.57	43.64	7.09	2.09	1.58	0.76	176

Table 15 – The V-TI characteristics of the various core first and arm first stars synthesised in this work

3 Conclusions

The synthesis of a range of polymers by ATRP for testing as VMs by Lubrizol has been completed and documented in chapters 2 and 3. Tests were run to ascertain their viscometric properties. While the core first stars show an almost uniform improvement in both VI, absolute viscosity and SSI versus the 8420 linear baseline, the arm first stars show more dramatic properties. The VIs for the arm first stars are markedly higher than the baseline sample. However, above a critical chain length, approx 8-9 arms, the SSI rises to almost three times that of 8420 for a near doubling of VI.

There were a number of trends identified in this work. The core first star samples were found to have an increasing absolute viscosity at -40°C with the number of arms in the star. However, this was the opposite found for the arm first star samples where the absolute viscosity dropped with increasing number of arms in the star.

The majority of polymers were found to be thickeners according to Selby's definition of VMs.[4] All of the arm first stars were however found to be V-TIs.

4 References

1. T. Yuki and Y. Ota, US2003104955, 2003.
2. A. M. Nassar, N. S. Ahmed, R. S. Kamal, A.-A. A. A. Azim and E. I. El-Nagdy, *Pet. Sci. Technol.*, 2005, **23**, 537-46.
3. A. Jukic, M. Rogosic and Z. Janovic, *Ind. Eng. Chem. Res.*, 2007, **46**, 3321-27.
4. T. W. Selby, *ASLE*, 1958, **1**, 68-76.
5. B. G. Kinker, *Chemical Industries (Dekker)*, 2003, **90**, 329-53.